2021

NOVEL NEW MODELING PROCEDURE FOR INDUSTRIAL MACHINERY WITH NONLINEAR CONNECTIONS

Steven Whitican
Michigan Technological University, smwhitic@mtu.edu

NOVEL NEW MODELING PROCEDURE FOR INDUSTRIAL MACHINERY WITH NONLINEAR CONNECTIONS

By

Steven M. Whitican P.E.

A DISSERTATION

Submitted in partial fulfillment of the requirements for the degree of

DOCTOR OF PHILOSOPHY

In Mechanical Engineering – Engineering Mechanics

MICHIGAN TECHNOLOGICAL UNIVERSITY

2021

This dissertation has been approved in partial fulfillment of the requirements for the Degree of DOCTOR OF PHILOSOPHY in Mechanical Engineering – Engineering Mechanics.

Department of Mechanical Engineering - Engineering Mechanics

Dissertation Advisor:	*Dr. Jason Blough*
Committee Member:	*Charles Van Karsen*
Committee Member:	*Dr. Gregory Odegard*
Committee Member:	*Dr. James DeClerck*
Committee Member:	*Dr. Paul Sanders*
Department Chair:	*Dr. William Predebon*

Table of Contents

List of Figures

List of Tables

List of Abbreviations

ASM	Acceleration Surface Method
CoFEM	Component Finite Element Analysis
CNC	Computer Numerical Control
DAQ	Data Acquisition Device
DOF	Degree of Freedom
FBS	Frequency Domain Substructuring
FE	Finite Element
FEM	Finite Element Model
FRF	Frequency Response Function
FNSI	Frequency Domain Nonlinear Subspace Identification
GUI	Graphical User Interface
HB	Harmonic Balance
HT	Hilbert Transform
IHBM	Incremental Harmonic Balance Method
MAC	Modal Assurance Criteria
MDOF	Multiple Degree of Freedom
MPC	Multi Point Constraints
pLSCF	Poly-reference Least Squares Complex Exponential
RAM	Random Access Memory
RCSA	Receptance Coupling Substructure Analysis
SDOF	Single Degree of Freedom
SEREP	System Equivalent Reduction Expansion Process
TCP	Tool Center Point

Abstract

Given current timelines for rolling out production at volume, the ability to model portions of the production process is of paramount importance. To model production, high-fidelity models of production assets must be obtained. The production assets are comprised of linear and nonlinear structures. The linear structures are well understood and defined. Significant work has, and is, being done to understand the nonlinear components. This work focuses on developing and correlating a model of a nonlinear component. The component studied and modeled is a linear guide. Linear guides are bearings which facilitate translational motion of machine axes. An accurate model of a linear guide is necessary to achieve an accurate model of a machine tool (production asset). Concepts of nonlinear structural dynamics are utilized and extended for use with linear guides. This work provides an accurate model of linear guides. The linear guides are fully tested to extract the nonlinear characteristics. The guides are found to exhibit a softening nonlinearity. Upon characterization of the nonlinearity, additional testing and validation are performed to develop a model. The harmonic balance method is utilized to conduct a numerical simulation of a set of linear guides The model is then correlated.

1 Introduction & Literature Review

In recent years, significant research has been conducted to study industry 4.0, or digital factory. These terms can carry different connotations to those involved. The crux of digital factory is the complete understanding and monitoring of all plant systems. According to a 2017 report, Digital factory is expected to contribute to 12% efficiency gains over five years [1]. The same report indicates that nine out of ten companies are moving towards digitization.

Efficiency gains are not only of interest to the end user, but to the equipment producers as well. In factories which are responsible for machining of parts, precepts from digital factory prove very useful. Embracing digitization allows for virtual prototyping of parts and processes, understanding of asset health, and optimization of process. These concepts lead the end user to shortened time to market by means of simultaneous engineering, reduced and scheduled down time, and full utilization of production assets.

In order to take full advantage of these benefits, factories employing CNC machinery require methods of tracking and modeling their production assets. Of particular interest is the CNC machinery itself. Metal removal processes are extremely sophisticated. Many models are required to accurately predict the behavior of the process and the machine. Figure 1 is presented to show there are two components to accurately capturing the characteristics of a CNC machine.

The right-hand branch of Figure 1 describes some of the critical aspects to be understood regarding the production process. These aspects involve determining process stability and surface finish. While the list (albeit short) on the right hand side is production process specific, the list on the left hand side is equally as important.

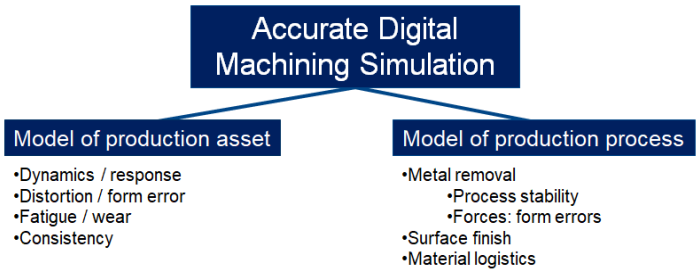

Figure 1 Processes involved in machining simulation

The list on the left-hand side of Figure 1 indicates the critical knowledge to be had regarding the production asset. Though the process may be known, and various authors endeavor to expand human knowledge of the production process, models must also be constructed of the production assets. The production asset will often define the success or failure of the production process. A prescient example is the computation of stability for a milling operation. The stability lobes will be heavily dependent upon the dynamics of the machine tool structure in addition to the process parameters (blades in cut, material combination, etc.).

In order to develop a model of a production asset, the underlying dynamics of the asset must be understood. The asset, as with many other types of commercial structures, is comprised of linear substructures connected at nonlinear joints. The precepts of linear modal analysis may be used to understand each *independent* substructure involved in the construction of a machine, but more is required to understand the behavior of the joints.

Some critical connections to be modeled in machine tools are bolted joints [2], bearings, linear guides, and ballscrews [3] [4] [5]. Bolted joints are well understood and may be approximated by a contact patch. Bearings are also well understood and modern research has even begun to account for gyroscopic moments of the rolling elements within the bearings. Effort has also been made to understand the dynamics of ballscrews and parametric models have been developed to aid machine designers in their task. Linear guides are identified as a nonlinear component which may benefit from greater research.

Accurate modeling of linear guides proves to be critical in modeling of the entire machine tool structure. Figure 2 depicts plots acquired across a set of linear guides during modal testing of a CNC machine. Each plot corresponds to a linear guide on the machine structure in the right side of the image. For example, the upper left hand plot represents data acquired on the upper left guide. These plots were acquired during sine sweep tests and are a comparison of responses across a linear guide. The plots were computed as follows: frequency response on the carriage side was subtracted from frequency response on side ‘b’. The plots were then normalized to determine the gain across the guide.

It is evident from the data that any model must involve, or be able to account for the frequency dependence of the guide. The linear assumptions fall apart first at approximately 200 Hz where a machine resonance exists. At frequencies greater than 350 Hz, the linear assumption becomes invalid.

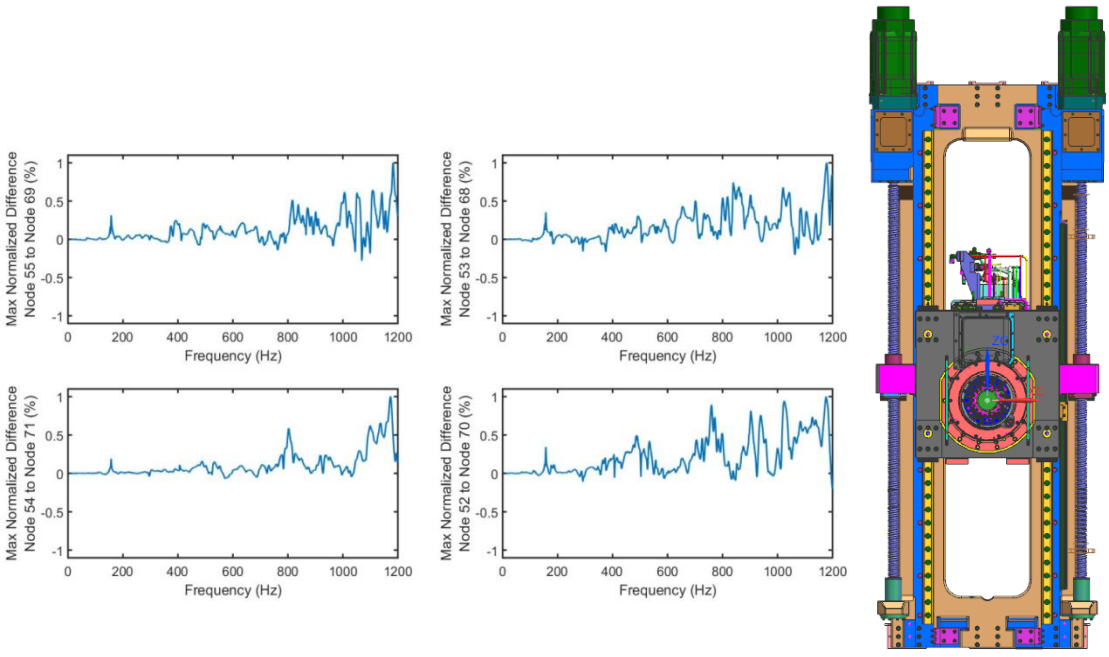

Figure 2 Deviation from linearity across the spectrum over linear guides. Each trace corresponds to a linear guide under a corner of the carrier to the right.

Research into modeling linear guides is varied and diverse. Models have been proposed which are analytically based, experimentally based, or utilize a combination of analytical and experimental techniques. This work pertains to the modeling of linear guides. Linear guides are meant to facilitate low-friction motion of machine axes across one another. Linear guides are very beneficial for machine tool development as they may be quickly replaced. The guides are modular. Linear guides also minimize maintenance requirements. As the guides come with a specified preload, they do not require tightening and adjustments as box ways do. Guides come in standard shapes and sizes and are very compact. Some examples of linear guides are given in Figure 3.

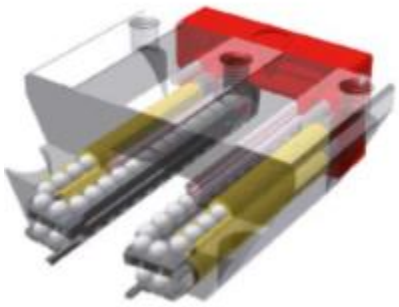

Figure 3 Linear guide section with rolling elements shown.

Linear guides are made up of two basic subassemblies: a rail and a truck. The rail possesses some load-bearing profile on which the truck rides. Manufacturers have varying paradigms on which rail profile is optimum. Linear Guides contain rolling elements: either balls or cylinders. The architecture of the rail is defined by the type of rolling element. The rolling elements recirculate through pathways in the truck block to facilitate lubrication and cooling. Linear guides are preloaded. There are various methods for preloading the guides which are beyond the purview of this work. The application of the preload means there is an initial strain on the system. This initial strain ensures that stiffnesses are better replicated from built-up assembly to built-up assembly. It also helps keep the guides from ‘dresser drawer-ing’ when a load is not applied at a central location.

For the purposes of this work, Schneeberger provided linear guides for testing. The novel test regime and model construction strategy are applicable to any type of linear guide. The scheme for construction and evaluation are also applicable to any nonlinear machine element. Future plans include utilizing the developed characterization and assembly scheme to model other nonlinear machine tool connections including ballscrew thrust bearings, ballscrew nuts, spindles, and table bearings.

Linear guides may be understood from two perspectives: quasi-static and dynamic. Quasi-static models are derived assuming negligible inertia effects. Numerous authors have published on the topic of modeling quasi-static nonlinear characteristics of linear guides. Popular quasi-static modeling techniques involve characterization of the guide by Hertzian contact or by Finite Element Model (FEM).

Quasi-static models have the advantage that they are entirely derived from the system physics. Measurements (aside from Hertzian coefficients) are not required to satisfy the model forms. The lack of measurement requirements is very useful to the analyst who is trying to predict system response for a machine in the design phase. Quasi-static models do not accurately account for the guide properties as a function of frequency. In order to account for guide stiffness and damping as a function of frequency, dynamic models are necessary.

A number of dynamic models for linear guides have been proposed. Dynamic models typically require some structure with physical linear guides to measure. Some dynamic models contain more physical intuition than others. Models developed are based on the Chebyshev Polynomial, Inverse Receptance Coupling, and Finite Elements.

This chapter will review current literature on modeling of linear guides. The models discussed are placed in logical order of simplest to most complex.

1.1 Assumptions of Present Models

Assumptions, though necessary in the construction of a mathematical model, often oversimplify the model and inhibit its deployment. Assumptions plague modeling of linear guides. Assumptions utilized in modeling of linear guides include:

Rigid blocks or rails

The guide block or rail may be assumed rigid. This does not allow for the truck to open or fold under high tensile or compressive loading.

Rigid rolling element set

Assumption of a rigid rolling element set attributes the entirety of the assembly stiffness to the guide block and rail. No attempt is made at quantifying the contact of the rolling elements.

Quasi-static behavior

Quasi-static indicates a mechanical process occurring at a strain rate low enough that inertia effects may be neglected. In the case of linear guides, quasi-static models neglect frequency dependent stiffness and damping.

Linear dynamic behavior

Linear dynamic models idealize the entire stiffness of the guide to a single stiffness value. This stiffness value may be easily incorporated in a dynamic finite element model.

Testing of a single guide is representative of testing of an entire platen

Models based on experimental data can be built based on the testing of a single guide. In typical structural application, guides are used in sets of two, four, six,

etc. Test regimes ideally excite the guide in the tensile / compressive direction when in practice the guides will be under combined loading.

Stiffness only in the direction normal to the platen

Certain models which have been proposed neglect the rigidity of the linear guide in all but the tensile / compressive directions. The linear guide also exhibits moment and lateral carrying capacities. Capturing the characteristics of the linear guide in the lateral direction becomes significant particularly when the guides are suspending structural elements on a wall.

1.2 Present Modeling Techniques

The first, simplest model considered is an orthotropic model of the linear guide. Guo et. al. proposes an orthotropic model [1] of linear guides. In this technique, the directional static stiffnesses of the guide are captured by the moduli which make up the matrix of Equation 1. This model has the capacity of describing the stiffness of the guide in all six degrees of freedom. An orthotropic model possesses a compliance matrix shown in Equation 1. The matrix relates directional strains to directional stresses by directional moduli. Note that in Equation 1 the rotational terms are not related to the translational terms.

$$\begin{Bmatrix} \epsilon_x \\ \epsilon_y \\ \epsilon_z \\ \gamma_{xy} \\ \gamma_{xz} \\ \gamma_{yz} \end{Bmatrix} = \begin{bmatrix} \frac{1}{E_x} & -\frac{\mu_{yx}}{E_y} & -\frac{\mu_{zx}}{E_z} & 0 & 0 & 0 \\ -\frac{\mu_{yx}}{E_y} & \frac{1}{E_y} & -\frac{\mu_{zy}}{E_z} & 0 & 0 & 0 \\ -\frac{\mu_{zx}}{E_z} & -\frac{\mu_{zy}}{E_z} & \frac{1}{E_z} & 0 & 0 & 0 \\ 0 & 0 & 0 & 1/G_{xy} & 0 & 0 \\ 0 & 0 & 0 & 0 & 1/G_{xz} & 0 \\ 0 & 0 & 0 & 0 & 0 & 1/G_{yz} \end{bmatrix} \begin{Bmatrix} \sigma_x \\ \sigma_y \\ \sigma_z \\ \tau_{xy} \\ \tau_{xz} \\ \tau_{yz} \end{Bmatrix}$$

Equation 1

where:

$\epsilon_x, \epsilon_y, \epsilon_z$	directional strains
$\gamma_{xy}, \gamma_{xz}, \gamma_{yz}$	cross strains
E_x, E_y, E_z	directional youngs modulii
$\mu_{yx}, \mu_{zx}, \mu_{zy}, \mu_{zx}$	Poisson ratios
G_{xy}, G_{xz}, G_{yz}	cross shear modulii
$\sigma_x, \sigma_y, \sigma_z$	directional stresses
$\tau_{xy}, \tau_{xz}, \tau_{yz}$	cross stresses

The authors derive terms relating directional moduli of Equation 1 to directional stiffnesses of a machine tool joint.

The authors validated the model against two blocks glued together at a mutual surface. The model was used to predict the first three natural frequencies with good results. Though the model yields a fast solution and exhibited good results in the test case, it suffers from a number of shortcomings.

The orthotropic model may account for directional stiffness, but it cannot account for nonlinear effects. A model of this format can neither account for dynamic or quasi-static nonlinearity. The entirety of the guide is reduced to a number of elements in the Finite Element Model (FEM), neglecting effects of rollers. Preload is captured by the model as a function of the stiffnesses used to compute the moduli. For the purposes of this work, the model is insufficient because of its frequency independence.

The orthotropic model, like many of the models proposed, is frequency independent. A more sophisticated model, which is still frequency independent, is computed on the precepts of Hertzian Contact.

Development of Hertzian contact models typically involves the assumption of rigid truck blocks and rails. This type of model attributes the entire compliance of the linear guide to the rolling element set. This inherently limits the model validity to low loading. It is typical for a CNC machine to experience very high loads, some machines being designed to sustain loads in excess of 10 kN. Under high loading such as this, the assumption that the entirety of the compliance is due to the rolling element set is not valid.

Figure 4 depicts a model for a ball roller guide [2]. The diagram was developed as the basis of the work done by Dhupia et. al. This model accounts only for the rigidity of the balls in the rolling element set. This model does not account for the change in contact angle the ball undergoes during loading and unloading. Critical values for the model such as ε and P_0 are determined by experiment. This model is formulated specifically for balls in the rolling element train. This model would require work to derive expressions for use with a cylindrical rolling element train.

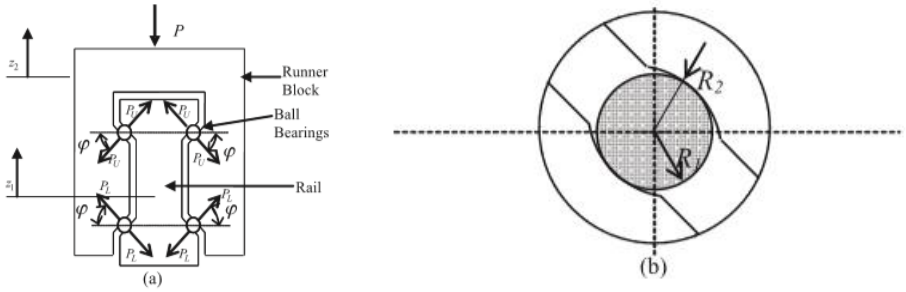

Figure 4 Ball roller guide mathematial schematic for model developed in [6]

The model proposed in [6] for relative displacement across the linear guides is given by equation (2). The authors account for the case of excessive load by augmenting the derivation for stiffness. Under conditions of excessive load, some rolling elements may lose contact with their track. This is an example of a model developed primarily for quasi-static purposes.

$$\boldsymbol{\Delta z = \left(\epsilon P_L^{\frac{2}{3}} - \epsilon P_0^{\frac{2}{3}}\right)\sin(\phi) = \left(\epsilon P_0^{\frac{2}{3}} - \epsilon P_U^{\frac{2}{3}}\right)\sin(\phi)} \tag{2}$$

The authors offer expressions of P_l and P_u which may be solved iteratively utilizing the load on the guide, P. With the knowledge of P_l and P_u, Δz may be determined.
The method described above accounts for only the normal translational degree of freedom of the guide. The authors do not attempt to characterize the lateral or rotational properties. It is also worthy to note this model does not account for the change in angle

Φ as load is added to the guide. Angle Φ will change based on the direction and magnitude of the load.

Adding to the work done by Dhupia et. al., Kwon creates a five degree of freedom model to account for the translational and rotational stiffness [7]. The researchers utilized coupled simulation methodology in which they determined the guide distortion attributable to the rolling elements and the associated reaction loads. The reaction loads were then applied to a Finite Element Model (FEM) and the total distortion computed. The researchers exemplified the importance of including the effects of carriage rigidity, as shown in Figure 5. It is visible from their FEM that the carriage will tend to spring open under load.

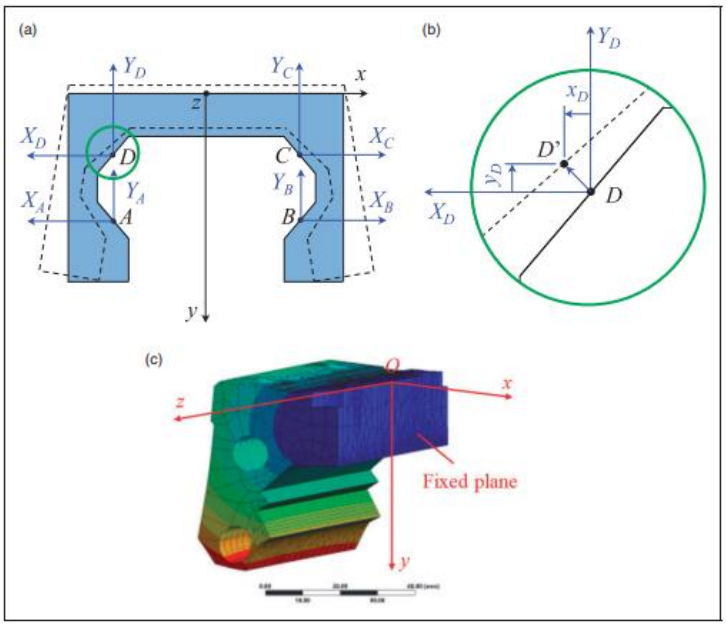

Figure 5 Distortion of linear guide under load [7]

This model is capable of accurately capturing the quasi-static properties of the linear guide, but results were not reported on its accuracy in depicting the frequency dependence of the linear guide. Kwon describes the importance of considering preload in mathematical stability of the guide models. Models with low preload had convergence and stability issues, whereas models with higher preload possessed smoother results. Outputs from the proposed model were compared against a commercial program

developed by a bearing manufacturer. Correlation testing on physical guides was not accomplished. The model proposed by Kwon *et. al.* predicted the stiffness characteristics of the linear guide with the same success as the commercial program.

Rahmani and Bleicher performed experiments on a set of linear guides to determine normal and angular stiffness characteristics [8]. The authors developed a test arbor with which to load and measure the linear guides. The arbor and some distortion plots from their work is shown in Figure 6.

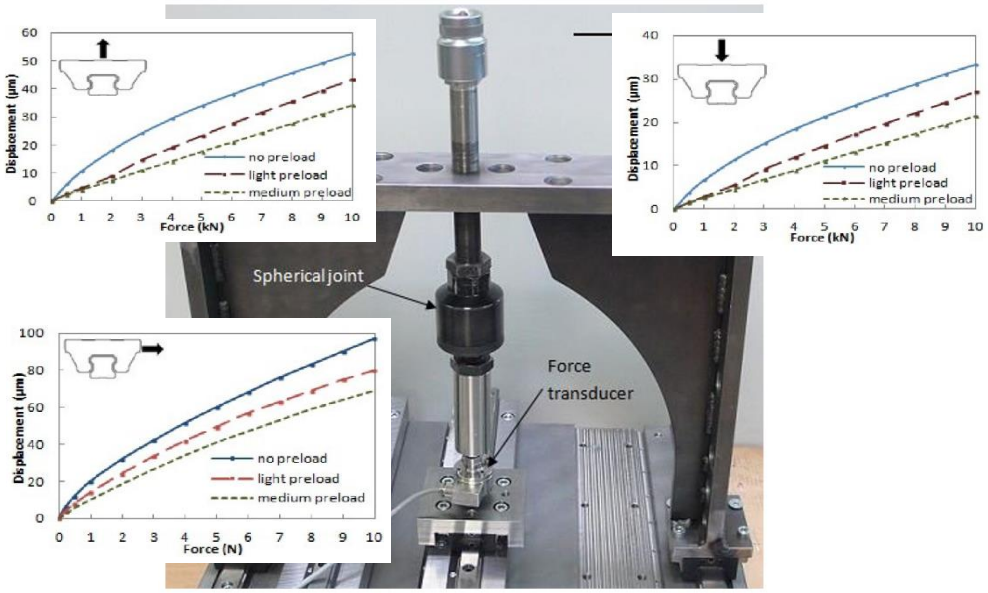

Figure 6 Linear guide test arbor and results [4]

The test rig consisted of an arbor between which three linear guides were tested. The authors were able to successfully measure the static stiffness characteristics of linear guides of varying preload. They found nonlinear behavior was more prevalent in linear guides with lower preload. Rahmani and Bleicher were also able to measure pitch and yaw characteristics of linear guides. They proposed a model for the linear guides based on Hertzian contact and found the analytical model to be 30-35% stiffer than the measurements. The authors used the Hertzian model for normal stiffness only, not lateral, pitch, roll, and yaw.

Yet another methodology for simulating linear guides is CoFEM, or Component Oriented Finite Element Modeling [9] [9]. The CoFEM methodology involves creation of FEMs of the sub-components comprising a structure. Examples of meshes on the various sub-components are shown in Figure 7.

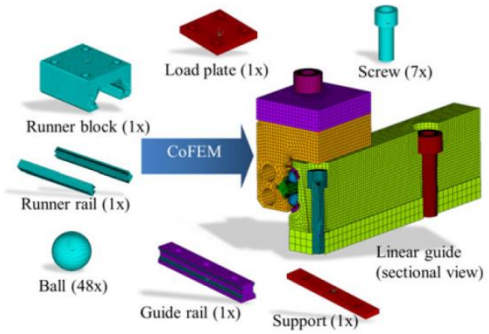

Figure 7 CoFEM building block representations. Each item circling the assembly to the right is a sub-component which is instanced to build the full model.

The CoFEM methodology was experimentally validated with a static and dynamic data set. Three models were developed and compared for computational efficiency and accuracy. The first model considered involved rigid balls in the rolling element train. The modulus of the elements surrounding the balls (the contact region) was modified to match the equivalent elastic modulus. The authors define equivalent elastic modulus based on Hertzian theory. The authors found this method to be highly accurate but computationally intense. A comparison of results between the RiBEM approximation and the full model is shown in Figure 8.

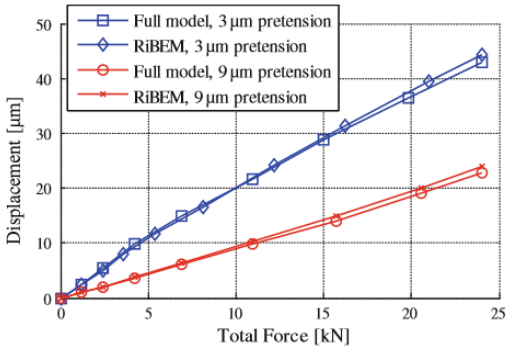

Figure 8 Comparison of RiBEM modeling methodology to full FEM [9]

Due to the computational intensity of the RiBEM method, Dadalau et. al. proposed two more levels of abstraction: RoCS – Rolling Contact Spring, and FiCS, Fixed Contact Spring. The rolling contact spring model applies a pretension element in conjunction with a stiffness element to approximate the contact characteristic of the balls in the guide. As loading on the guide varies, the angle of contact changes.

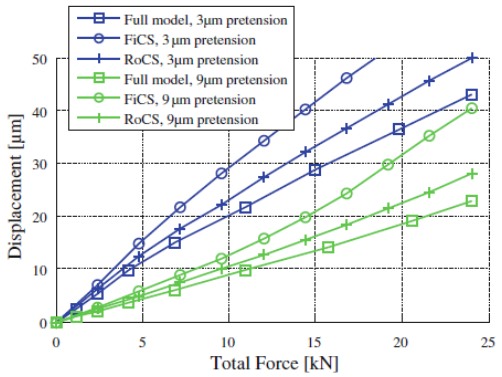

Figure 9 Comparison of CoFEM modeling schemes [6]

The Fixed Contact Spring model does not account for rotation of the balls under loading.

Dynamic testing consisted of developing an ingenious test rig which provided inertia to excite the guide in all degrees of freedom (DOFs). Results obtained by the CoFEM method were very agreeable. The model was able to accurately predict natural frequencies and stiffness characteristics of the testbed.

Two shortcomings are evident from this modeling methodology. The first is the large number of DOFs required to accurately represent the guide. Though this model was able to accurately predict natural frequencies of a guide in an assembly, the solution time was very long. Secondly, the validation testing involved only a single guide. As stated previously, guides are typically applied in a series. A benefit of the CoFEM methodology is its predictive nature. Guides need not be tested in order to determine model coefficients.

Dhupia *et. al.* developed a model based solely on test data [6]. The authors fit a Chebyshev polynomial to data acquired from shaker testing. The Chebyshev polynomial

was of the form of Equation 3. The results for the computed restoring force surface are shown in Figure 10. The authors utilized a 100 lbf shaker exciting a single linear guide in the direction of pull. The limitations outlined previously also apply to this model. A single guide is tested in isolation, and in a single direction. Furthermore, this test scheme utilized an electrodynamic shaker which precludes application of static preload. The guides will be under some static preload during operation due to the weight of machine tool axes.

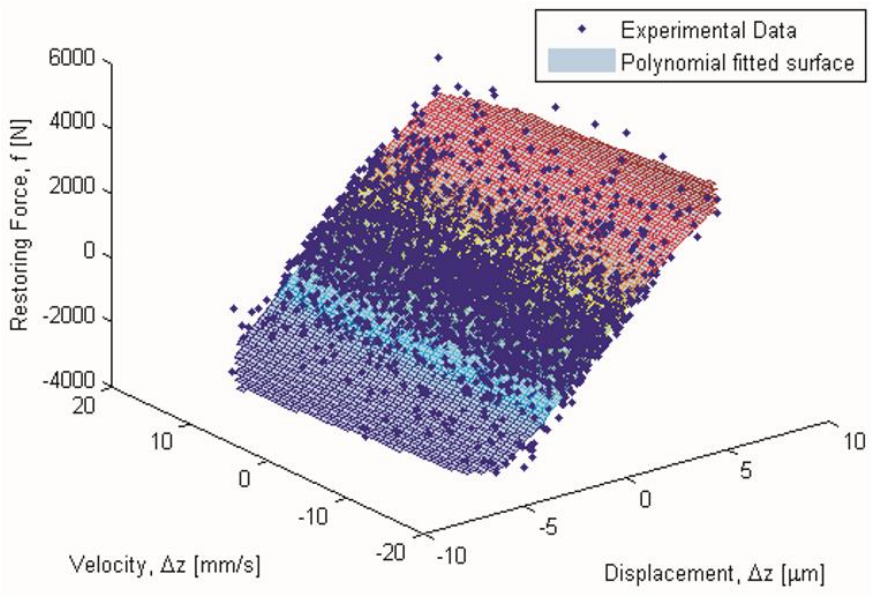

Figure 10 Data curve fit to parametric surface [6] for use with modeling the linear guide.

$$f(\Delta z, \Delta \dot{z}) = \sum_{i=0}^{N_x} \sum_{j=0}^{N_y} C_{ij} T_i(\Delta z) T_j(\Delta \dot{z})$$

Equation 3

where the coefficients are functions describing the surface.

Returning to a model based on Hertzian contact, Kong *et. al.* proposed a more sophisticated methodology utilizing concepts of nonlinear dynamics such as the Incremental Harmonic Balance Method (IHBM) to study linear guides [10]. The

Harmonic Balance Method (HBM) was used to compute a variety of Frequency Response Functions (FRFs). The various FRFs were computed for varying mean and alternating loads on the guide.

The proposed method assumed the carriage and rail to be rigid. Kong *et. al.* made a meticulous analytical study of various design characteristics of the linear guide. Design features such as preload, number of rolling elements, and rolling element contact angle were investigated. Accommodation was made in this model for variation of ball contact angle under loading. A predominant theme of Kong's study was the determination of the threshold displacement. The threshold displacement is the inflection point between the piecewise nonlinearities.

Altering design parameters (roller quantity, contact angle, etc.) it was observed that threshold displacement and system stiffness could be optimized. System stability was also discussed in detail by investigation of eigenvalues. Study of the eigenvalues determined what type of bifurcation the linear guide would experience and hallmarked when the system was entering a chaotic region of the response.

The final modeling methodology discussed involves Receptance Coupling Substructure Analysis (RCSA). RCSA and Inverse Receptance Coupling Substructure Analysis (IRCSA) have gained significant popularity in modeling of machine tool spindle – tool holder – tool systems [11] [12] . The IRCSA method yields an FRF to describe the joint. Approximating the joint as an FRF is very advantageous as the frequency characteristic of the joint may be captured.

RCSA modeling methodologies typically involve assembling components with their FRFs in a cascading order. Figure 12 depicts the cascading nature of RCSA computations. Using the terminology from [11], in the first stage, the framework and ram are coupled. The machine in question has a quill (ram) that feeds out towards the work. The framework possesses the guides which connect and provide axis motion of the ram. In the second stage, the framework-ram are connected to the column. In the third stage the column-framework-ram are connected to the base. The components are coupled based on compatibility conditions which are enforced.

The assembly sequence is described above. Characterization of the linear guide occurs in opposite order of the assembly sequence. Stiffness and damping are assumed for a single joint (linear guide). Equation 4 is used to describe the extracted joint. This represents the joint as a SDOF system in x, y, and z as noted in the subscripts on the diagonal of the matrix. More degrees of freedom may be utilized to describe the joint requiring more measurements on the structure. With substructuring techniques of this type, more measurements will tend to increase numerical noise in the coupling algorithm and degrade results. In Equation 4, *k* denotes stiffness, *c* denotes damping, *i* is the complex operator, and *w* is the evaluation frequency.

For measured data, the nonlinearity is implicitly included in the FRF. The fact that the nonlinearity is present in the FRF makes this a popular methodology. Use of a particular data set makes the assumption that the nonlinearity possesses the same influence regardless of excitation level.

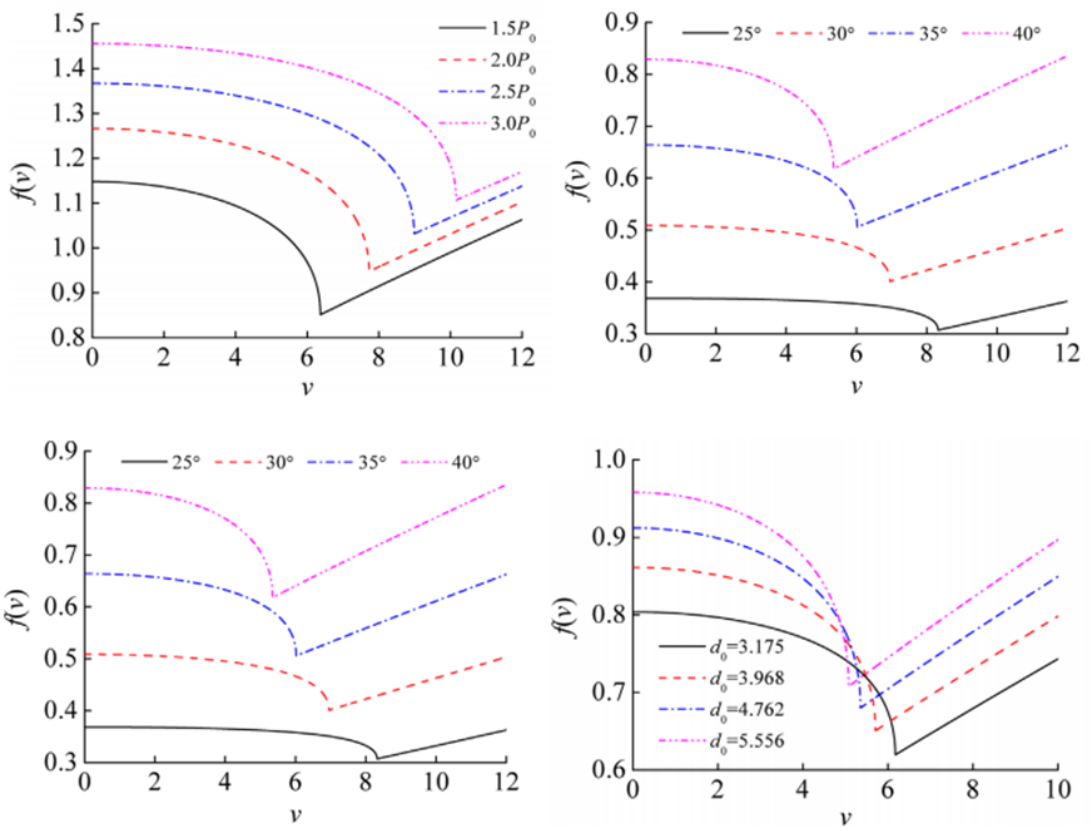

Figure 11 [7] Study of inflection points for varying linear guide designs.

$$\left[H_{n_{j)}}^{J_j}\right] = \begin{bmatrix} \frac{1}{k_{J_j n_j)_x} + i * c_{J_j n_j)_x} * w} & 0 & 0 \\ 0 & \frac{1}{k_{J_j n_j)_y} + i * c_{J_j n_j)_y} * w} & 0 \\ 0 & 0 & \frac{1}{k_{J_j n_j)_z} + i * c_{J_j n_j)_z} * w} \end{bmatrix}$$

Equation 4

where

H is the transfer function
k is a stiffness parameter
c is a damping parameter
w is a frequency parameter

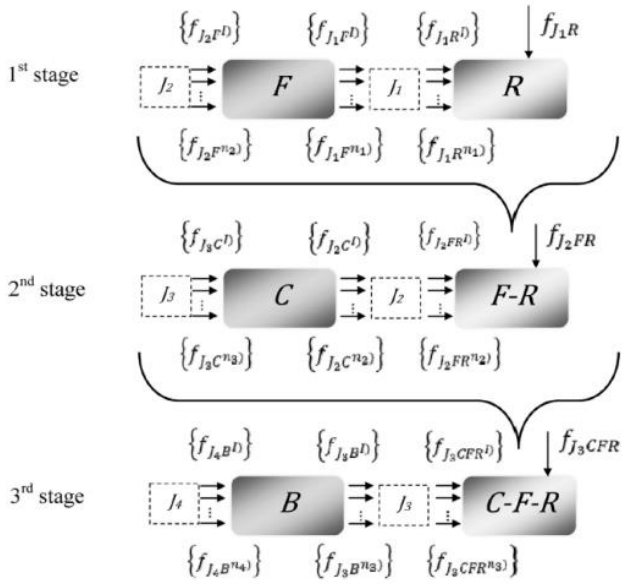

Figure 12 [11] Example of how RSCA is utilized to model machine tools. The assemblies must be cascaded together.

It is of paramount interest to achieve a fully accurate model of a CNC machine for predictive use. Machine tools are comprised of linear substructures (columns, rams, platens) the dynamics of which are easy to predict. Complexity is introduced when predicting the dynamics of a built up machine tool structure due to nonlinearity and damping introduced in joints. Joints in machine tool structure are more sophisticated and require more advanced treatment than those in typical structures because joints in machine tool structures facilitate motion. The dynamics of the machine tool structure may vary greatly based on the axis position, adding yet more difficulty to accurate prediction of dynamics.

The discussion in this chapter has centered on linear guides. Linear guides are the joint which facilitates linear motion between two axes of a machine tool. Present modeling techniques have been reviewed and their inadequacies discussed. Future work will rely on the precepts of nonlinear dynamics to characterize linear guides. The work will concentrate on determining the form of the nonlinearity. The Acceleration Surface Method (ASM) is proposed for determination of the nonlinear form. Once the form of the nonlinearity associated to the linear guides is established, its parameters are to be

determined. A proper FEM may then be constructed with minimal dimensionality for use in machine tool simulation. Initial testing and modeling is to be done on a test stand developed to isolate the dynamics specific to the linear guides. Once the guide model is developed, it is to be deployed and validated against the test stand and against a commercial high-production CNC machine.

1.3 Conclusion

Linear guides have been the subject of some study. An accurate, appropriate model of linear guides is crucial due to their function in machine tools. Current work has been heavily centered on analytical modeling of guides and comparison with given commercial software. Many of the current modeling methodologies are quasi-static, meaning they do not take into account the dynamics of the linear guide. The aim of the subsequent work is to develop a test-based model of linear guides. This model would account for the quasi-static nature of the guides as well as their dynamic properties.

The work presented in this dissertation develops a novel test-based model for linear guides. The methodology presented may be utilized to couple machine tool linear substructures with nonlinear connections. The methodology may be extended for use in modeling spindles and other systems with bearings.

Additions to the field include:

Advanced testing of linear guides in a practical setting

A test stand is proposed which exemplifies the practical application of the guides. The test stand is designed so the guides are excited as though they were operating on a machine tool. Similar mode shapes are experienced by the test stand as those exhibited by machine tool axes. As highlighted above, the majority of existing work tested the guides individual. The existing work did not conduct a thorough investigation of the guides in a realistic setting. In addition to the realism presented by the test stand, practical industrial

equipment was utilized in the work. This included a servohydraulic shaker and modal mallet.

Proposed 5 DOF model of the linear guides

Further definition is provided in following chapters of this idea. The linear guide exhibits stiffness in all axes except the axis of motion. Rigidity is provided by a ballscrew or linear motor in the axis of motion. A 5 DOF model is presented in this work which includes linear and nonlinear coefficients.

Coupling technique utilizing nonlinear methodologies to compute frequency response functions

Previous work has focused on utilizing nonlinear methodologies to solve the guides. This work concentrates on utilizing nonlinear methodologies to solve the system. The end goal is to achieve an accurate FRF which may be handed to a program for use in calculating stability. The guides are simply a stumbling block to achieving the FRF. Recognizing this fact, the model of the guides must be simple enough to roll out and not confuse itself in the larger suite of calculations.

A commercially viable solution

There are other methodologies for solving nonlinear problems in structural dynamics. Most do not achieve the commercially deployable goal. In the research of this work, one of the more promising opportunities was the use of IWAN elements in the model to account for nonlinearity. The IWAN elements could be parameterized to account for the effects discussed in the next chapter. Commercially available code (except code developed for use with Sandia National Laboratories) has no capability of modeling with IWAN. This work proposes an elegant solution which may be used simply alongside commercial codes. In this work, a minor transition to MATLAB is required for computation of the FRFs. Given the NL_Vib code utilized, when deployed, the

practitioner need not have advanced knowledge of methods for solving nonlinear problems.

2 Model Construction and Baseline Testing

To create a proper model, some baseline testing was conducted. The procedure used towards development of the model took a two-path approach. A FEM was created alongside physical hardware. The FEM was utilized for transducer placement optimization. A detailed discussion of the baseline FEM is given in this chapter. The baseline testing is also discussed in this chapter. A discussion is provided on the high stiffness and damping of machine-tool elements with respect to modal testing practices.

2.1 Test Stand Development

The test stand was developed specifically to exemplify the practical use of linear guides. The guides were installed most similarly to their field application. Linear guides are typically applied in sets of two, four, six, etc. The test stand was developed to accommodate four or six linear guides. Testing was completed with both configurations. Figure 13 gives an example of a linear guide with the degrees of freedom labeled.

Guides exhibit stiffness in five degrees of freedom:

- tension and compression (k_x)
  Please note that in practice, the guides exhibit different values for k_x in tension as opposed to compression. The baseline linear models discussed in this chapter were incapable of accounting for the non-linear stiffness. This will be addressed in a later chapter.
- lateral (k_y)
- axial (k_z)
- rotation about axis of motion (r_z)
- rotation normal to plate (r_x), and
- rotation about lateral direction (r_y)

No stiffness was assumed in the model for k_z. The axial stiffness (k_z) is minimal compared to the lateral, tensile, and rotational stiffnesses and was neglected. In standard practice, the properties along the axis of the guides are determined by the means of linear motion. The means of linear motion is typically provided by a power screw or linear motor. The procedure utilized in this work may be utilized to characterize ballscrews or linear motors.

Given the dimensions of the linear guides, the five active DOFs must be accounted for. The linear guides are relatively long compared to their width. This indicates that moment reactions from the rolling set are not negligible. This work finds it critical to include rotational degrees of freedom for an accurate model of the guide. In practice all DOFs of a guide will be exercised. Lumping all stiffnesses into only lateral and tensile values leads to inaccurate estimation of mode shapes and natural frequencies.

Considering the importance of rotational degrees of freedom, they are extremely difficult to excite, measure, and quantify. Whereas translations can be measured directly, rotations must be measured indirectly. It is not possible to measure the most sensitive locations for rotation because they are often inside the bearings. To that end, rotational degrees of freedom must be extrapolated or interpolated based on translation data. For the purpose of this work, the rotational degrees of freedom were utilized to tune the model. Very good results were obtained on this basis. Rotational and translational degrees of freedom were utilized in a model updating scheme described in a later section.

The purpose of this work is to develop a five degree of freedom model. The five degree of freedom model was to lump the parameters particular to each direction. The rotational degrees of freedom were utilized to increase MAC with extracted test modes. Tuning also was used to minimize the relative difference between experimental and analytical natural frequencies. It was not the desire of this work to account for all of the minute physics of the linear guide. Previous attempts have been made at capturing the full physics of the guide. These full-physics models lack the capability of use in a built-up structure. The purpose is to guide the research towards an accurate fast-solving model which may be utilized for making engineering decisions.

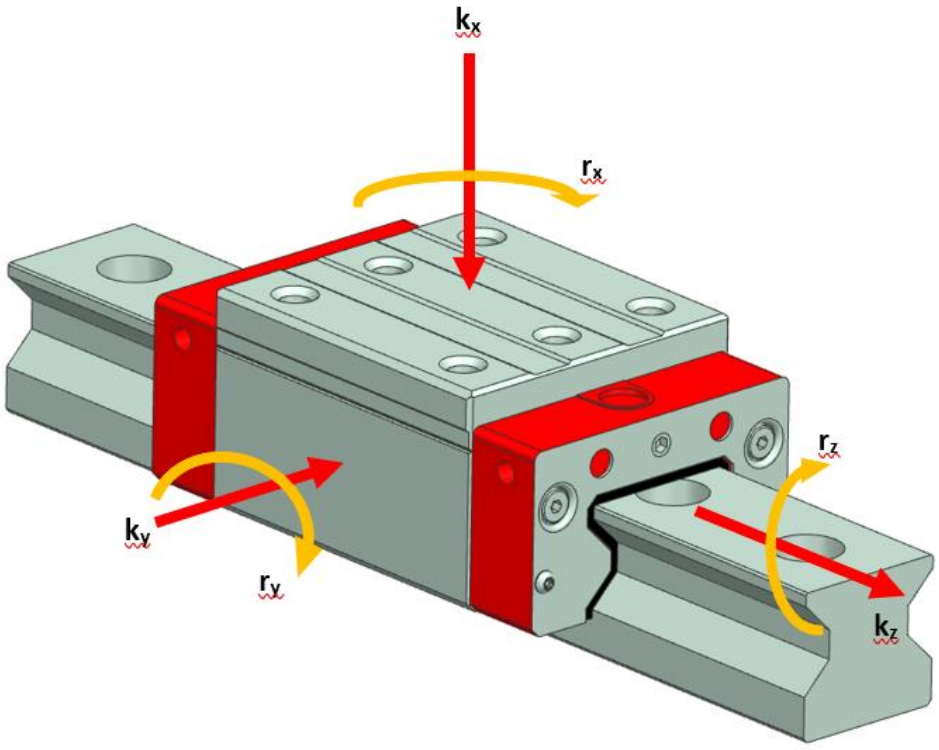

Figure 13 Degrees of freedom of a linear guide expressing stiffness.

The test stand was arranged in such a way that the top plate would exhibit flexible dynamics, yet be rigid enough to be representative of a machine tool. In order to limit the

dynamics introduced to the system by the lower bracket, it was bolted to a rigid machine base. This type of arrangement is common with machine tool dynamics. Figure 14 shows an image of the test stand which was utilized to study the linear guides. The gray base to which the test stand was mounted was leveled to the floor. The base was of ductile iron construction with heavy internal reinforcement.

Further detail on acquisition of driving point measurements is shown in Figure 15. The center of the plate was utilized (flagged as 4079, the node number for the FEM) as a driving point for measurements normal to the plate. Measurements lateral to the plate were acquired at position 4068. 4079 was chosen to excite the flexible shell bending modes. 4068 was chosen to excite the rigid body mode where the upper plate twisted over the lower plate.

The test stand is free to move in the axis of the tucks. Primary resistance to motion is due to friction induced by the weight of the plate above, preload within the guide bearings, and viscous effects.

The test stand was excited by several means which are covered later in the text. The first critical task performed was to build a baseline FEM and determine optimum locations to place transducers. Nodes in the vicinity of the guide truck were connected to a common point utilizing CBUSH elements. CBUSH spiders were utilized to distribute the effect of the truck out over its proper surface without introducing spurious stiffness to the system. CBUSH elements were utilized as opposed to RB3 (interpolation) elements for the purpose of export to MATLAB. NASTRAN eliminates DOFs when constrained. It is critical to maintain the DOFs by not using MPCs or constraints when exporting. Stiffness elements are preferrable to maintain the full system matrices for import and use with MATLAB. MATLAB codes developed by other firms may be able to handle the missing DOFs. The MATLAB code developed for this work relied heavily on the boundary matrices which NASTRAN can be set up to export.

Figure 14 Image of the test stand utilized to characterize the nonlinearity of the linear guides.

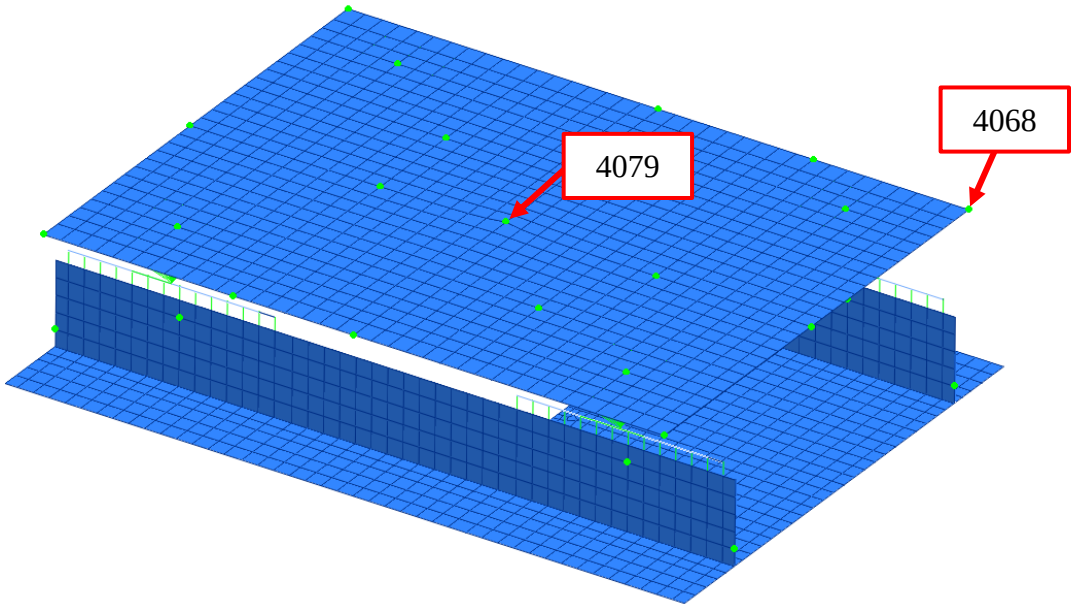

Figure 15 Image of test stand with driving points indicated in red boxes.

The test stand was abstracted utilizing shells, beams, and stiffness elements. This abstraction was done foreseeing the solution techniques downstream. While solid elements are capable of reproducing the geometry with high fidelity, they are computationally costly and do not yield many parameters for tuning and updating the model. The DOFs for computation were to be kept to an absolute minimum due to the solution techniques planned for the nonlinear portions of the problem.

Holes were idealized out of the model. For the model, effects of the joint between the guide and plate are assumed negligible. Based on the analyst's experience with structures of this type, the bolt spacing is close enough to enforce a linear connection when properly torqued. Energy levels for excitation were too low to drive the joints nonlinear. This is the typical case for industrial machinery. The base frame, to which the guide rails are mounted, is a weldment. The weldment was developed to ensure full penetration of the weld bead between the individual components. The full weld penetration ensured the most linear behavior possible.

The model utilized several types of elements. Primarily, shell elements were utilized. Shell elements approximated the top plate and lower structure. The shells were all linear. In order to ensure ample properties for update, the attachment from the lower structure to the machine base was simulated by 0D stiffness elements. These elements work to apply a stiffness at the indicated notes. The stiffness is indicative of the joint between the assemblies. The nonlinear elements were approximated by 6DOF stiffness elements. The 6DOF elements were connected with stiffness spiders to the plate and the lower assembly. The spiders approximated the physical size of the linear guide truck at the interfaces. The elements and their sizes corresponded to good correlated models of the structure.

The test stand was bolted to a cast iron machine base. The bolts connecting the test stand to the machine base are spaced to ensure the most linear connection with constant contact. Bolts were tightened using a torque wrench. The torque applied represents the guidelines of the bolt manufacturer. The torques for various bolts may be found in Appendix A.

The machine base, shown in Figure 14, was assumed to be rigid and was not included in the model. It was observed that inclusion of the machine base was not significant to obtaining an accurate model. The machine base was significantly more rigid than the surrounding structure and did not have a strong influence on the acquired measurements. The structure of the base was heavily webbed with thick side walls. The side walls were reinforced with more webbing to the central structure.

A discussion was just had on the full system. The discussion contains some observations made during testing of the full system. Prior to the assembly of the hardware, each individual component was tested.

2.2 Models of constituent components.

Creation of an accurate nonlinear model necessitates accurate component models. The major component contributing to the flexible modes was the top plate. To ensure the data being fed to the nonlinear model was correct, the top plate was tested as outlined below. Impact testing was conducted, and mode shapes were extracted. The mode shapes were compared with those computed by the FEM. The constituent models were then tuned. The underlying assumption was that the constituent structures behave in the linear regime. This assumption is proven valid by the testing.

The top plate of the test stand was tested independently prior to installation to the linear guides on the lower structure. Figure 16 depicts the model used for correlation testing. Impact testing was performed for the sake of parameter extraction. The test plate was suspended from multi strand v-belts to provide unconstrained boundary conditions. The suspension frequency was validated as being less than 10% of the first flexible natural frequency of the plate. It is important to consider the weight of the plate juxtaposed against the supporting system.

Figure 17 depicts the MAC between the mode shapes extracted from the test and from the FEM. The MAC showed good agreement between the test and the model. To maximize the MAC, it was found that alteration of FEM model parameters was not necessary. The MAC was maximized by offsetting the DOFs pertaining to the test by half the thickness above the plate. This was necessary because the FEM considered the top plate as a midsurface. The actual transducers were placed on the surface of the plate. Being on the top surface of the plate made the transducers more subject to translation along the axis of the plate. To be clear, the MAC was enhanced by improving the physical fidelity of the correlation model as opposed to altering mechanical parameters (mass, density, modulus) of the finite element model.

The MAC agreement achieved was greater than 90% in all cases and the observed sequence of modes was respected. Figure 17 shows the mode for mode agreement of the test data and finite element data.

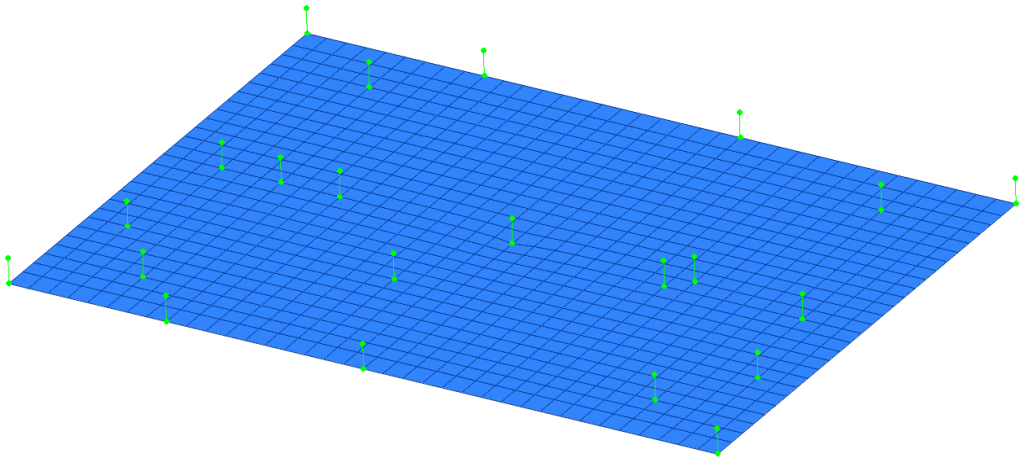

Figure 16 Correlation model representing modal test of top plate.

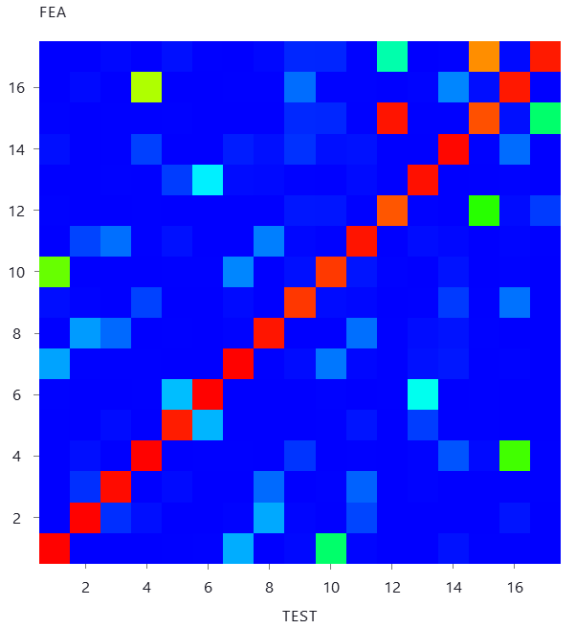

Figure 17 MAC between experiment and analysis.

Figure 18 shows a comparison of FRFs from the test and simulation. Qualitatively, the comparison of driving point FRFs matches up very well. The damping assumptions made in the model were accurate based on the relative shapes and amplitudes shown in the figure.

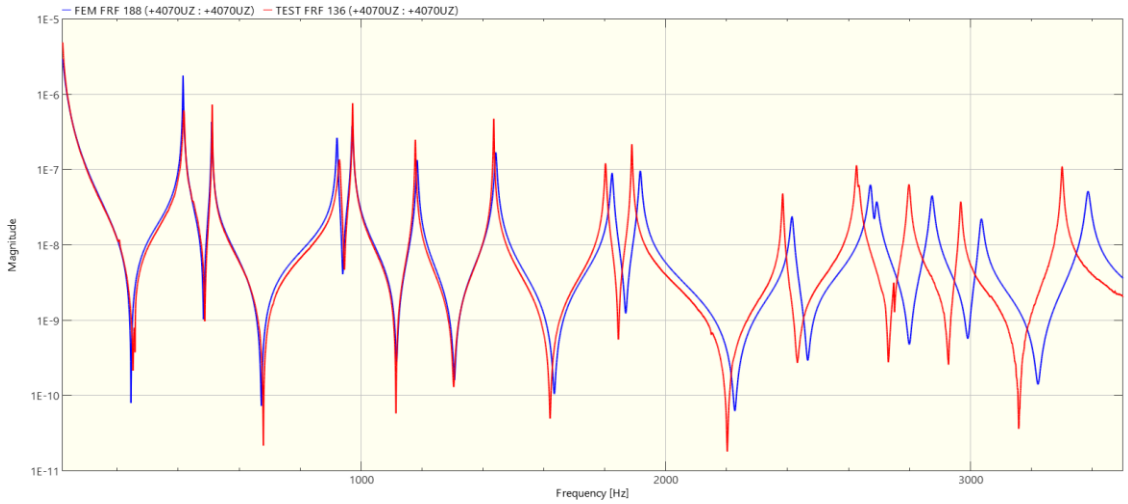

Figure 18 Comparison of driving point FRFs (red FEM, blue Test).

Figure 19 displays the correlation metrics for the FRFs. The correlation metrics account for all measurements acquired normal to the top plane of the plate. The correlation metrics show a good match, except in the immediate vicinity of resonant frequencies. Immediately at resonant frequencies, agreement between the measured and computed FRFs drops off. The agreement also drops off at frequencies greater than 2 kHz.

The degradation in correlation was due to the additional stiffness presented by the formulation of the elements. The higher-order modes require more flexibility to accurately depict. The inaccuracy was not in the bandwidth of interest, so was not further investigated. Higher order modes rarely affect machine tools or machining. In the engineer's experience, structural modes lower than 800 Hz are critical and spindle modes up to 3 kHz are critical. Certain cutting operations can excite higher order spindle modes and cause chatter conditions. These operations do not have enough energy to excite through the spindle into the structure.

To establish a more accurate model at higher frequencies, a thorough study of the formulation of the connections between shell elements must be conducted. Because this work was targeted towards the lower structural frequencies, study of the higher order modes is beyond the present scope.

It did not require significant effort to achieve correlation between top plate simulation and experiment. It is reasonable that simple correlation could be achieved with a model such as this. The top plate model was developed to not introduce complicated dynamics. This was done to ensure the guides could be more thoroughly studied without spurious dynamics from the top plate. The top plate was a dimensionally held at the edges by milling and was Blanchard ground for precise thickness.

Though the top plate was simple to model, and very good correlation was achieved, the remainder of the system presents difficulties. A reduction in model size was examined in an effort to keep solution times within reason.

Reducing the Model Size

In addition to the basic correlation testing conducted on the top plate, a convergence study was performed. A study of the natural frequencies was conducted based on the mesh size applied to the top plate. The plate was unconstrained for the purpose of the study. Meshes were built with element sizes ranging from 300 mm to 1 mm. Figure 20 shows the results for the convergence study. The modes in the band of interest converged with a mesh size of approximately 50 mm. The criterion was a change in natural frequency of 5% or less from the previous size.

For the final assembled model, a 50 mm mesh was applied to the top plate. Figure 21 depicts the comparison of natural frequencies between the FEM and the test. The natural frequencies align well for the 50 mm mesh. Figure 22 depicts the MAC between the mode shapes computed using the 50 mm mesh and the test. The MAC was very good between the test and simulation.

With an agreeable model for the top plate, the system was assembled and a model of the full system was attempted. The next section reviews the acquisition of data for deriving the type and strength of nonlinearity associated to the linear guides.

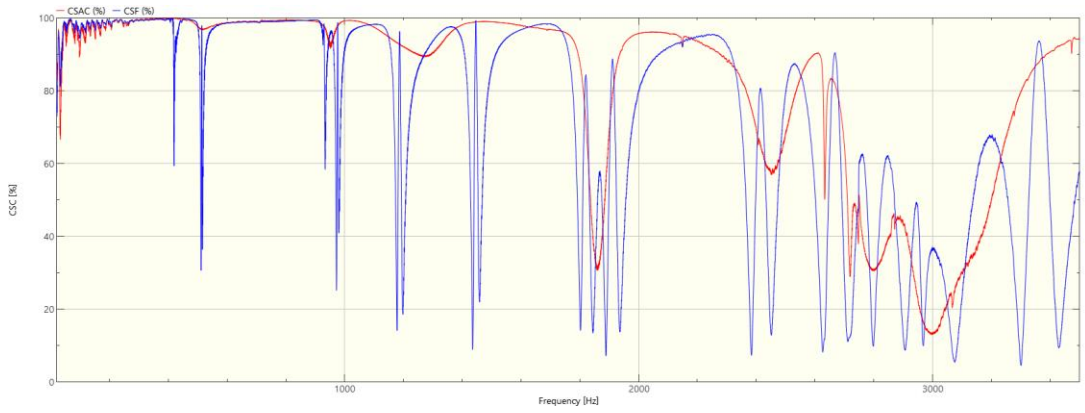

Figure 19 Correlation criterion for FRFs. Comparison of test data and analysis.

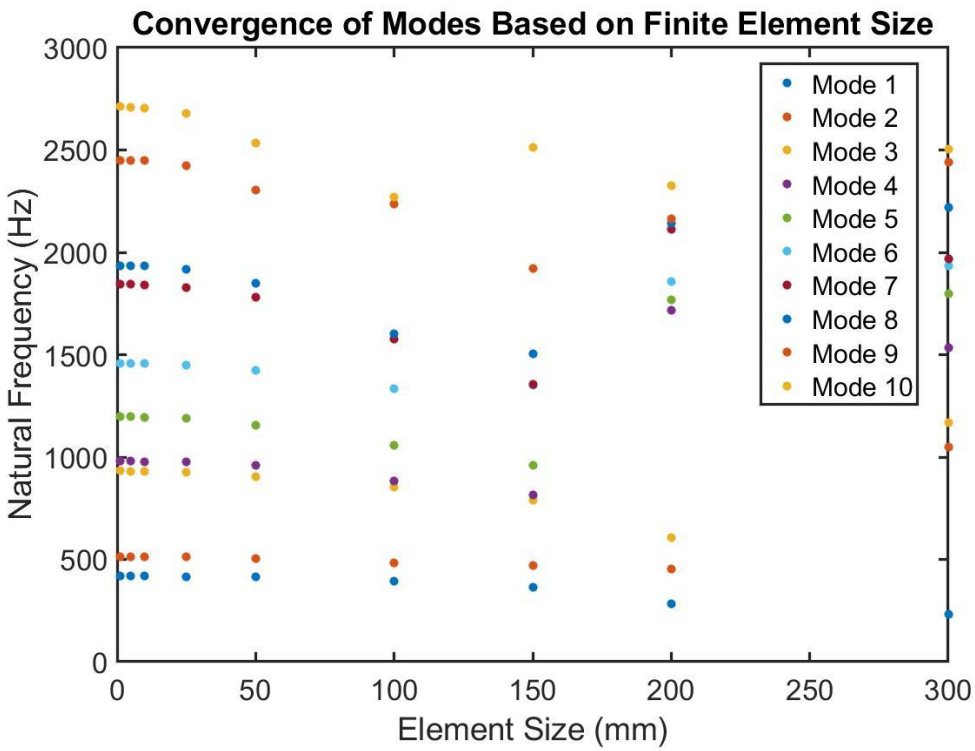

Figure 20 Element size vs. natural frequency convergence study.

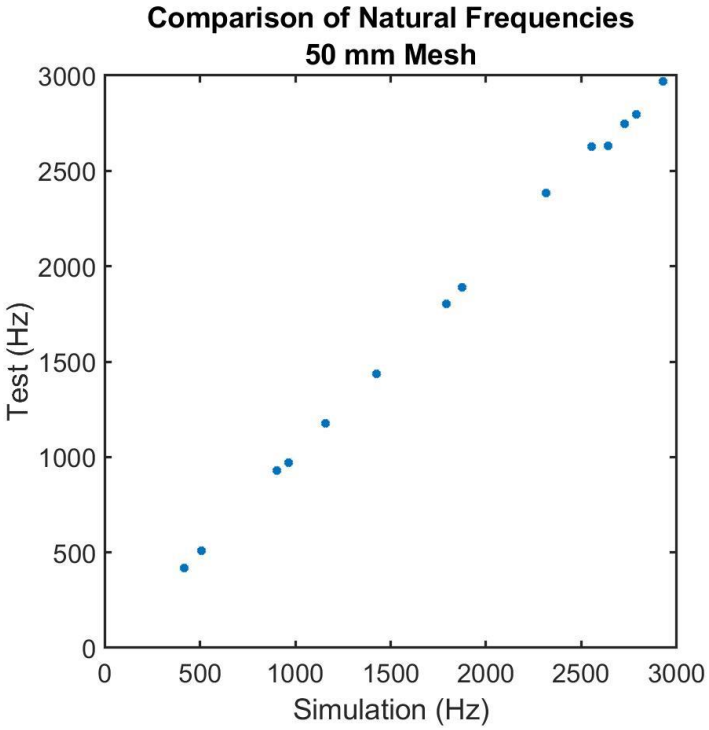

Figure 21 Natural frequency agreement between simulation and test.

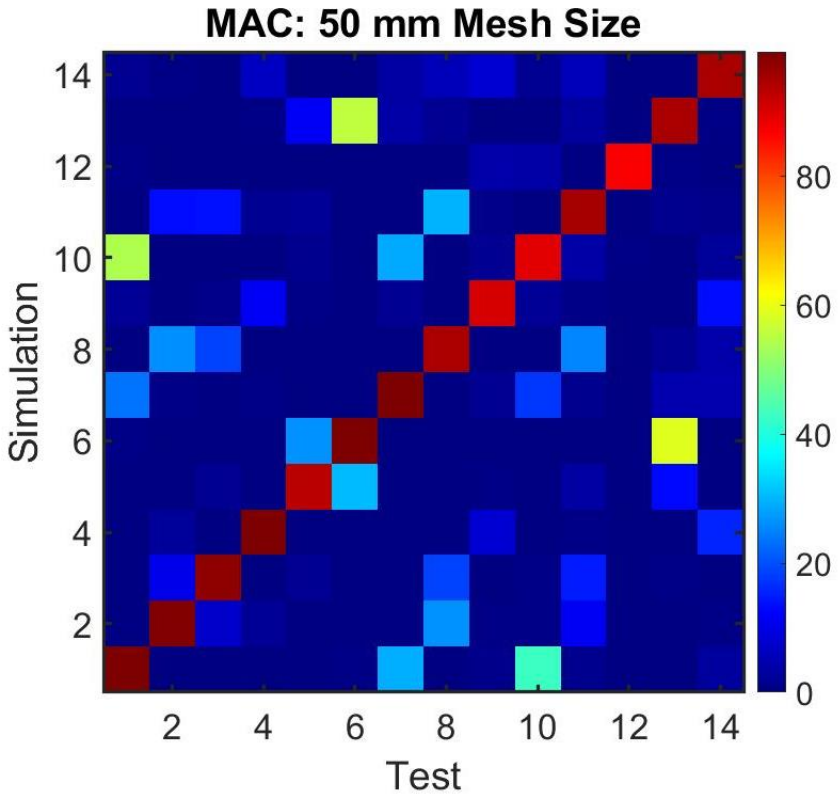

Figure 22 MAC between simulation and test for 50 mm mesh size.

2.2.1 Model of Guide

Previously attempted models of the linear guides were presented in Chapter 1. Commercially viable models of the linear guides are presented in Chapter 3. For the purposes of this work, it was critical that the guide be represented by a lumped parameter model with five degrees of freedom. Efficiency and compactness were desired from the model. More than five DOFs would violate the intent of the engineer to develop an efficient model. Each degree of freedom was to represent an axis of translation or rotation in which the guide exhibited some rigidity.

2.3 Test Procedure

The linear guides were subjected to a thorough test regime complete with varied methods of excitation. The goal of the work was to utilize modern nonlinear techniques for modeling the system. Significant effort was put forth to test with varying excitation strategies. Different nonlinear techniques require different types of data for their characterization schemes. The rigidity of the test setup renders some of the test regimes less effective. The work conducted here was able to determine which test regimes produced good results and therefore the corresponding identification algorithm could be

utilized, and which produced marginal or poor results rendering the corresponding identification algorithm unsuccessful.

Equipment utilized to test the linear guides included:

- 1000 lbf servo-hydraulic shaker
- 100 lbf voice coil shaker
- Modal hammer
- Modal mallet

The varied test setups were attempted for utilization with different forms of nonlinear parameter extraction. With the presentation of each excitation scheme, strengths and weaknesses are herein discussed. Along with the strengths and weaknesses, light is also shed on what was learned about the structure.

Two concepts which have received significant attention in the literature are ASM (acceleration surface method) and FNSI (frequency domain nonlinear subspace identification). The hope of this work was to follow a parallel path to the literature and utilize ASM to identify the form of the nonlinearity and FNSI to characterize the nonlinearity. Put differently, FNSI would be utilized to extract the nonlinear coefficients. The success of this is presented in two parts below with the respective excitation regimes.

Two forms of testing are required to accomplish ASM and FNSI. This is to say that the portion of ASM is presented with swept sine testing and FNSI is presented with broadband testing. A simple Single Degree of Freedom System (SDOF) is presented to exemplify the points made.

$$1e5\sin(\omega t) = \ddot{x} + 3\dot{x} + 2e6x - 1.6e5x^3$$

Equation 5

where:

x is displacement
ω in angular frequency
t is time

This system will be utilized to help understand some important strengths and drawbacks for each excitation regime.

2.3.1 Swept Sine Testing (for ASM)

Swept sine testing provides a fair trade-off between fidelity of characterization and duration of testing. Swept sine testing was conducted in this work for the purpose:

- to establish a ‘snapshot’ response for the system,
- to conduct homogeneity checks, and

- for use with ASM.

For the purposes of the swept sine testing as well as the other types of testing discussed in this report, the article was fully instrumented with accelerometers. The accelerometers were all calibrated against a known artifact. The placement of the accelerometers was conducted manually as described in Chapter 3 with the goal in mind of minimizing off-diagonal MAC. Accelerometers utilized in the testing were predominantly 100 mV/g. Areas where significant response was observed were instrumented with 10 mV/g accelerometers.

A VXI was utilized to acquire the data. The VXI system was configured to allow variable front-end gain. The gains were set and adjusted based on the results during the testing. Gains were set to maximize the use of the system. A VXI 1434 card was fortunately found and utilized for shaker control. All input was processed through VXI 1432 cards. Signal processing and acquisition was handled with m+p SO Analyzer. Further processing was conducted in MATLAB as necessary.

2.3.1.1 Snapshot System Response

Swept sine testing can be very helpful to establish the topology of the system dynamics. It is critical to understand the topology of the system before further time is spent in investigation. Swept sine testing was utilized in this fashion for the work presented. Figure 23 shows an FRF collected by swept sine testing from 400 Hz up to 3.5 kHz. This test was conducted to determine where the most dominant modes of the system were located. Regions studied further involve the three mode clusters identified at approximately 500 Hz, 900 Hz, and 1200 Hz. These three clusters were identified as those governing the structural response. Additional detail as to the characteristics of these modes is presented below.

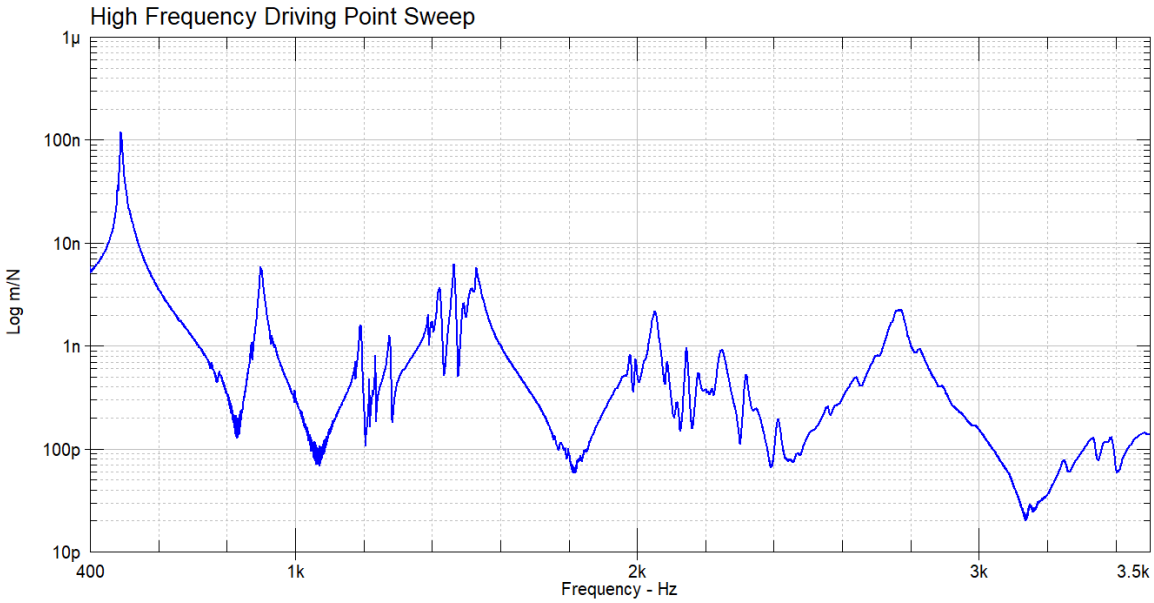

Figure 23 FRF at driving point 4079. Swept sine excitation 400 Hz to 3500 Hz.

2.3.1.2 Homogeneity Checks

After the system topology is established, homogeneity checks may be utilized to determine how the responses are affected by level of input energy. A nonlinear mode will present differently in the FRF for different forcing levels. For the conducted homogeneity checks, the shaker was arranged over the center of the top plate and sine sweeps were completed from 400 Hz to 1250 Hz. The results are shown in Figure 24.

It is evident that the lower frequency modes were subject to variation in the force level. The homogeneity check reveals a softening effect. This is to say that as force level or energy input level to the system increases, the natural frequencies of the modes decrease. This is contrary to what the engineer expected to see. The engineer was expecting to find a hardening affect due to the compression of the rolling elements during the cycles of vibration. The softening effect may be associated to the geometry of the linear guide truck. As amplitude of vibration increases, the compliance of the guide truck becomes active in the cycle. As the guide truck participates in the cycle, the ‘c’ shape around the rail opens. As the guide truck compliance becomes a part of the overall computation, the system becomes weaker causing the natural frequencies to decrease.

Figure 25 and Figure 26 show close-up views of the nonlinear portions of the response. Included in the plots are measurements taken with burst random excitation and hammer excitation. Figure 25 shows a close-up of the first cluster of modes. The hammer data is seen to ‘smear’ the nonlinear energy over a variety of frequencies surrounding the mode. The ‘smear’ is to the left indicating a softening nonlinearity. This is discussed further later in the report. It may be seen that as energy is increased into the system, the natural frequency decreases and the amplitude increases.

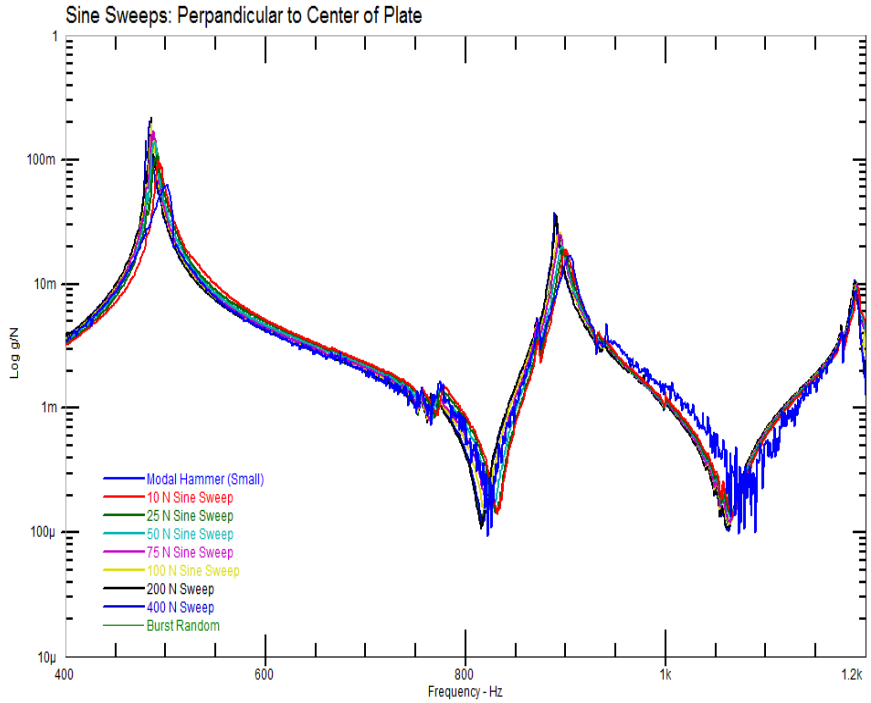

Figure 24 Homogeneity check at driving point, center of plate (location 4079).

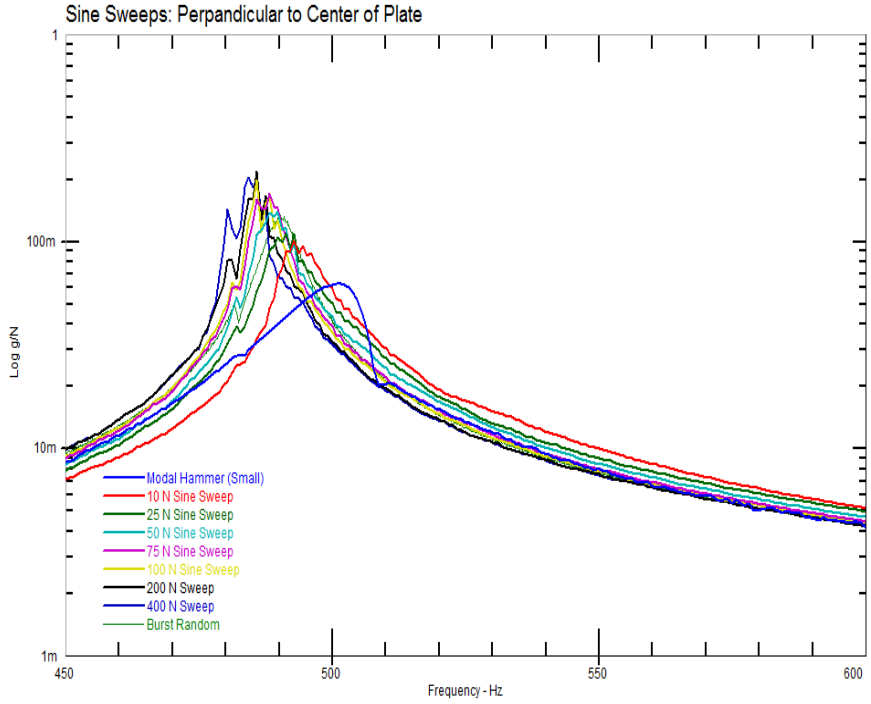

Figure 25 Homogeneity check at driving point, center of plate (location 4079) zoomed in on first cluster of modes.

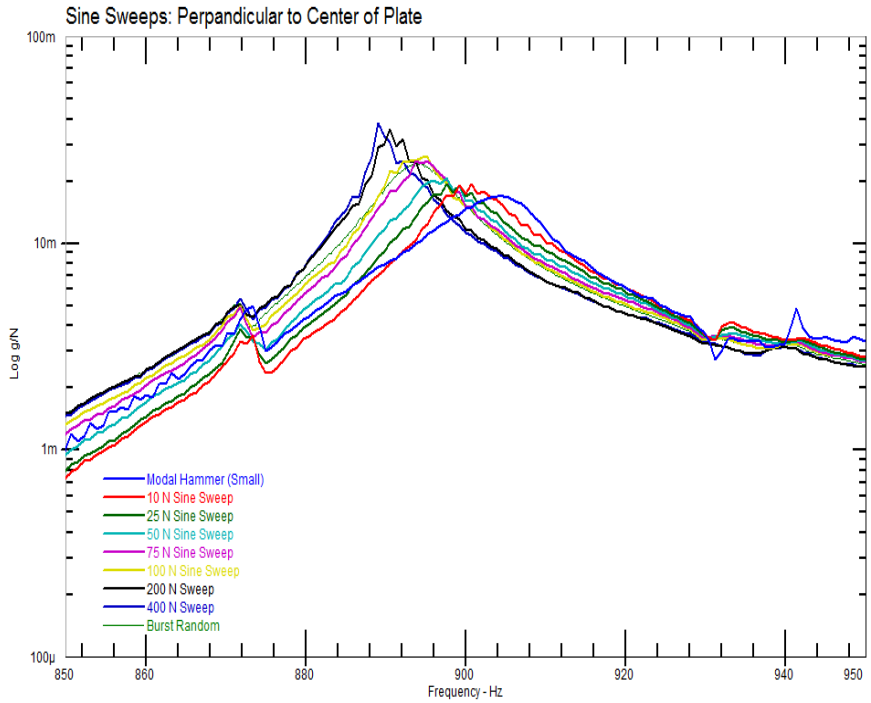

Figure 26 Homogeneity check at driving point, center of plate (location 4079) zoomed in on second cluster of modes.

Figure 26 shows a closeup of the second cluster of modes. Similar observations may be made to the second cluster of modes. As energy is increased into the system, an overall softening effect is observed. Along with the softening effect is an increase in amplitude. Notice that the dominant mode at approximately 900 Hz is affected by input energy, but the tertiary mode (870 Hz) was not appreciably affected by input energy.

The third cluster of modes did not exhibit any nonlinear characteristics and is not addressed here. As displacements decrease at higher frequencies it is reasonable to assume that the nonlinear effect observed and modeled here is not observed at the higher frequency.

A challenge of acquiring swept sine data is the inability to totally control the input spectra. The frequencies are swept through at a defined rate (slewing rate) and there are times during the sweep that the system cannot keep up with force level adjustments. This is to say that if a force level of 10 N is desired across the entire spectrum, there may be some areas where 9 N is achieved, and 15 N is achieved. This problem is satisfied in a subsequent section by application of sine dwell testing.

Swept sine testing is required due to the continuous time traces collected. The time traces may be utilized with ASM.

2.3.1.3 ASM

Sine sweeps may be conducted and the responses across a joint of concern processed into the acceleration surface. The acceleration surface is a visual depiction of the damping and stiffness characteristic of the joint. The acceleration surface method aids in the visualization of the nonlinearity. Nonlinear form may be determined by ASM. If the nonlinearity involves hard stops against which an object bumps, the amplitude between the stops may be determined by ASM.

Consider the SDOF system presented above as a practical example. The displacement response was computed for a sweep between 250 and 350 Hz. The results are shown in Figure 27. Some information may be gleaned from the trace, but the exact form of the nonlinearity may not be determined simply by looking at the time data. Based on Figure 27 it is evident that a strong nonlinear distortion is present. The fact that the distortion occurs above the resonance peak gives a clue as to the form.

A far more helpful method for determining the form of the nonlinearity is to use ASM. An ASM plot takes the acceleration, velocity, and displacement and plots them on a three-dimensional plane. Figure 28 shows the acceleration surface for the mode being considered.

With respect to Figure 28, the form of the nonlinearity was much more easily observed. The formulation of the system in Equation 5 reveals a cubically softening nonlinearity. Clues as to the type of nonlinearity are evident in the time domain data, however, it becomes very explicit when viewing the acceleration surface. Several challenges come about when using this method on a physical structure.

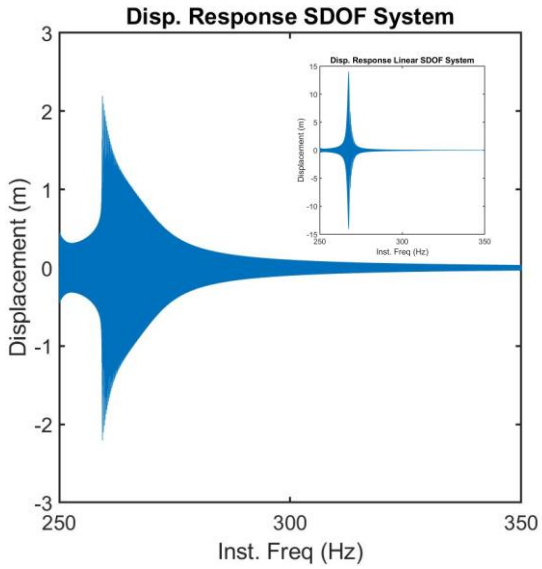

- Figure 27 Time-domain response of a SDOF system. Inset panel is for the linear system.

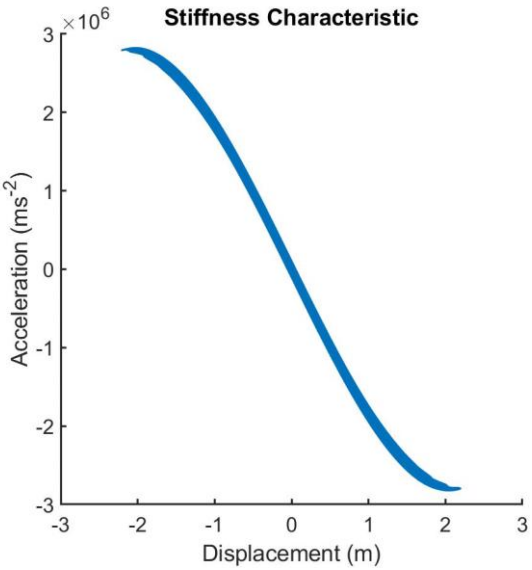

Figure 28 Cut in acceleration surface showing the stiffness curve.

The first challenge occurs when there is a high modal density. When there is significant modal density, it is not evident which mode is being studied. The second challenge involves noise in the data. Noisy data provides a significant challenge for computation of the acceleration surface. The quality of the surface struggles. This leads in to the third challenge, the noisy data provides challenges for integration of the data. Data is likely to be acquired from an accelerometer. Velocity and displacement must be computed from the accelerometer measurements. Noise in the data may be compounded through the computations of velocity and displacement.

To return to a specific discussion on the application of technique to study of the linear guides, ASM data is presented below. As indicated above, ASM must be conducted on a mode by mode basis. This presents a challenge in the case of the linear guides as each peak in the FRF shown in Figure 24 is representative of a cluster of modes. A curve fitting algorithm was used to identify natural frequencies and mode shapes. Further discussion is provided in the sine dwell section as to the linearity of each specific mode.

ASM proved challenging to separate out the effects of each mode. Future research may study the application of a modal filter to the data. The challenge therein primarily being the validity of a modal filter on a nonlinear data set. The data presented in Figure 29 includes some bleed-through from other modes in the near vicinity of the nonlinear mode of interest.

Further study of the first nonlinear mode yielded the plot as shown in Figure 29. With careful study of the data, a softening result may be observed. The red spline was applied by the analyst after study of the data. Additional spurious data points in the plot were contributed by neighboring modes. The softening nature of the mode corresponds to what was found earlier in the homogeneity checks.

It is worth noting that the ASM technology was developed with aerospace testing in mind. Aerospace structures are typically relatively weak and undamped. Industrial machinery presents the opposite consideration. Several critical aspects were necessary to obtain a quality stiffness curve from stiff and highly damped experimental data:

- All filtering must be conducted with zero phase filters. MATLAB's filtfilt command was used extensively in the computation of the acceleration surfaces. As the signals must be integrated from acceleration to velocity, then again to displacement, significant delay may be introduced if not handled properly. ASM compares acceleration, velocity, and displacement at each instant. It is supremely important that the fidelity of each instant is not violated in the computations, otherwise the wrong datapoints will be plotted. When the wrong datapoints are plotted, the analyst is either left with a confusing mess or an inaccurate plot which will lead to the wrong conclusions as to the property of the system.
- Quality data must be captured. For ASM to work, quality data must be captured. It was important to set up the front-end gains to avoid overload and to also make best utility of the DAQ's range.

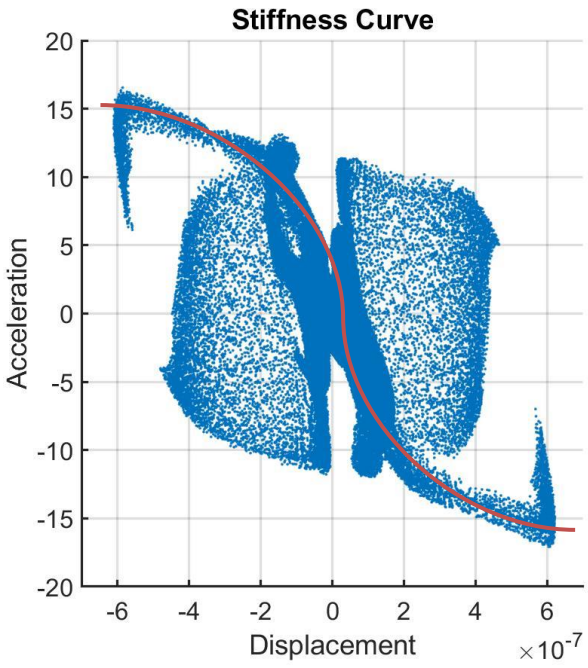

Figure 29 Stiffness curve calculated from the acceleration surface. The red spline was added by the analyst after interrogation of the data.

2.3.2 Stepped Sine (Sine Dwell Testing)

Sine dwell testing is a legacy method for characterization of nonlinearity. Sine dwell testing may be used to ensure proper energy is utilized to excite the structure at every frequency of interest. In sine dwell testing, the excitation frequency is increased incrementally or logarithmically at the 'slewing rate'. A major benefit of stepped sine and swept sine testing is that the slewing rate may be positive or negative. This means that the dynamics of the system may be thoroughly investigated by approaching the mode from higher frequencies or from lower frequencies.

Sine dwell test results for the example system depicted by Equation 5 are shown in Figure 30 and Figure 31. The results shown were computed by a MATLAB algorithm utilizing a Simulink model of Equation 5. Figure 30 again shows the same softening tendency as seen above in Figure 28. Another way to depict the system characteristic is with backbone curves. An example backbone curve is shown in Figure 31. The backbone curve compares the natural frequency to the input force level.

An advantage to the sine dwell technique is the accuracy in force input level that may be achieved. As opposed to swept sine testing where a force level is dynamically fed back and updated in sine dwell testing the system steps from frequency to frequency and

adjusts energy level before data is captured. Stated differently, sine dwell testing selects a frequency and adjusts the input energy until the desired value is achieved. Only after the desired value is achieved does the system catalog the data pertaining to that spectral line.

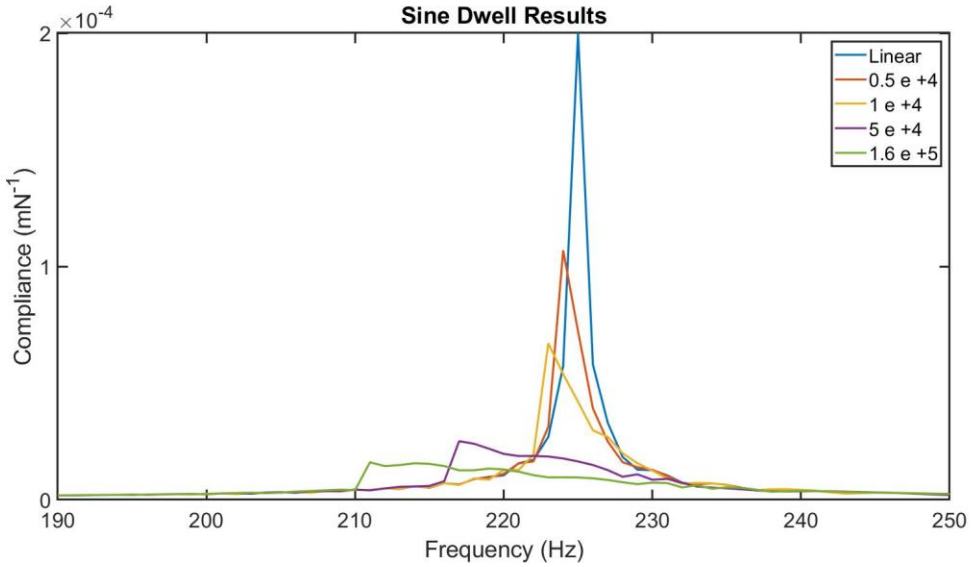

Figure 30 FRF homogeneity check with sine dwell testing.

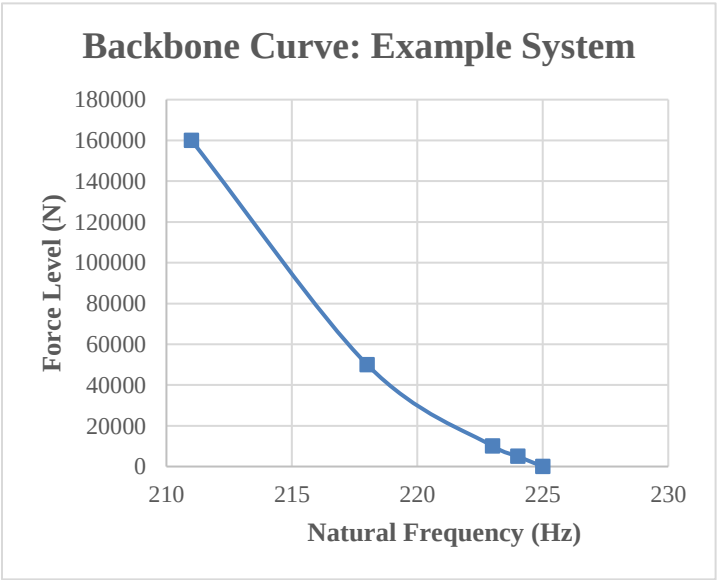

Figure 31 Backbone curve for the example system presented in Equation 5.

Sine dwell testing was utilized in this context to establish backbone curves.

Of the test regimes, sine dwell is the most time consuming. The time-consuming nature of the procedure can be a drawback when test schedules are tight. Sine dwell testing may be most efficiently performed by seeking out several bandwidths that define the response and focusing on them. A preliminary test may be conducted to locate the system modes. In this case, the preliminary test for the linear guides is shown in Figure 24. Once the system modes are located, a bandwidth around the mode may be selected for further testing. These bandwidths of interest may include the nonlinear modes of the system.

Sine dwell testing was utilized extensively in this work. Swept sine testing, while capable of detecting and categorizing the nonlinearity, could not be utilized to characterize the nonlinearity. Given the stiff nature of the structure, the feedback could not keep up to maintain a consistent input spectra. Sine dwell testing may also be utilized to slowly step through a portion of the response which is modally dense in order to help with the extraction of the many modes. Sine dwell testing, through the use of backbone curves, may also be utilized to characterize the nonlinearity.

The challenge of this work is the number of degrees of freedom to be quantified. In this case, there are five nonlinear coefficients sought out.

Figure 32 through Figure 35 show FRFs acquired at the top and lateral locations for the first two sets of modes. The figures depict positive and negative slewing rates. From the sets of data, several conclusions may be drawn:

- The nonlinearity is not dependent upon slewing rate: it does not matter whether the natural frequency is approached from below or above, the same characteristic is observed.
- The dominant modes are nonlinear and tend to be softening.
- As energy increases and natural frequency decreases, the amplitude increases until forcing is sufficiently high. Then the amplitude decreases slightly.
- As the force level increases, the observed damping decreases.

Backbone curves for the system are shown on a per mode basis in Figure 36 - Figure 43. The backbone curves presented were for the first eight modes. The higher order modes [of interest] did not present any nonlinear artifacts.

Table 1 organizes the data presented in the backbone curves. The purpose of Table 1 was to lay out the definition of which modes behaved in the most nonlinear fashion. Based on the results for the table, modes 2,3,4,6, and 7 presented as the mostly nonlinear modes of those of interest.

These modes must be captured with the nonlinear model. The nonlinear model, presented in subsequent sections, attempts to do so by defining which of the degrees of freedom are most active in the linear mode shape and associating a nonlinear term to it.

It is worth noting that with the swept sine testing, the 200 N sweep did not detect the reduction in response amplitude. This is due to the better controlled input force that sine dwell testing offers as described above.

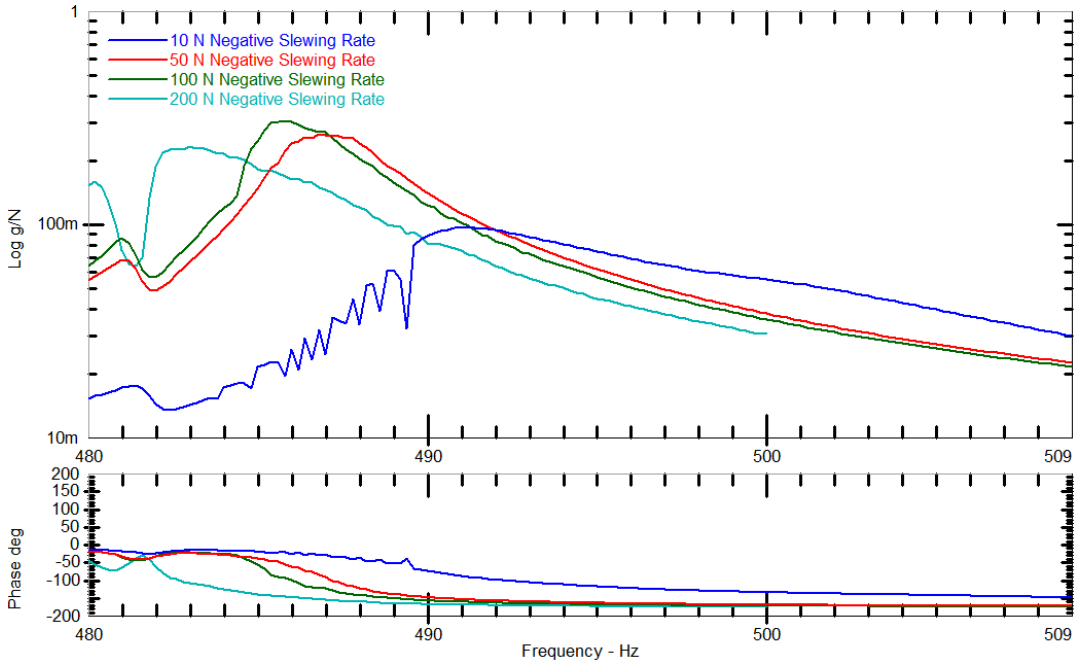

Figure 32 Sine dwell homogeneity check, 4079z with negative slewing rate. First mode cluster.

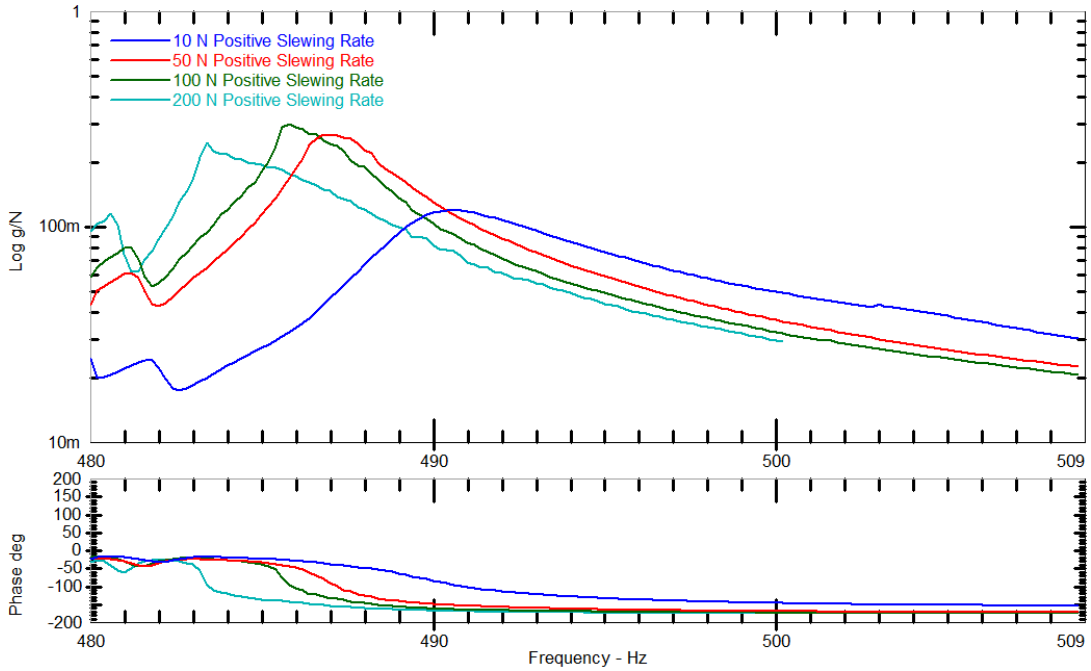

Figure 33 Sine dwell homogeneity check, 4079z with positive slewing rate. First mode cluster.

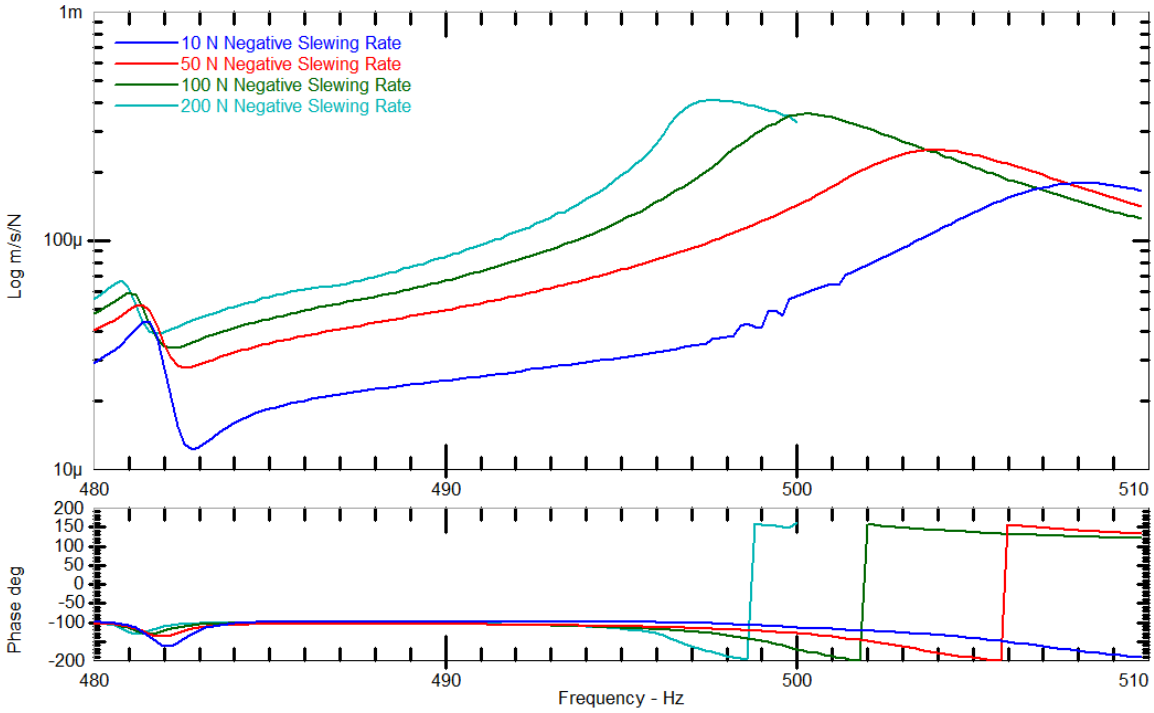

Figure 34 Sine dwell homogeneity check, 4068y with negative slewing rate. First mode cluster.

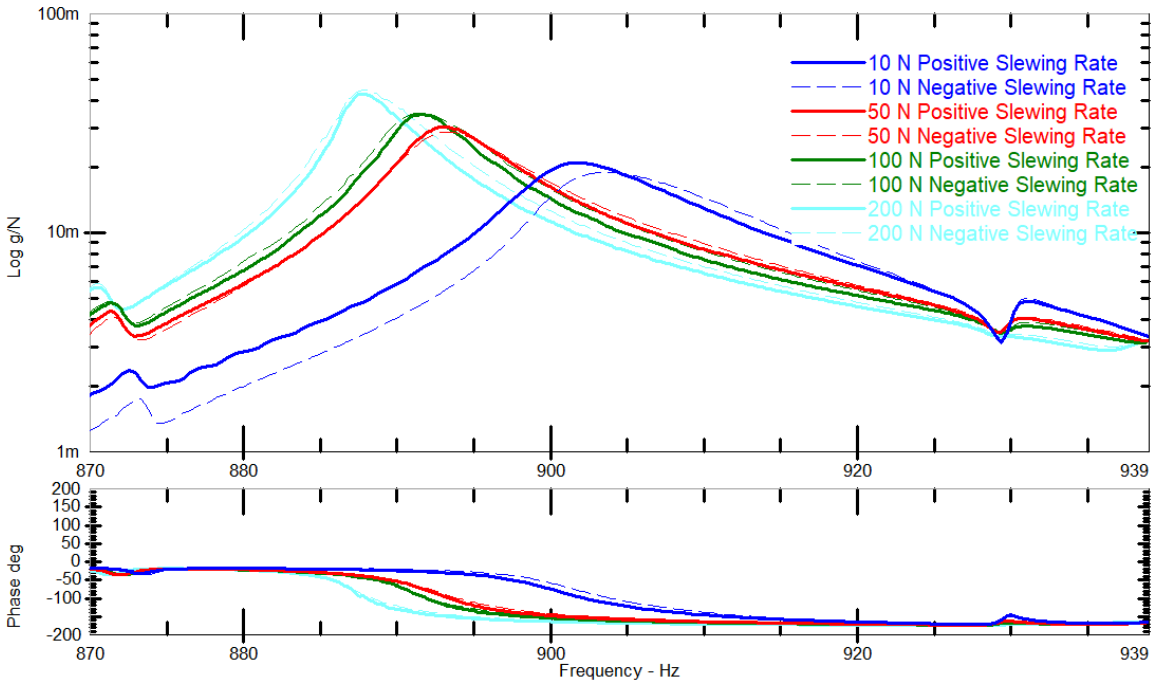

Figure 35 Sine dwell homogeneity check, 4079z with positive and negative slewing rate. Second mode cluster.

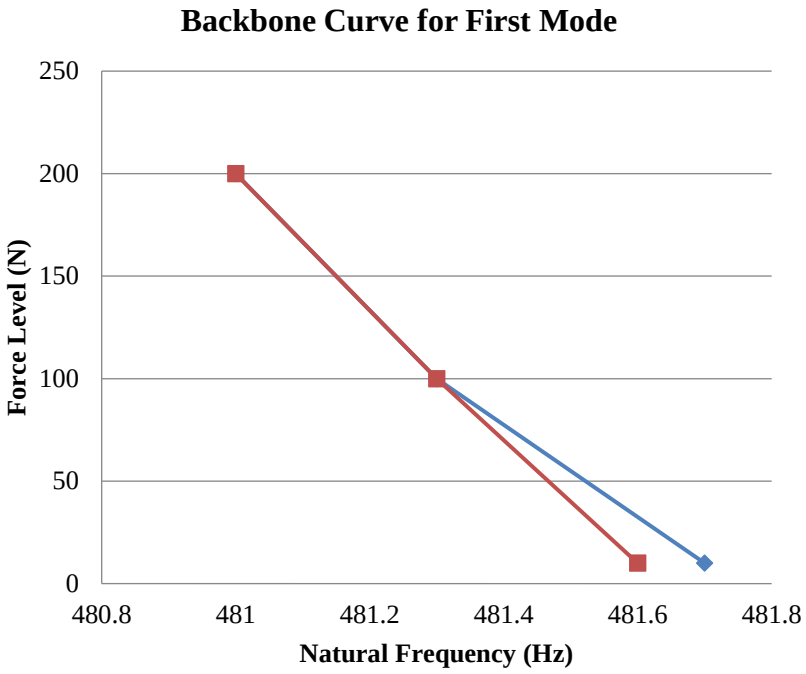

Figure 36 Backbone curve for the first mode.

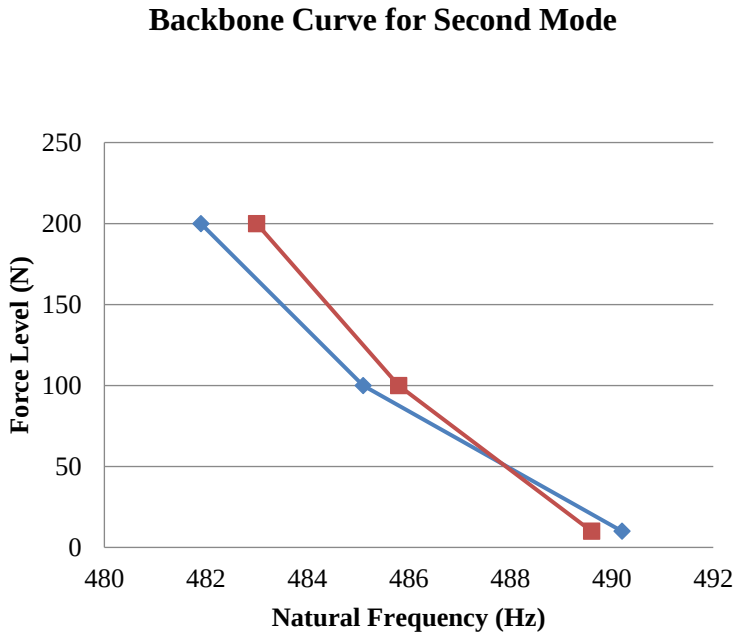

Figure 37 Backbone curve for the second mode.

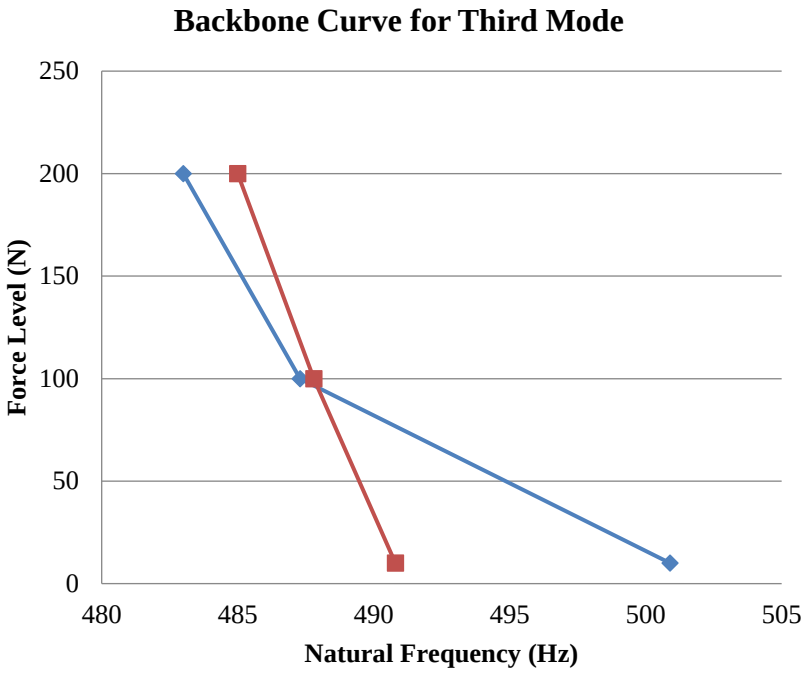

Figure 38 Backbone curve for the third mode.

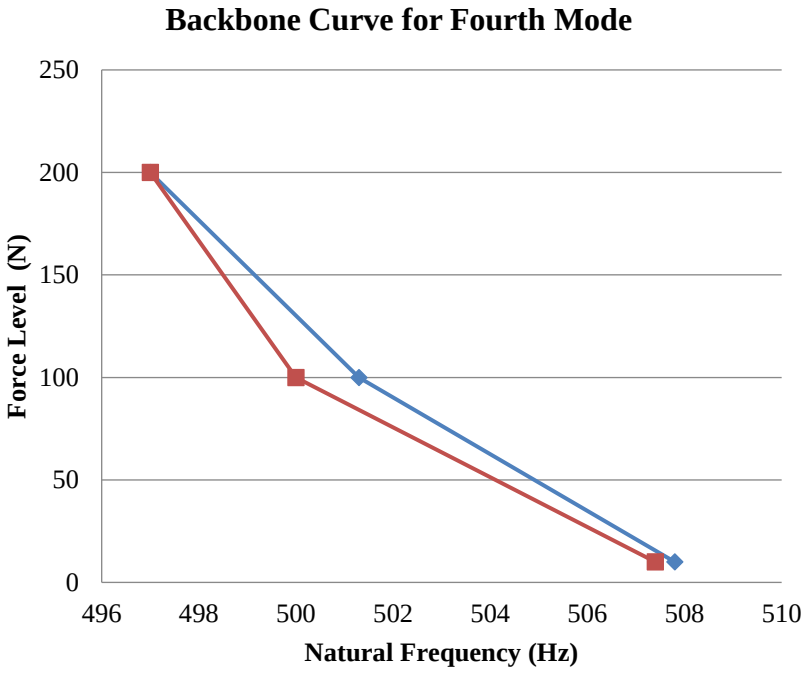

Figure 39 Backbone curve for the fourth mode.

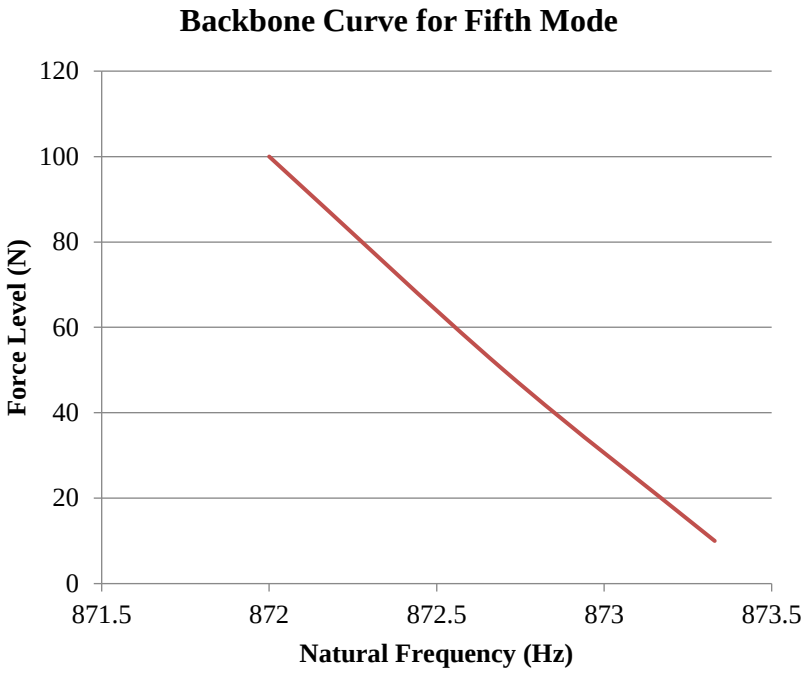

Figure 40 Backbone curve for the fifth mode.

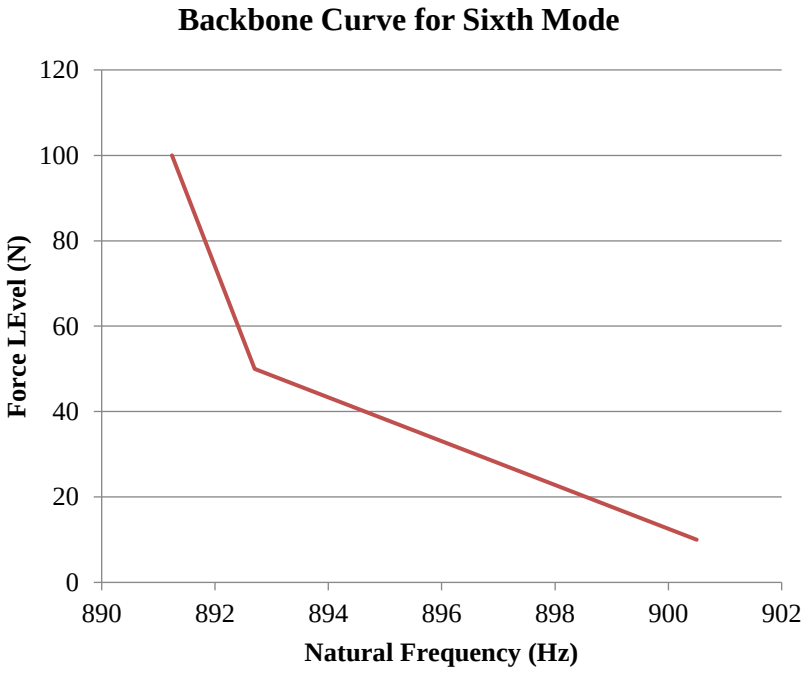

Figure 41 Backbone curve for the sixth mode.

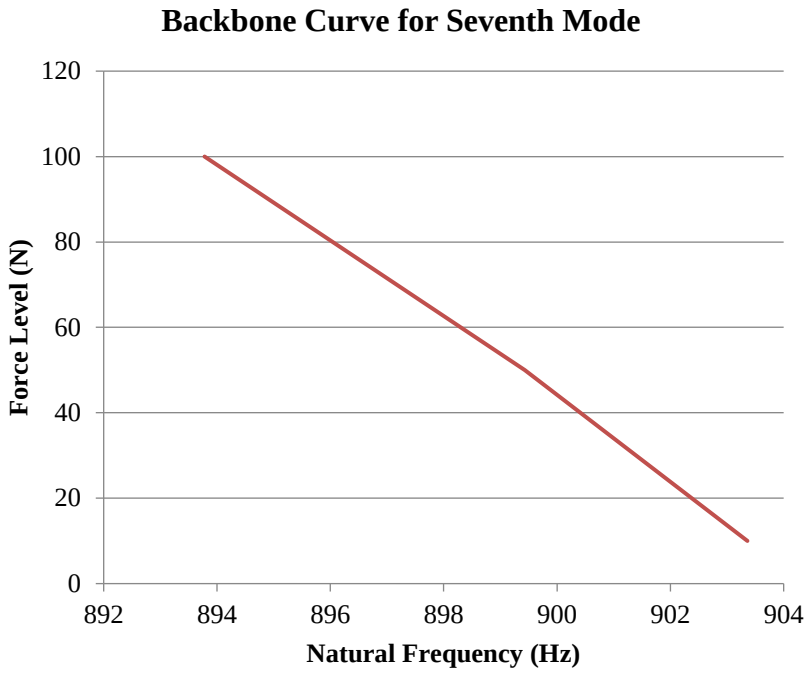

Figure 42 Backbone curve for the seventh mode.

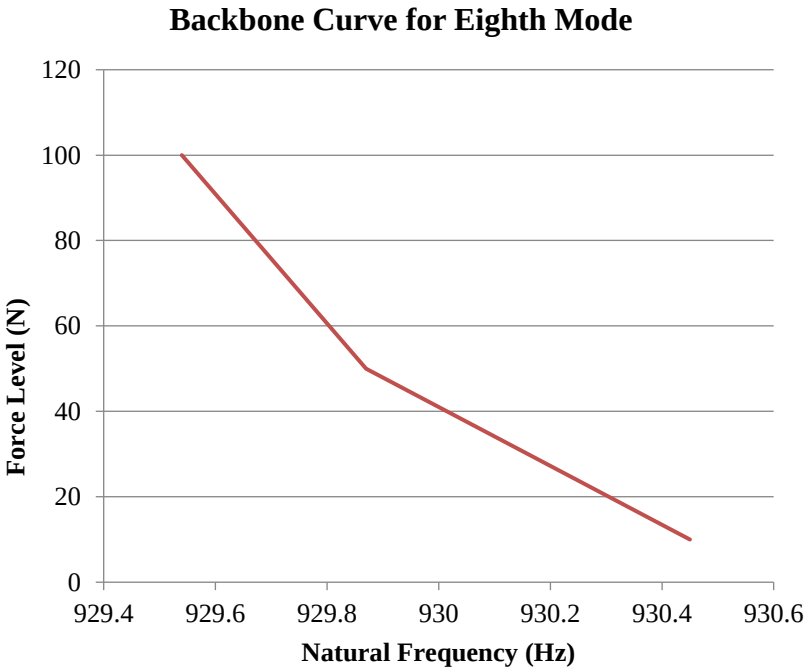

Figure 43 Backbone curve for the eighth mode.

(Hz)	Mode 1	Mode 2	Mode 3	Mode 4	Mode 5	Mode 6	Mode 7	Mode 8
Natural Frequency Difference	0.6 (0.1%)	8 (2%)	17 (4%)	11 (2%)	2 (0.2%)	15 (1%)	23 (1%)	1.5 (0%)

Table 1 Difference in natural frequency between low excitation level and high excitation level.

2.3.3 Impact Testing

Impact testing may be used for certain applications when characterizing nonlinearity. The Hilbert Transform (HT) has been used successfully on SDOF systems. When the modes are closely spaced, the HT based techniques cease to work. Given this consideration, impact testing was fruitful for collection of baseline data but could not be utilized to characterize the nonlinearity. Impact testing was also useful for establishing the model for the top plate. The top plate behaved in a linear fashion before being coupled to the linear guides.

Certain artifacts are evident in the FRFs when nonlinearity is present in a data set. The shape of the FRF as well as the shape of the coherence function both indicate presence of nonlinearities. Impact test data was presented alongside the sine sweep data of Figure 25. As indicated earlier, the lobing to the left is indicative of a softening nonlinearity.

What is evident from the data is that not all modes extracted by means of harmonic (sine based) testing are clearly excited and extractable. The impact test data tends to linearize the system by means of how the input spectra is applied.

2.3.4 Broadband Testing (Shaker)

Broadband testing proves fruitless in testing of this type. These structures are significantly stiff. Broadband testing was attempted with the 1000 lbf servo-hydraulic shaker as well as the voice coil shaker.

The servo-hydraulic shaker has system limitations which prohibit it from imparting enough energy to the structure in the bandwidths of interest. The first mode of interest for the structure was approximately 450 Hz. Figure 44 shows the system response curve for the shaker. The shaker was not capable of producing significant force in the bandwidth of interest. For a very stiff structure, the peak force capability of the shaker drops off at 100 Hz. At the frequencies of interest, the peak force capability of the shaker is approximately 100 lbf [448 N]. The shaker can produce more than enough force for the harmonic testing discussed earlier, but it is not capable of conducting broadband testing in the frequency of interest.

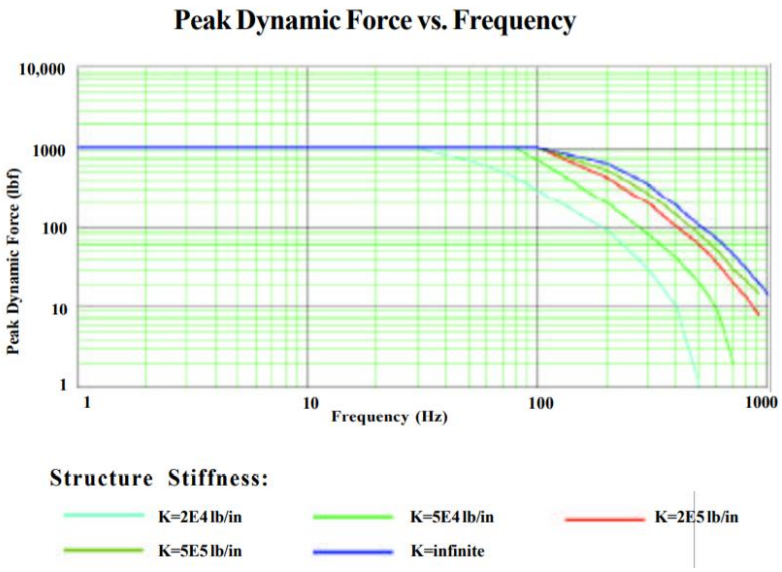

Figure 44 System characteristics of servo hydraulic shaker with large hydraulic power unit.

The voice coil shaker, though capable in the bandwidths of interest, could not impart enough energy in the broadband regime to acquire quality data at a sufficient force level. The underlying linear system could be successfully identified, but the shaker could not impart enough force to excite the nonlinearities.

Great care was taken in developing the input signal for use with broadband testing. A signal was created in MATLAB and filtered so only the required frequencies were present. The bandwidths studied were limited to those within 50 Hz of the nonlinear resonances. The input signals were repeated 100 times in MATLAB and exported for use with m+p Analyzer. The purpose of the repetition was for use with FNSI, which requires steady state data for identification of the nonlinear coefficients. When computing results with FNSI, the first several periods where transients decay are omitted from the data to be processed.

For the FNSI algorithm mentioned above to function, periodic random data is necessary. Quality periodic random data could not be obtained from testing of the structure at higher forcing levels. Given this, the use of FNSI on the machine tool structure was abandoned due to lack of necessary test equipment.

It is worth noting here that successful applications of FNSI have been benchmarked on aerospace structures which are lightly damped and not significantly stiff.

Figure 45 shows a comparison of FRFs collected by the various broadband excitation techniques. The data is inconsistent from measurement regime to measurement regime. The data also exhibits extremely poor signal to noise ratio. The data was not fit for curve fitting or parameter extraction.

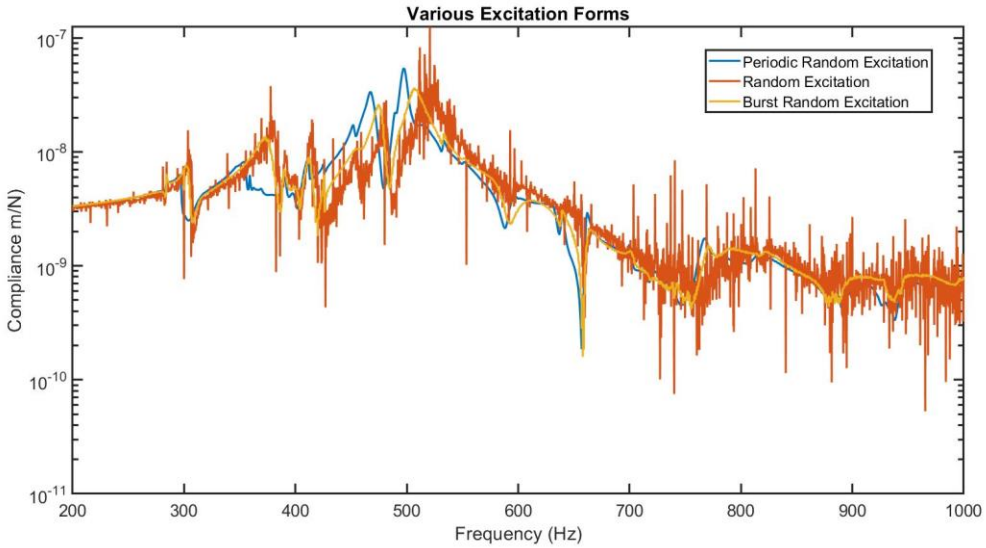

Figure 45 Comparison of results from broadband excitation techniques.

2.4 Study of Nonlinearity

The purpose of this model was pertaining to machine tool structural modes. Structural modes here involve modes of the platens, base, and cross slides. Spindle modes are considered separately as higher frequency spindle modes can have a strong affect on machining dynamics. Modes of the structure typically occur at lower frequencies. For this reason, modes between 400 and 1.2 kHz were selected for further study.

Three clusters of modes were chosen in particular for further study. The bandwidths selected for study were 480-500 Hz, 867-947 Hz, 1166 Hz – 1211 Hz. Figure 46 shows the sections of the response which were selected. The red portions of the response were gathered by sine dwell testing. The blue response was gathered by swept sine testing.

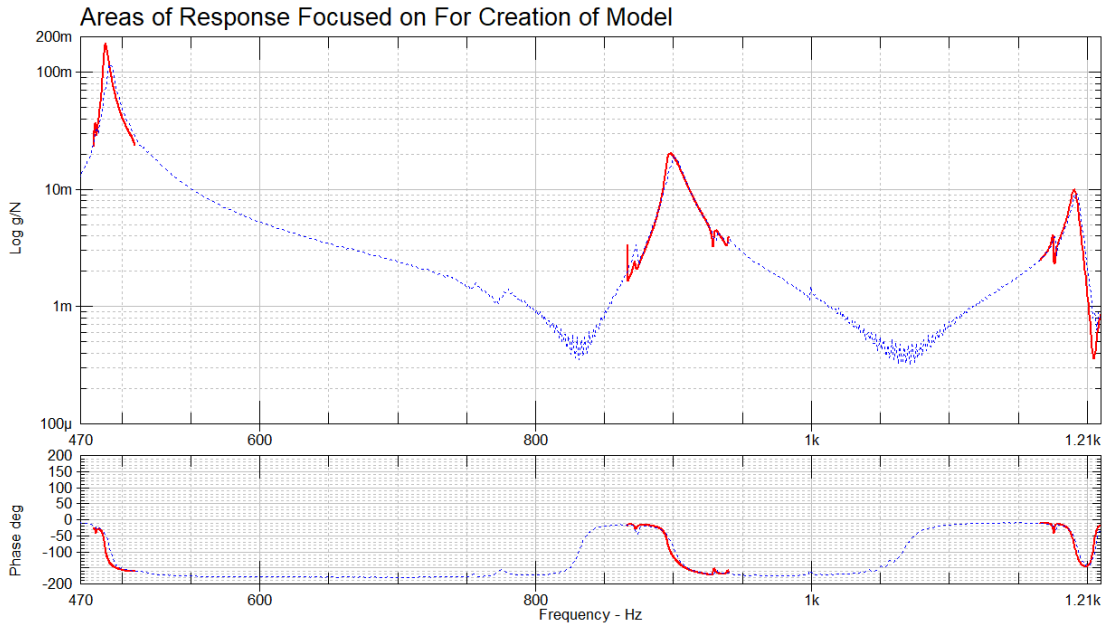

Figure 46 Areas of response studied in detail are shown in red.

Multiple sets of swept-sine data were captured. Excitation levels were 10 N, 20 N, 50 N, 100 N, and 200 N. The amplifier utilized was incapable of operating more than 200 N. Sine dwell tests were conducted with frequency (slewing rate) increasing and decreasing. 10 N was utilized to extract the underlying linear system. The results shown in Figure 46. Figure 46 shows a softening relationship with excitation energy. The natural frequency tends to decrease as energy increases. The damping ratio also decreases as energy increases. The shift in natural frequency is most pronounced between 10 and 50 N. 100 N does not significantly shift from 50. At 200 N, the natural frequency further decreases and the damping decreases. The phase portion of the plot shows a sharp transition at the primary mode in this bandwidth.

2.5 Conclusion

This chapter covered the acquisition of data which is used in subsequent chapters for development and tuning of the system FEM. Various methods of data acquisition were presented and discussed. Broadband techniques were not utilized in this work due to the lack of enough energy to excite the nonlinearity. It is critical to recall when viewing this work, the majority of techniques in publication were developed specifically for automotive or aerospace applications. Automotive and aerospace applications do not exhibit the high levels of stiffness and damping found in machine tool structures.

Due to the significant stiffness of the test structure, the testing relied heavily on sine dwell and sine sweep testing to characterize the nonlinearity. Homogeneity checks were conducted and it was found that the system exhibited a softening characteristic. ASM was also utilized to extract the model form from sine sweep testing.

Based on the results presented above, the analysis proceeded with a nonlinear model of the linear guide. The technique utilized to solve the model utilizes a time-domain approach. Nonlinear stiffnesses were computed as a part of integrating the equations of motion. The nonlinear coefficients were arrived at by optimizing the computed FRFs to match the test data.

This approach had the benefit of being more predictive. For cases involving virtual prototyping and the design cycle a more predictive model is desirable. Due to the solution technique, this procedure is very time consuming. There are a number of other pathways that may be taken to arrive at the result. Some of the techniques are described in this work. The primary purpose of this work was a predictive model. The work does not endeavor to minimize other techniques which may be more useful for a fully developed product. The purpose of this work was mostly for use with prototyping designs.

3 Current Commercial Capabilities: Initial Model and Linear Model Updating

Current capabilities of commercial code are centric on predicting linear natural frequencies and responses. To accurately capture the dynamics of bearing elements (such as linear guides), nonlinear modeling must be utilized. Commercial code does not yet account for structural nonlinearities in an efficient manner.

Prior attempts have been made to analytically model linear guides which are discussed in Chapter 1. The purpose of this work is to measure the characteristics of the linear guides and create a nonlinear dynamic model and modeling procedure. The linear guide model and methodology may be utilized for modeling an entire machine tool.

It was found in Chapter 2 that the linear guides possess a softening nonlinearity. This means that the natural frequency decreases as energy input increases. The ultimate model must capture this characteristic. Typical eigensolution based strategies cannot account for this softening effect.

The purpose of constructing the test stand was to isolate the linear guides with a dynamically simple yet practical system. It was shown in Chapter 2 that the top plate which governs the dynamics of the structure was easily modeled. The mode shapes and natural frequencies were easily predictable. The simplified nature of the test stand makes extraction of the properties of the linear guides much more definite and simple.

3.1 Pretest and Transducer Placement

Common transducer placement algorithms were attempted with varying levels of success. For the final models presented here, the transducers were manually placed in such a way that the off-diagonal MAC would be minimized. In the engineer's experience, transducer placement algorithms work significantly better for aerospace and academic structures than for stiff compact machine tool structures. The algorithms may work better for physically large machine tool structures such as gantry mills which more closely approximate a space frame. Based on experience, it is more efficient with the structure considered in this work, to manually place the transducers while studying the off diagonal MAC.

Modes were chosen which are analogous to those typically seen in machine tools. Special consideration was given to those modes identified as nonlinear in the previous chapter. The identified modes were the ones which govern the response of the system. These modes required accurate modeling to properly approximate the FRFs which would be used in the 'big picture'.

Given the nature of the test article, the mode shapes were expected to be robust while the natural frequencies were free to shift with force level. Given the engineer's experience

this is a fair assumption. It is typical in machine tools that the natural frequencies can shift while the associated mode shapes remain the same. Based upon that assumption, the mode shapes were utilized to track the natural frequencies in the curve fitting stage of the project. The modes were curve fit with a commercial pLSCF algorithm.

Some modes in machine tools have more influence on Tool Center Point (TCP) dynamics ('big picture') than others. TCP dynamics strongly influence the performance of the machine during operations. The dominance of the mode based on the driving point FRF determines its influence on machining performance.

Great effort may be taken by machine tool companies to identify these modes which are deleterious to machine performance. If the mode cannot be mitigated in the design phase, energy absorbers may be required. If the mode is not properly designed in the final release, it may be a constant pain to application engineers who will have to select tooling which does not excite it.

The major modes of concern are those at 500 Hz (fist plate bending), 946 Hz (plate potato chip mode), and 1494 (second potato chip mode). These modes are shown in Figure 46, Figure 52, and Figure 54. Other modes of concern were the 605 Hz tipping mode, shown in Figure 48 and the 634 Hz twisting mode shown in Figure 49.

The mode shapes extracted from the FEM are shown below in Figure 47 through Figure 57.

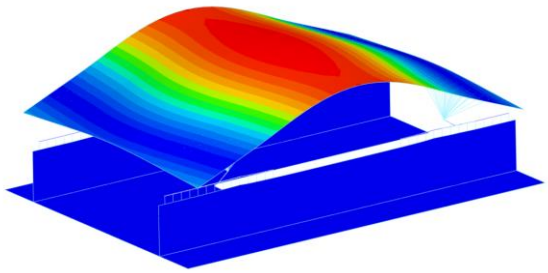

Figure 47 502 Hz First bending mode of the plate most sensitive to k_x and r_y.

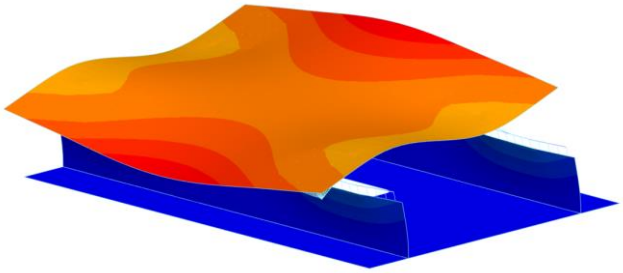

Figure 48 605 Hz Tipping mode over the linear guide rails mainly involving r_z.

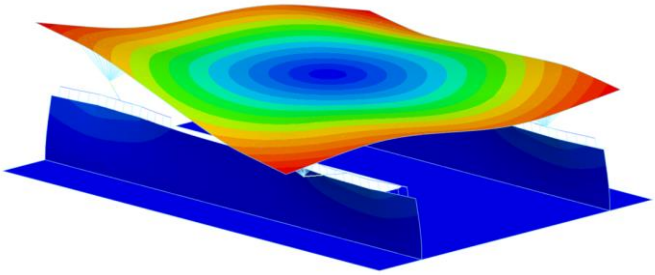

Figure 49 634 Hz Torsional mode of the plate, mainly exercising the k_y of the linear guides.

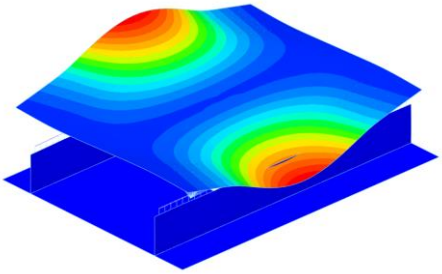

Figure 50 819 Hz Twisting mode of plate over linear guides.

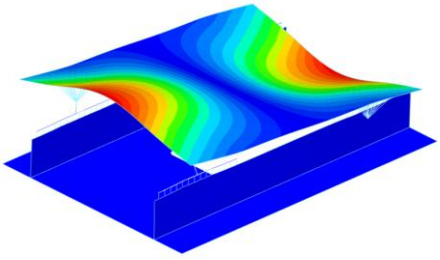

Figure 51 936 Hz Twisting mode of plate over linear guides opposite to 819 Hz mode.

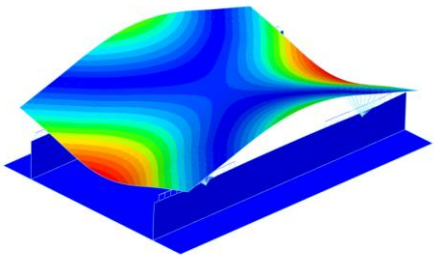

Figure 52 946 Hz First potato chip mode of top plate.

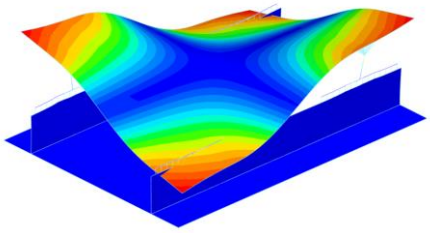

Figure 53 1450 Hz First Shell mode.

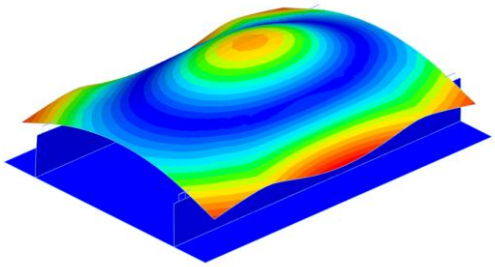

Figure 54 1494 Hz mode.

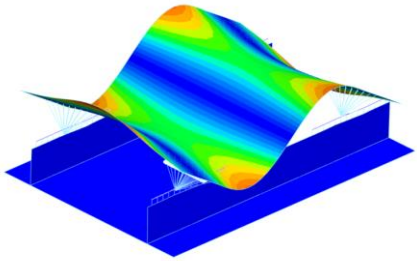

Figure 55 1610 Hz Second bending mode of plate over linear guides.

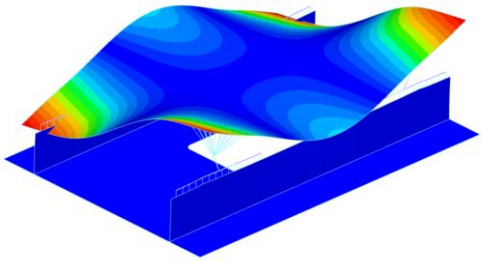

Figure 56 1678 Hz mode.

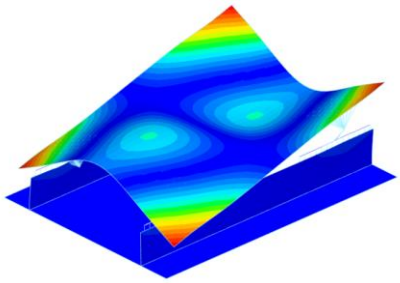

Figure 57 2054 Hz mode.

3.2 FE Modeling Process

Existing techniques of solving the model will be reviewed in this section prior to the discussion on utilizing modern nonlinear techniques to compute FRFs. The goal of this work is to lump the properties of the linear guide to a single nonlinear element. Other attempts, reviewed in Chapter 1, have been made to accomplish this. This section practically examines methods available to the FE practitioner within commercial codes.

The common practitioner must rely on elements built into commercial solvers. A joint may be represented by an individual or series of rigid or parameterized connections. This work utilized the CBUSH, and RB2 elements from NASTRAN to approximate the linear guides. Table 2 is used to track and display the various natural frequencies computed with different idealizations. The green rows are those specifically tracked and utilized for tuning as they dictate the response.

Several observations may be made regarding sensitivity of parameters to change in natural frequency. The first plate bending mode was most sensitive to the rotation of the linear guide about the y-axis. The tilting mode was sensitive to k_y. The tilting mode was fine tuned by adjustments made to k_y. The potato chip mode was fine-tuned by adjustments to r_z.

The long first side mode (892 Hz Test) was evident in the response. This mode was most sensitive to adjustment in k_z. Adjustments in k_z yield unphysical results in the system. This mode manifests approximately 2+ orders of magnitude stiffer than the other modes of interest. For this reason the mode is neglected and no stiffness is associated to k_z.

Alterations in k_z tend to affect other modes which are of more significance in the computation of the responses.

When the system matrices were computed, proportional damping was assumed for the top and bottom plates. These values for damping were evaluated based on the unconstrained testing of the individual components. The assumption in this work was that the damping added from the assembly was entirely attributable to the linear guides. This assumption proved very good as the results exhibited decent correlation.

Viscous coupling damping terms were estimated and optimized. In the case of damping, the k_z direction was utilized. Viscous effects on k_z cannot be neglected as that is the direction of travel for the guides. There are a number of physical phenomena which are approximated by the damping associated to this direction. To list a few physical phenomena, the damping associated to the k_z direction approximates the oil film effects in the bearing, the rolling of the bearing elements, and the friction of the lip seals against the rails.

Table 2 Comparison of natural frequencies based on modeling technique.

Hz	*Mode #*	*Test Model*	*RB2*	*CBUSH (Manufacturer Values)*	*CBUSH (Tuned Values for Linear Instance)*
First Plate Bending	1	490	1078	395	490
Tilting Mode	2	481	724	459	508
Twisting Mode	3	503	1471	466	535
Long Side First	4	892	1424	710	821
Potato Chip	5	899	1723	741	902
Short Side First	6	872	1957	780	963
Cup	7	1191	2264	1278	1518

a: For RB2 there is an additional mode present in the computations that is analogous to the second bending mode of the plate. This was not present for the other models

b: For the CBUSH (Manufacturer Values) model, an additional mode was present with a nodal cross at the center of the plate. This was the first twisting mode of the plate.

3.2.1 FEM with RBE2 Elements

According to the literature, linear guides may be modeled as rigid links. To confirm this concept, the test stand model was retrofitted with rigid links to represent the stiffness of the guides. The rigid connections do not allow compliance across the joint. The computed modes occur at significantly higher frequencies than when the CBUSH elements are utilized. Whereas the first mode may be accurately depicted with the use of CBUSH elements, use of RBE2 elements do not accurately capture the system dynamics.

Modeling the guides as rigid links proved to be a most inaccurate method. The stiffness in rotational degrees of freedom are a major source of error when utilizing RB2 elements to model linear guides. By feature of the rolling elements and weakness of the guide blocks, the assembly is not completely rigid. Figure 58 and Figure 59 show the FRF comparison between the RB2 model and the experimental data.
The red FRFs were acquired by low-energy sine dwell testing. The red FRFs were taken as the ‘truth’ data set. The blue curve represents the FRF computed utilizing RB2 connections. It is evident from the figures that the RB2 had predicted the first bending mode of the plate approximately 500 Hz too high. The order of the modes was also reversed. In reviewing the shapes associated to the natural frequencies listed in

Table 2, the first bending mode of the plate occurs at Mode 4 (1061 Hz) for the RB2 connection. The truth data indicates that the first bending mode of the plate was mode 3 (489 Hz).

The slope of the top plate is critical for defining the mode shapes and thus the FRFs. Figure 60 is a good example of the spurious stiffness the rigid links cause. The slope of the top plate in the first mode shape decreases at the guide connections. This is due to the spurious rotational stiffness which the rigid connections impart on the system. The experimental model shows a continuous curvature for this mode while the rigid links hold the top plate. Reference Figure 47 for the correct mode shape.

A comparison of the mode shapes and natural frequencies is provided in Table 2. The best possible comparison is provided. Please note that for the RB2 connections, the mode shape comparisons are approximate at best.

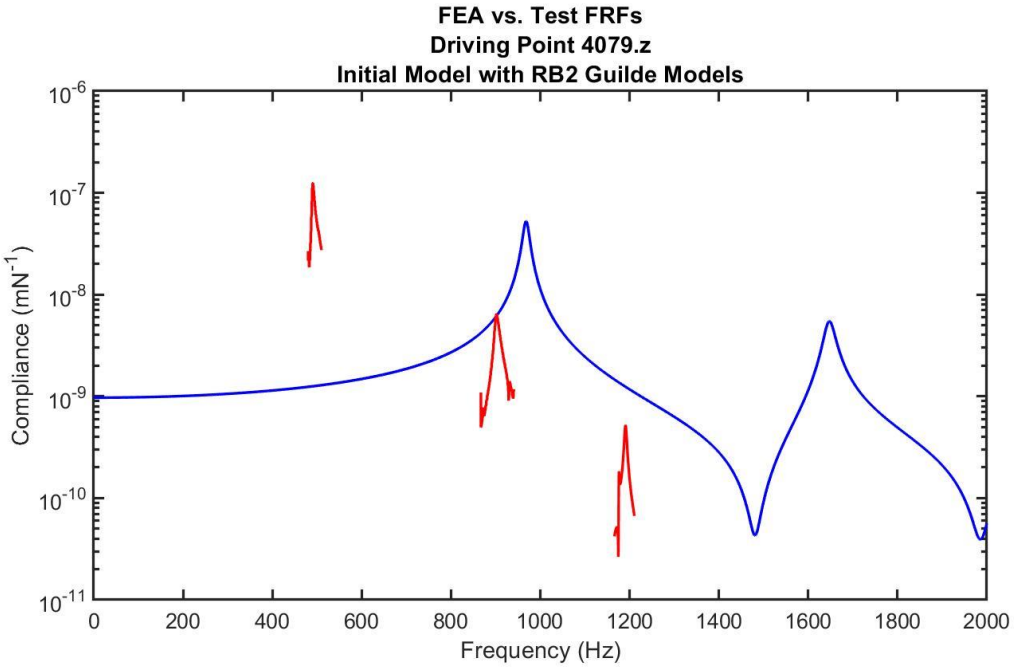

Figure 58 Comparison between computed and measured FRF. Measured FRF from 10 N sine dwell data. FRF acquired at 4079.z. (blue – computed, red – experimental)

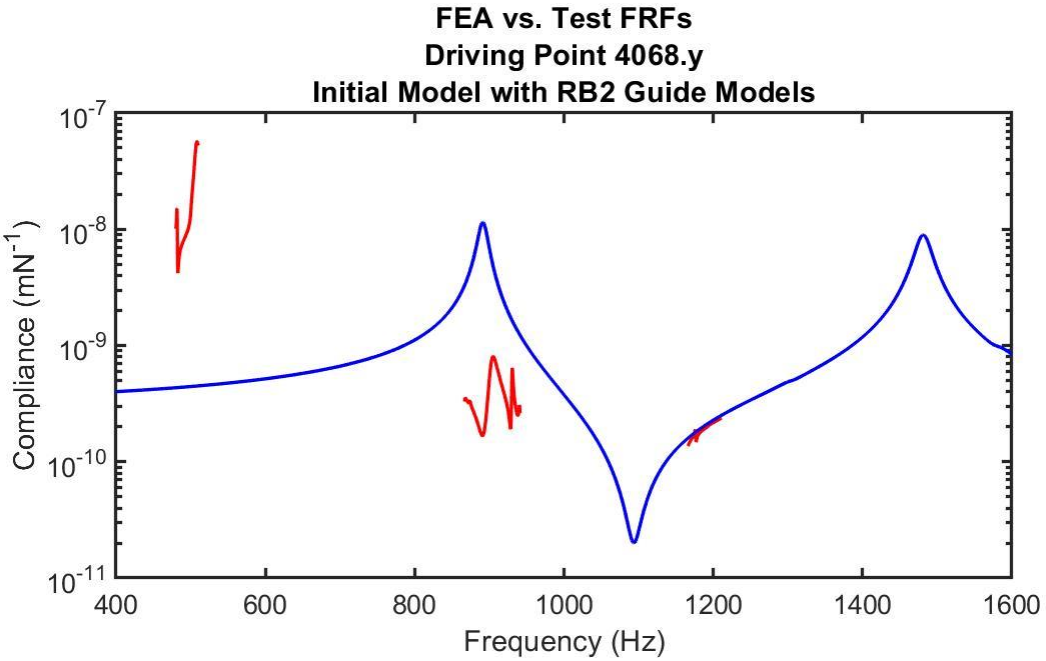

Figure 59 Comparison between computed and measured FRF. Measured FRF from 10 N sine dwell data. FRF acquired at 4068.y. (blue – computed, red – experimental)

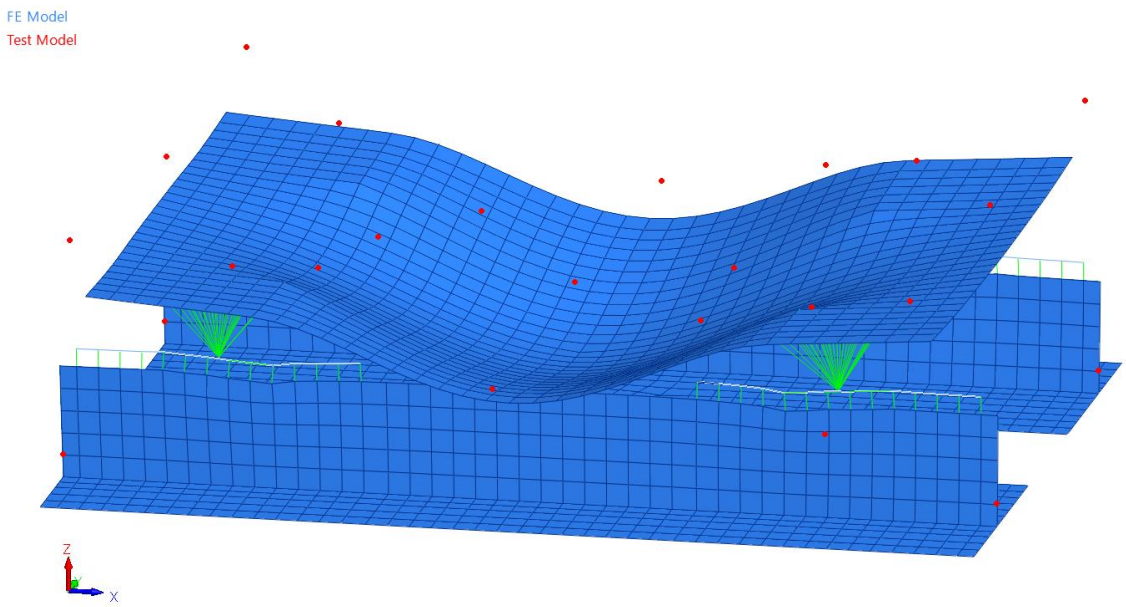

Figure 60 First bending mode of top plate utilizing RB2 connections.

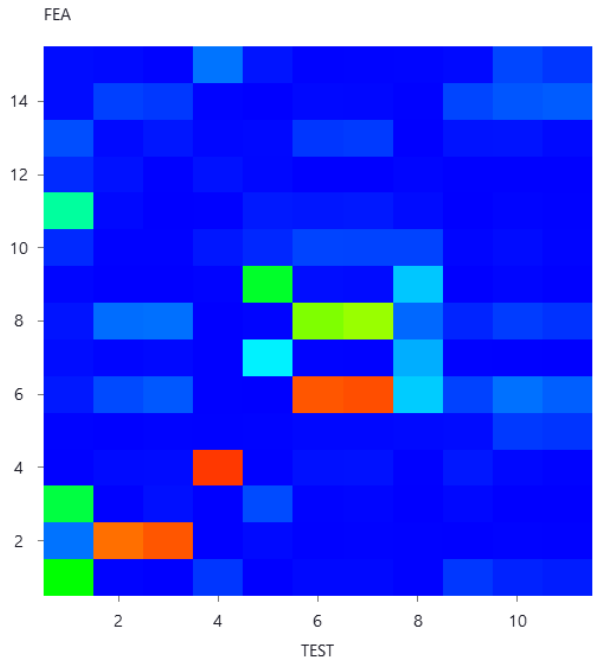

Figure 61 MAC: RB2 model to modes extracted from 10 N sine dwell testing.

3.2.2 FE Model with CBUSH Elements: Supplier Values

Linear guide manufacturers provide nominal values for stiffness in lateral and axial degrees of freedom. Rotational degrees of freedom are typically not included in the data supplied by the manufacturer. The values the manufacturers supply are not test based. The values are determined by mathematical models. While the values may be adequate

and reflective of static tests of individual guides, they do not sufficiently capture the dynamic properties of the linear guides.

Table 2 provides a comparison of the natural frequencies and mode shapes for the various commercial guide models. Whereas with the rigid connections, the modes were computed stiff, with the manufacturer values the modes were computed too soft. The natural frequencies came in out of sequence. Without any accounting for rigidity of the rotational degrees of freedom, the mode shapes were predicted at lower frequencies than those measured.

The results of this work show that when modeling bearing elements, the rotational degrees of freedom are critical. The results from the RBE2 reveal that if RDOFs are approximated too stiff, the mode shapes are severely affected, and the modes come in too stiff. This section shows that not accounting for RDOFs produces responses and mode shapes at frequencies too low. The system without RDOFs represents as too weak.

When computing responses for industrial machinery, accurate depiction of the frequency and amplitude is critical. The frequencies present in the data serve to dictate where the regions of stability are present for manufacturing operations. The amplitudes help to determine the stable depths of cut.

Having exhausted the two common types of elements utilized to model linear guides, the work now progresses to utilizing the CBUSH 6 DOF stiffness element and performing some model updating to determine the rotational stiffnesses. Two methods were utilized for model updating in the following section. First, the values were manually tuned. Second, a commercially available software was utilized to update the models.

3.3 Linear Model Updating

In a model updating scheme, particular parameters are chosen which the user deems more uncertain. This is to say that the engineer reviews the model and identifies parameters which may have been misrepresented. In the case of this work, the uncertainty in the model is associated to the guides. The linear substructures are simple to model, and it has been proven in Chapter 2 that an excellent model had been obtained for the top plate.

The sensitivity of uncertain parameters is calculated against the desired altered outcome of the main structure. For example, a sensitivity analysis may be computed to see how much a natural frequency changes due to the alteration of a stiffness in the model.

For the sake of this analysis, manually tuning of the model is presented first as it was the most fruitful. Comments are then made regarding automated model updating. Automated model updating proved less fruitful and the results obtained were not utilized in this analysis.

3.3.1 FE Model with CBUSH Elements: Manually Tuned

A current standard for modling of linear guides is to utilize a 6-DOF stiffness connection. This connection accounts for rigidity in all translational and rotational DOFs. The technique allows for the tuning of the six stiffnesses associated to the linear guides.

In this section, the degrees of freedom were manually tuned to arrive at the desired mode shapes and natural frequencies. Model updating may be a very physical and practical endevor. In this case, only the values associated to the linear guides were addressed. Chapter 2 reviewed the initial simulation and correlation of the top plate and proved an accurate model had been achieved without alteration of the associated structure. Each of the four linear guides respective parameters were updated simultaneously. This was done to ensure a realistic result. Each of the guides are a manufactured product, the final values achieved should be very similar to one another. This helped prevent large differences in values of stiffness from guide to guide.

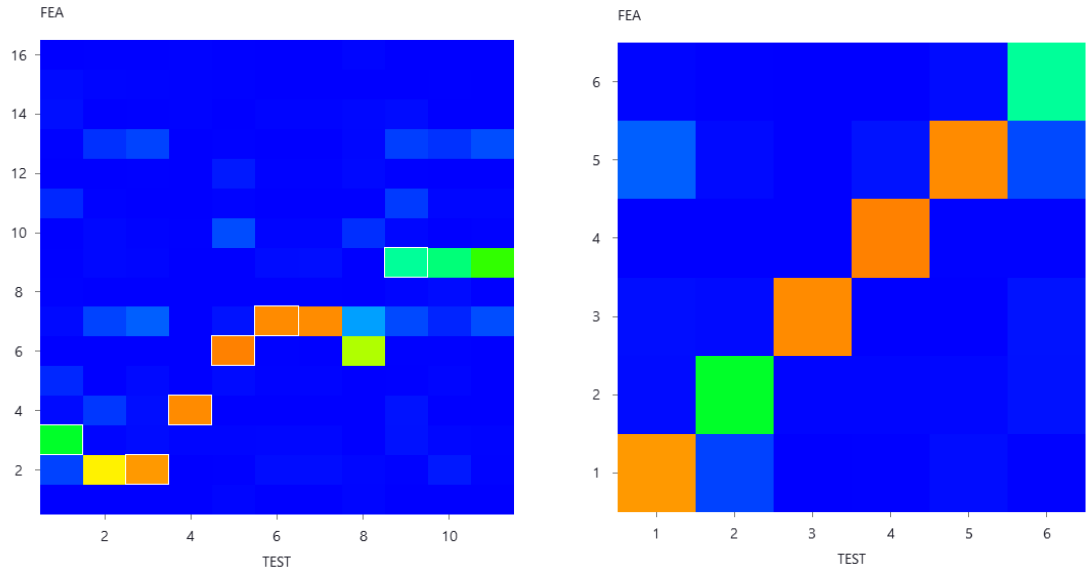

Figure 62 10 N Step Sine MAC Left Image: MAC all modes. Right Image: MAC paired modes.

The simulation results presented below represent manual tuning of the stiffnesses and damping targeting the first, second, and fifth modes. Recall from above that the only parameters altered are those pertaining to the linear guide. The balance of the parameters was to remain (with regards to stiffness and damping). This was again due to the fact that individual models of the parts had been correlated. The connection terms and uncertainties were to only be associated to the linear guides. The first bending mode of

the plate governed the response of the system. This provides a means of accurately depicitng the first mode. It can be seen that the MAC is in good agreement.

There were no damping values provided with the linear guides. The published values for stiffness of the linear guide were:

k_x=1.25e+09 N/m
k_y=1.25e+09 N/m

After the manual tuning of the model, the values arrived at were:
k_x = 1.4718e+09 N/m
k_y = 1.2633e+09 N/m
k_z = 0 N/m
h_x = 3.0790e+12 N/m
h_y = 1.7788e+12 N/m
h_z = 1.2390e+12 N/m

b_x = 8000 N/m
b_y = 8000 N/m
b_z = 1000 N/m
d_x = 1000 N/m
d_y = 1000 N/m
d_z = 1000 N/m

Interestingly, the values for k_x and k_y were very close. The error for k_x and k_y were 15% and 0.1% respectfully. The published values are close to accurate, however for the dynamic models – accurate rotational stiffnesses are critical. It can be seen above that the rotational values are significantly high.

Figure 64 and Figure 65 show the FRF comparisons between the measured and computed data. The computed data in these figures represents that from the manually updated model.

As stated earlier, the higher order mode in Figure 65 is most sensitive to axial stiffness. There is no practical axial stiffness in the model. When an axial stiffness is added such that the FRF matches (within that bandwitth) the other modes no longer correlate. Given the relative stiffness of this mode compared to the mode which drives the response – further correlation is not saught out.

Other modes may be seen in the test data which do not drive the response. These modes are neglected as they play an insignificant role in TCP respone prediction.

The results of the manual updating procedure have produced very good FRFs which are excellent for computation of analytical stability. These results are used in the subsequent chapter for the application of the nonlinearity. With the application of the nonlinaerity,

the model can accurately predict FRFs at the TCP for variable forces. This is to say that the FRF is predicted for higher thrust tooling, which plays a critical role in the manufacturing process. The next section reviews commercial software utilized for updating the model and discussses the benefits and weaknesses of the automated process.

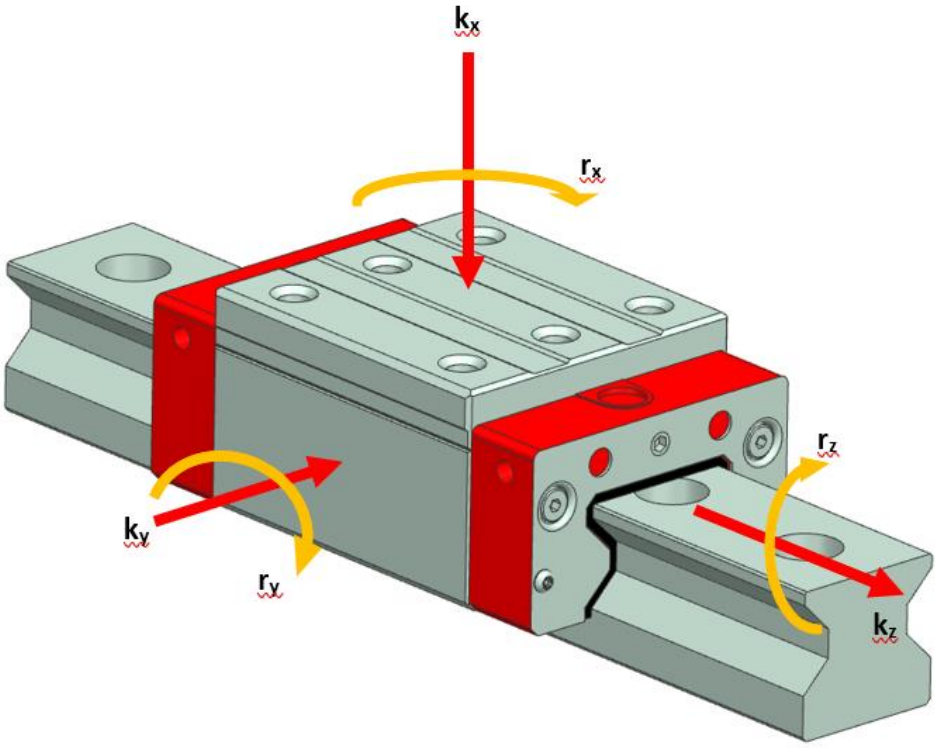

Figure 63 Directionality of extracted coefficients for linear guides.

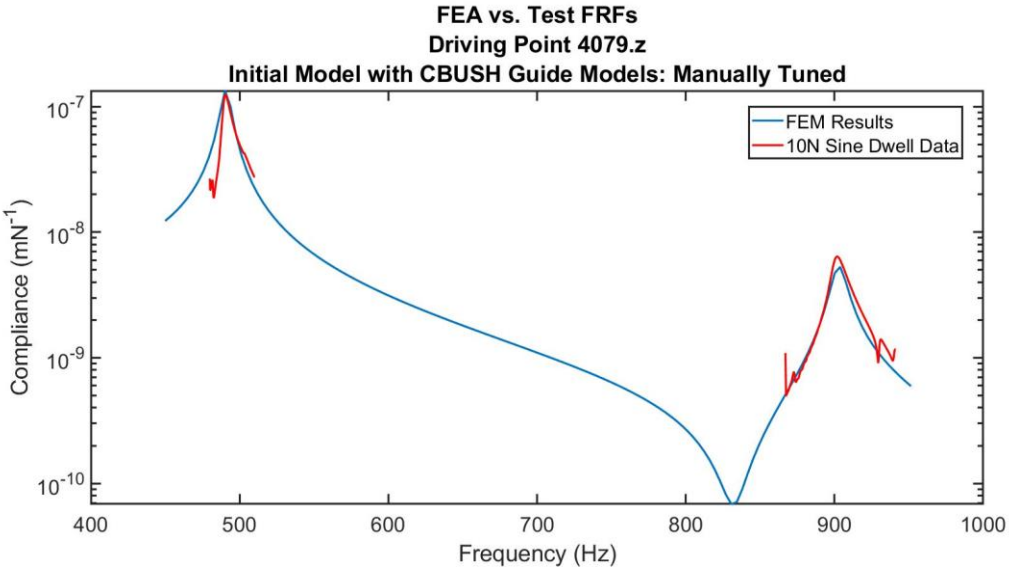

Figure 64 Comparison of FRF data. Red – Measured, Blue – Computed.

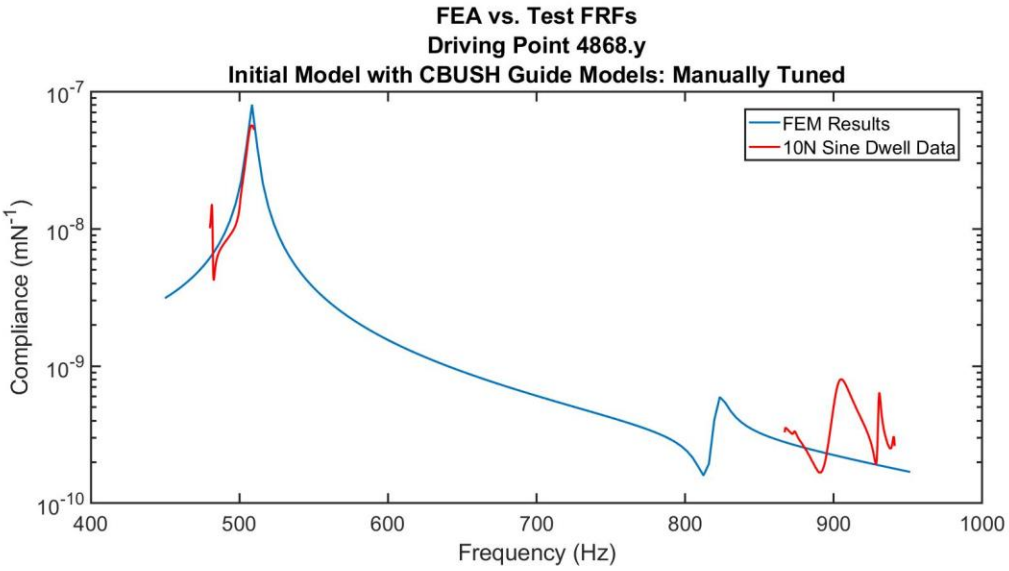

Figure 65 Comparison of FRF data. Red – Measured, Blue – Computed.

3.3.2 Automated Model Updating

An automated model updating scheme was utilized to extract the linear properties of the system. The model updating scheme was somewhat successful, through for the final work conducted the results for the manual scheme were utilized because they more closely approximated the lower-frequency modes.

FEMTools was the commercial software utilized for the model updating. The commercial software had various updating schemes available. For the sake of the model update, the natural frequencies were used along with the mode shapes. For the solver to converge to reasonable natural frequencies with reasonable stiffness estimates a decent initial guess was necessary for the rotational DOFs. The RDOFs were initially estimated at 80,000 Nm/rad. This allowed the algorithm a reasonable value to start with. Without a reasonable initial value, the algorithm was susceptible to local minima and would not arrive at the correct solution.

Figure 66 shows a plot of the natural frequencies. The MAC (pre update) is shown in Figure 67. The agreement between the test and FEA frequencies was not too bad. The largest error was approximately 16% at the lower order modes. The higher order modes were of less interest. Table 3 provides a comparison of the natural frequencies per model updating methodology.

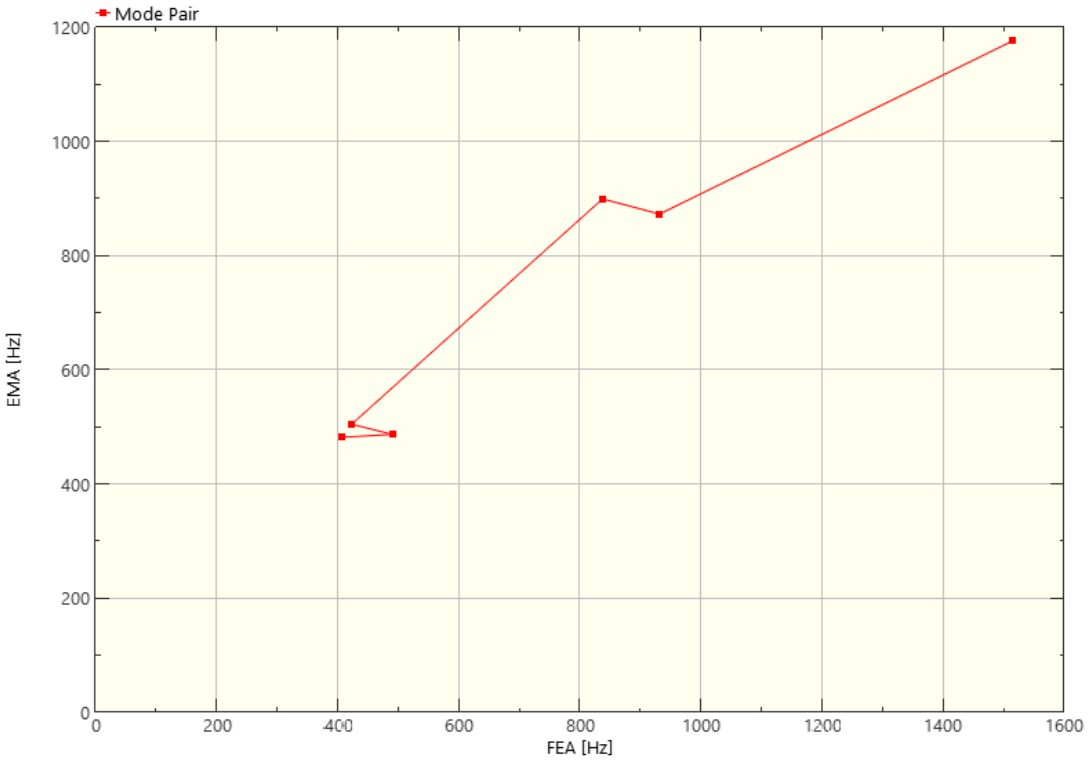

Figure 66 Plot of natural frequencies prior to the automated model update.

Mode Shape Pair	Fn Experimental	Difference Pre-Update	Fn Pre Update	Difference Post Update	Fn Post Automated Update	Difference Post Update	Fn Post Manual Update
1	481	-15.5%	407	-0.01%	481	-2%	471
2	487	0.8%	490	1.83%	495	0%	489
3	504	-16.2%	423	-1.78%	495	-1%	497
4	899	-6.9%	837	-7.34%	833	1.2%	910
5	872	6.8%	931	0.01%	872	-11%	968
6	1176	28.8%	1515	17.41%	1381	29%	1523

Table 3 Table comparing update results.

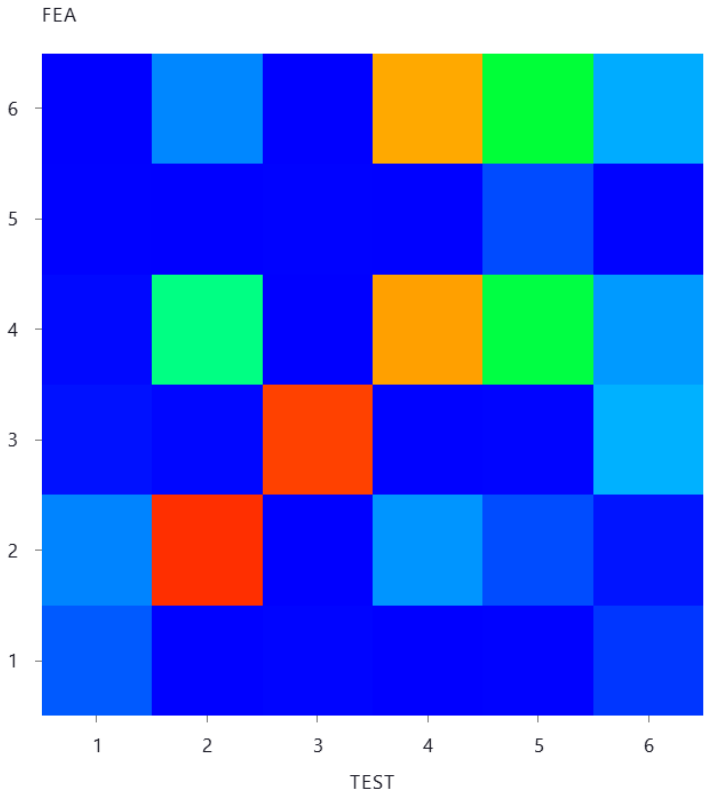

Figure 67 MAC Prior to the automatic model update.

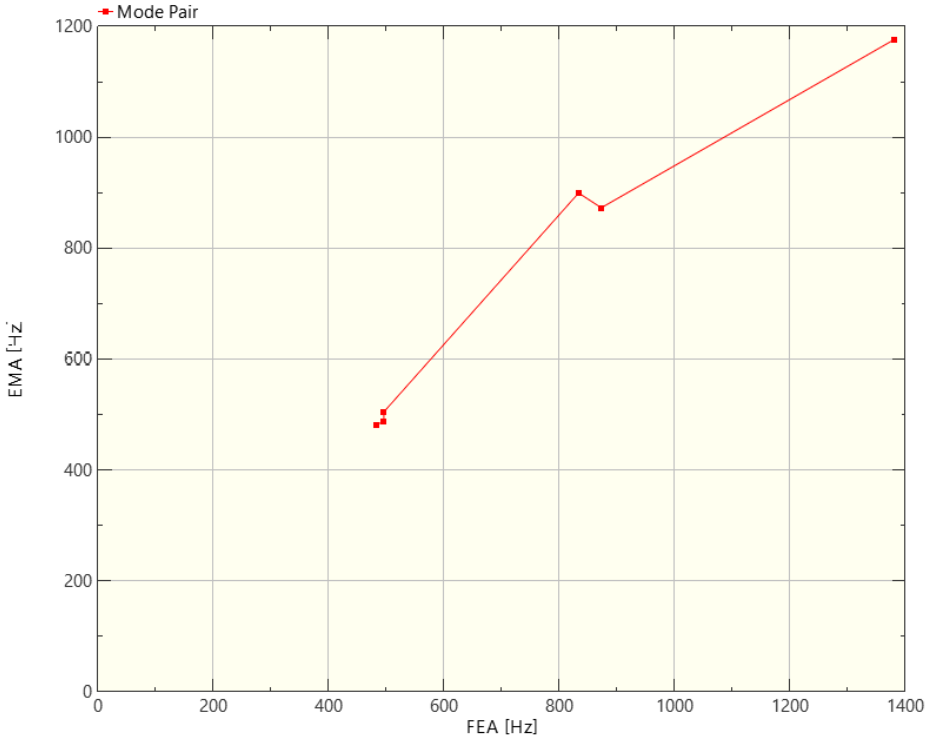

Figure 68 Plot of natural frequencies after the automated model update.

The model updating scheme utilized was CCABS. Better results were observed by setting a maximum parameter change to 0.5% and allowing the algorithm to slowly converge to the solution.

3.3.3 Shortcomings of Linear Model Updating

The linear model updating schemes were valid to a point. A very decent model could be obtained utilizing the linear model updating techniques. Better agreement was desired than that which could be achieved with the linear methodologies. The linear techniques could not account for the softening effects at higher forcing levels. It is important that the model account for the softening effects to accurately produce FRFs which would be used in the computation of stability lobes for machining.

3.4 Further reduced model: Reduction in DOFs of the base plate.

In the execution of the final modeling technique, it was found that a significant amount of computational effort was spent solving the base plate. Due to the nature of assembly of the base plate to the machine base, idealization was performed eliminating the lower portion of the weldment. The connection was replaced with 0-D stiffness elements as shown in Figure 69. The elements were updated to achieve the same performance as observed with the full base-plate model.

This pre-idealization of the base plate model removed 1500 DOFs allowing a significantly faster solve time for the system. Shrewd modeling idealizations of this type are necessary going forward, particularly for modeling of entire machine tool systems. Added DOFs significantly contribute to the computational burden.

As the system was to be solved utilizing modern nonlinear techniques, reduction of the active DOFs was an absolute necessity to ease computational burden. Both techniques which may be utilized to solve this system, shooting or harmonic balance, involve integration of the time domain equations of the system. Integration of the time domain DOFs can be a very computationally expensive process.

It is paramount that the analyst work to eliminate unnecessary DOFs when conducting the work. Other thoughts pertaining to the streamlining of the process are presented in the final chapter as opportunities for future research.

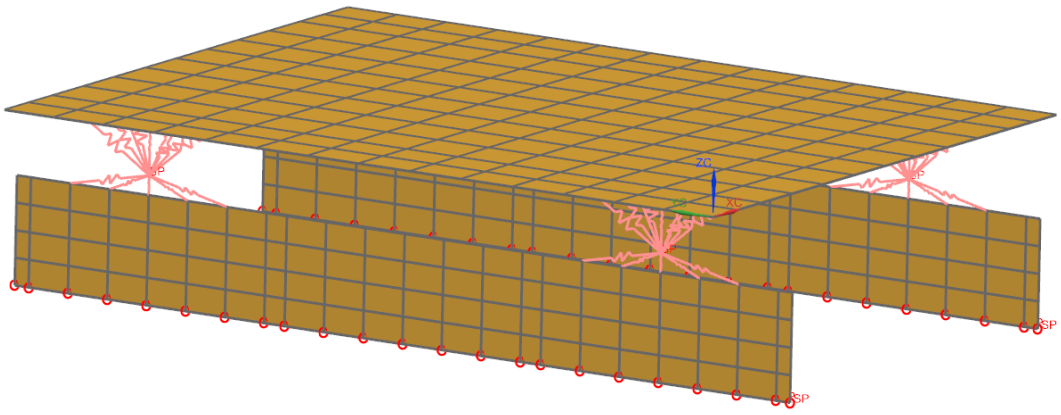

Figure 69 Model utilized for implementation in nonlinear analysis.

Other reduction schemes were attempted to reduce the dimensionality of the model. The other reduction schemes yielded no profitable results. The schemes attempted included Guyan Reduction, Dynamic Reduction, and SEREP. Each technique may be expounded upon for its own benefits and detractors, but none of the attempted techniques were able to help eliminate degrees of freedom from the model. Any of the techniques listed above produced a model stiffer than desired. The modes could no longer be precisely approximated. No additional reduction was applied for the final work.

When Guyan reduction was attempted, a minimized model could note be determined which accurately depicted the modal properties of the system. Guyan reduction resulted in a system which was too stiff. Several schemes were attempted to utilize Guyan reduction. First, more DOFs were added to the plate. A 10 mm mesh was utilized rather than the 50 mm mesh. Then the retained DOFs were selected and the reduction computed. The same results were observed. When reducing the system to a more manageable size, too much fidelity is lost.

SEREP introduced spurious modes. The introduction of the spurious modes made this technique undesirable for the reduction. All modes in the bandwidth of interest were to be retained. SEREP retained the selected modes, but the introduced spurious modes had to be removed. This inhibited the automated application of the technique presented in this work.

An alternate model updating and reduction technique may have been utilized which would have yielded a black-box model. A black box model was not within the interest of this work. The technique involved direct update of the system characteristic equations to

better match the test data. Techniques such as this destroy the fidelity of the system matrices. An attempt is made when formulating the system matrices to estimate parameters of a physical system. When this fidelity is lost, insight is also lost as to meaning of elements within the system. A direct update scheme may work well if the intention were to characterize a single system and use the updated model for predictive work. A major portion of the work presented here is to develop a model of a sub-component of a system which may be deployed when models of prototype equipment are desired.

4 Model Construction

The harmonic balance method plays a significant role in the work presented here. As indicated in Chapter 1, the purpose of this work was to define the characteristics of a set of linear guides in a practical setting. The nonlinear characteristics were to be determined and a modeling methodology developed. The practical application of this work caused several complications which are covered below.

4.1 Preparation of System Matrices

As modern nonlinear techniques are not yet available in commercial solvers, the work had to be conducted in MATLAB. The first challenge was to obtain the model from the pre-post processer utilized. This involved creation of a special MATLAB code to convert the boundary mass and stiffness matrices (output from NASTRAN) into meaningful system matrices which may be used for integration of the equations of motion.

```
DMIG    KAAX            0       6       1       0                       78
DMIG*   KAAX                            1                       1
*                       1               1 1.725780023E+11
DMIG*   KAAX                            1                       2
*                       1               2 1.822441600E+11
DMIG*   KAAX                            1                       3
*                       1               3 1.718459419E+11
DMIG*   KAAX                            1                       4
*                       1               3 8.893568558E+10
*                       1               4 8.055384402E+14
DMIG*   KAAX                            1                       5
*                       1               5 8.026189126E+14
DMIG*   KAAX                            1                       6
*                       1               1-1.118125718E+11
*                       1               6 8.105576949E+14
DMIG*   KAAX                            2                       1
*                       1               1-3.578002299E+09
*                       1               6 1.118125718E+11
*                       2               1 7.156004598E+09
DMIG*   KAAX                            2                       2
*                       1               2-1.324416000E+10
*                       2               2 2.648832000E+10
DMIG*   KAAX                            2                       3
```

Figure 70 NASTRAN .pch file output containing stiffness and mass matrices

The advanced nonlinear techniques presented here have not yet been adopted into commercial FE codes. The pre-processor utilized for this work was SIMCENTER-3D by Siemens. SIMCENTER utilizes NASTRAN language for computations. To that end, the first task was to develop a method to convert the stiffness matrix output from NASTRAN

to something readable and usable by MATLAB. The EXTOUT parameter may be enacted to request the boundary stiffness and mass matrices. MATLAB Code created to convert the .pch file generated by the EXTOUT parameter to full stiffness and mass matrices is presented in Appendix C.

A brief overview of the output format is presented here. Figure 70 shows a portion of the output file. Figure 71 shows a graphical depiction of how the file is formatted. The number circled in red indicates the dimension of the matrix. The mass and stiffness matrices from the FEM are square. The number circled in yellow represents the entry for the indicated location. The location is defined by the numbers circled in green and blue which indicate the element and its associated DOFs. The MATLAB code presented in the appendix may be studied for further understanding. The MATLAB code was rigorously tested and results compared to those calculated with the commercial solver.

Appendix C also presents MATLAB code utilized for post-processing. The NASTRAN input files (.dat) were converted by element and MATLAB plots created to visualize the generated data.

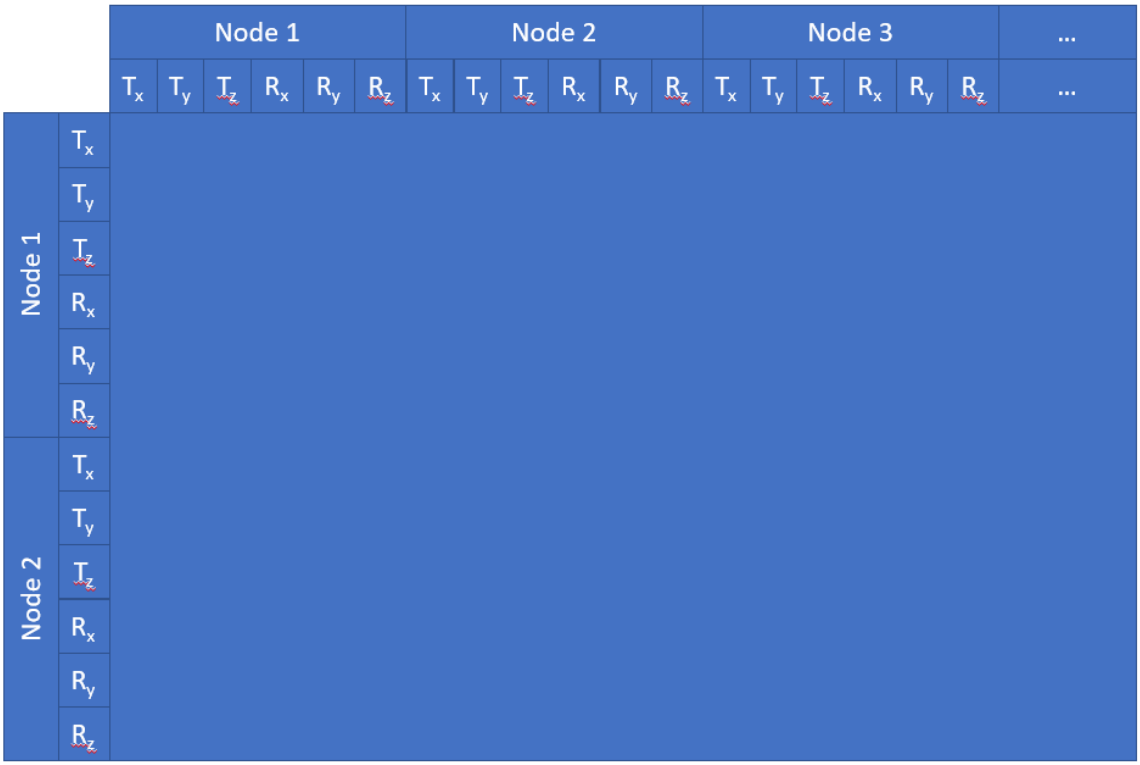

Figure 71 Format of mass and stiffness matrices exported from NASTRAN by EXTOUT parameter.

With a robust method to extract the necessary data for computations the work proceeded with a baseline trial. The MATLAB code utilized for the computations was provided by University of Stuttgart. The baseline model for validation of the procedure is presented

in Figure 72. A cantilevered beam was created with the commercial FE solver and a nonlinear connection added at the end. The nonlinearity mimicked the type of nonlinearity under study in this work. The nonlinearity was cubically softening. The equation for the nonlinearity may be determined from the model in Figure 72.

4.2 Exercise on Trial System

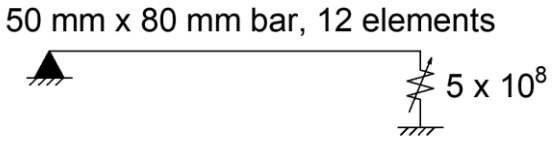

Figure 72 Mechanical schematic of the trial model.

The stiffness matrix of the trial system may be observed in Figure 73.

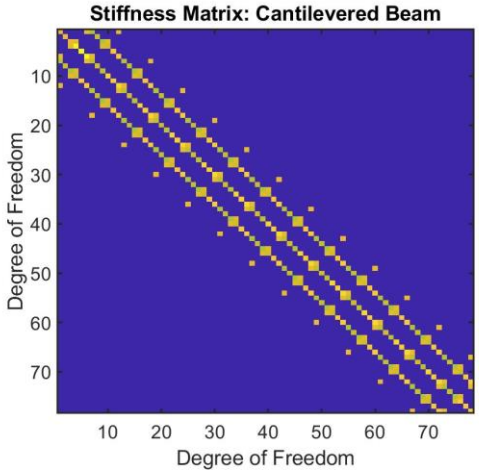

Figure 73 Stiffness matrix of the trial model.

Figure 74 shows the FRFs computed along the length of the beam. The driving point for all FRFs was the tip of the cantilevered beam. The FRFs were computed without the nonlinear attachment to validate the linear system prior to application of the nonlinearity. Exact agreement was observed between the FRFs computed with the direct method and those computed with the harmonic balance method.

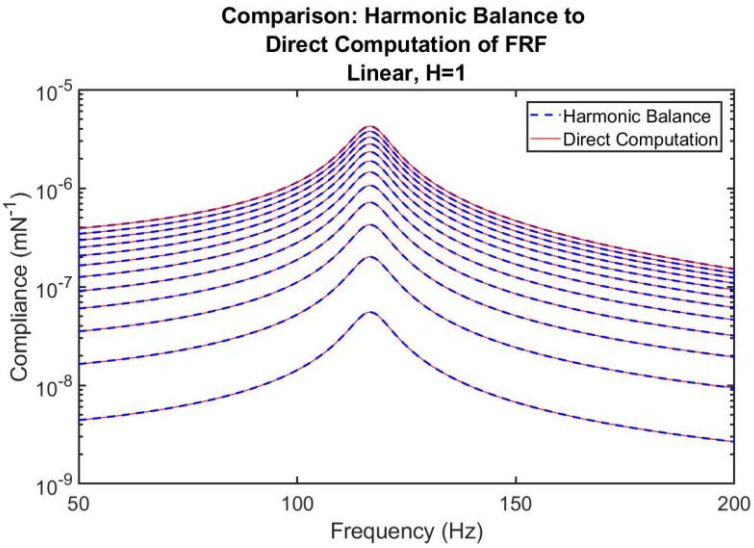

Figure 74 Validation of the harmonic balance code against the directly computed FRFs for the length of the beam.

The results when the nonlinearity is active are presented in Figure 75. The results mimic what was expected and confirm the validity of the MATLAB program and the modeling technique. The blue curve, indicating the FRF with the active nonlinearity tips towards lower frequencies. Seven harmonic were utilized the calculate the data presented in Figure 75.

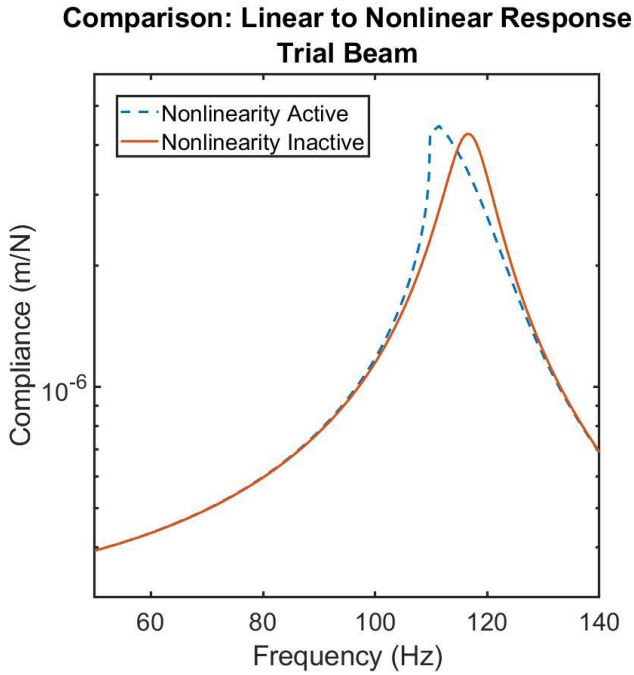

Figure 75 Comparison of the response of the linear system vs the nonlinear system.

The harmonic balance method breaks the computation down to the fundamental signal and its harmonics. The method computes and provides the contribution of each harmonic to the total response. In this manner, the system may be idealized. The fundamental concept of the method is that a system may be modeled by a combination of its constituent harmonics. An example of this is shown in Figure 76. Figure 76 shows a plot of each harmonic. The ordinate may be observed as an indicator of how much each harmonic contributes to the overall system response.

It may be observed that Harmonics 1 and 3 play a significant role in the response. The amplitudes of harmonics 1 and 3 are six orders of magnitude greater than those of harmonics 5 and 7. The amplitudes of harmonics 1 and 3 are also sixteen orders of magnitude greater than those of 2, 4, and 6. This matches expectations. The nonlinear system is an 'odd' system which means the odd harmonics present as dominant and the even harmonics are inconsequential.

There are a number of controls utilized when calculating the results with the harmonic balance method. The factors primarily adjusted in the computation were the continuation scheme and the step size. The inclusion of a number of harmonics may be considered as a method of system abstraction. For re-creating a measured response, perhaps three or five harmonics are all that are necessary as opposed to 10 or 11. In this way, computational efficiency may be further enhanced.

Figure 77 shows the output format of the data generated by the NLvib software. The data was processed into 3-dimensional matrices. The method extracts 'c0' which is the coefficient pertaining to the 0^{th} order harmonic. The method also extracts as many of the subsequent harmonics as are requested.

With a functioning workflow, the procedure was applied to the linear guide system. To re-iterate the process presented and added by this dissertation, the new and novel procedure involves:

1) Acquisition of modal data (this may be avoided if similar information is available for use)
2) Construction of baseline model
3) Update (tuning) of linear model with modal data
4) Application of nonlinearity to model
5) Solution of model with nonlinear technique such as shooting or harmonic balance

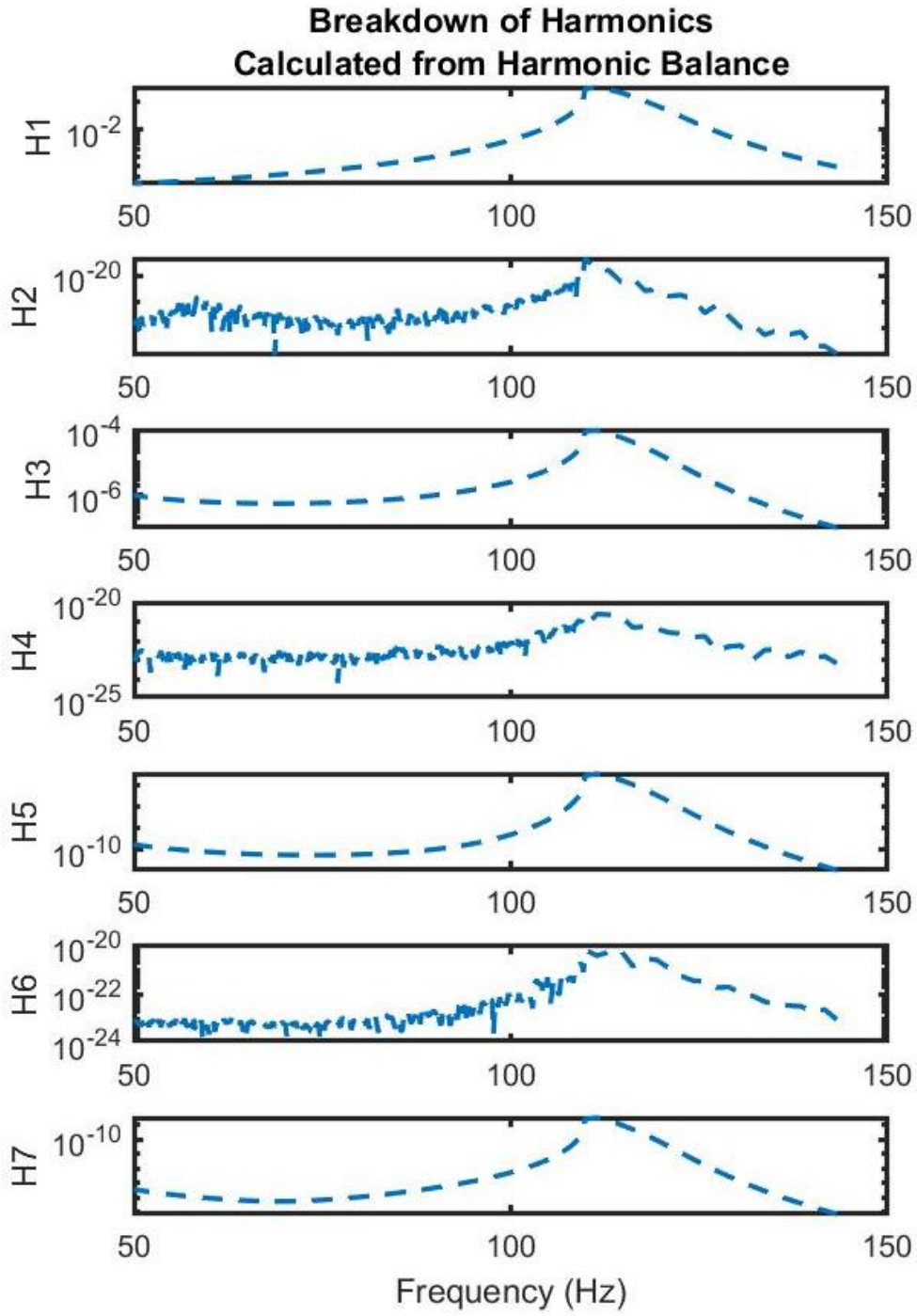

Figure 76 Harmonic breakdown of the response computed with the harmonic balance method.

4.3 Evaluation of procedure on linear guide test stand.

The stiffness matrix imported to MATLAB is shown in Figure 78. The figure shows the overall stiffness matrix. The substructures were assembled along the major diagonal of the matrix. This may be observed by the line representing the principle stiffnesses of the elements along the major diagonal of the matrix. Coupling terms between elements may be observed in the off-diagonal positions. Figure 79 shows a close-up view of the coupling terms. The coupling terms for the linear portion of the analysis are the same as those presented in Chapter 3.

The coupling terms occur diagonally which is consistent with the intent of this work. A 5DOF model was desired for the linear guides which did not account for cross products in the guides themselves. Only direct orthogonal and rotational stiffnesses were desired in the model. Nonlinear elements were combined with the linear elements depicted in Figure 79. Until the procedure is implemented into a commercial FEM code, a strong understanding of how finite element models are assembled is necessary for success.

This model exhibits 20 nonlinearities. Each nonlinearity is cubic and softening. The form of these nonlinearities is to exemplify the characteristics observed and discussed in Chapter 2. Though 20 nonlinearities may be present, only several are to be utilized for the tuning of the model. Also considering the purpose of this work: to establish a global model for the guides as opposed to an individual model, some nonlinearities are assumed to be equivalent.

In this case, all translational and rotational nonlinear terms for the respective guides are expected to be equivalent. This reduces the number of nonlinear coefficients to extract from twenty to five.

The starting point for the simulation assumed a common nonlinear coefficient for each of the cubic springs. Each coefficient was set to -5,000,000 N/m. It was found immediately upon conducting harmonic balance on a physical system that the computational expense is very high.

To verify the model, the linear response was first computed utilizing a single harmonic. The response required approximately four hours of computational time. Though this method is not insurmountable to make it more industrially advantageous improved methods for model reduction are necessary.

After the linear model was verified with one and three harmonics, the tuning of the nonlinear coefficients began. This procedure works well for this type of model and system because the nonlinearities are not significant enough to require many harmonics for proper approximation. More harmonics in the approximation require significantly more computational effort.

Output Data Format
C0
C0
DOF 1 cosine result, Harmonic 1
DOF 2 cosine result, Harmonic 1
DOF n cosine result, Harmonic 1
DOF 1 sine result, Harmonic 1
DOF 2 sine result, Harmonic 1
DOF n sine result, Harmonic 1
DOF 1 cosine result, Harmonic 2
DOF 2 cosine result, Harmonic 2
DOF n cosine result, Harmonic 2
DOF 1 sine result, Harmonic 2
DOF 2 sine result, Harmonic 2
DOF n sine result, Harmonic 2
DOF 1 cosine result, Harmonic H
DOF 2 cosine result, Harmonic H
DOF n cosine result, Harmonic H
DOF 1 sine results, Harmonic H
DOF 2 sine result, Harmonic H
DOF n sine result, Harmonic H
Frequency Line

Figure 77 Output data format for the harmonic balance software utilized.

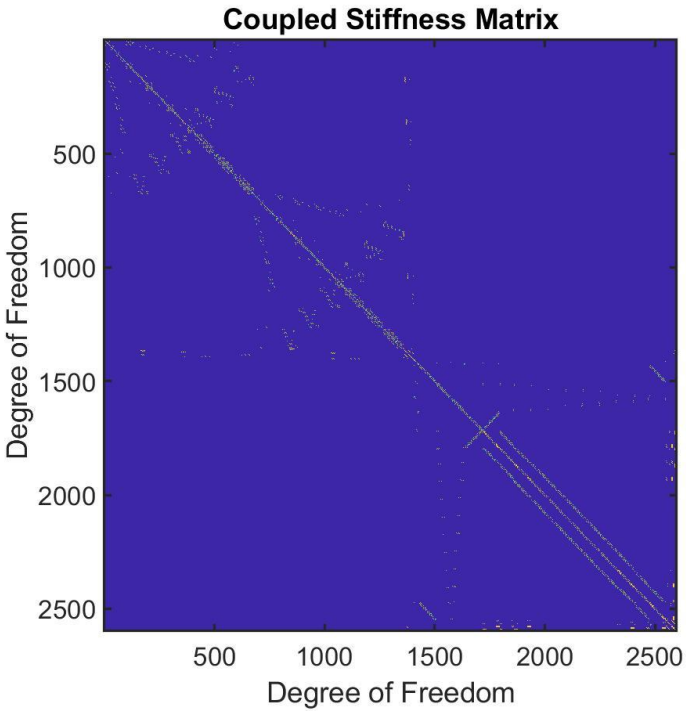

Figure 78 Overall view of the coupled stiffness matrix.

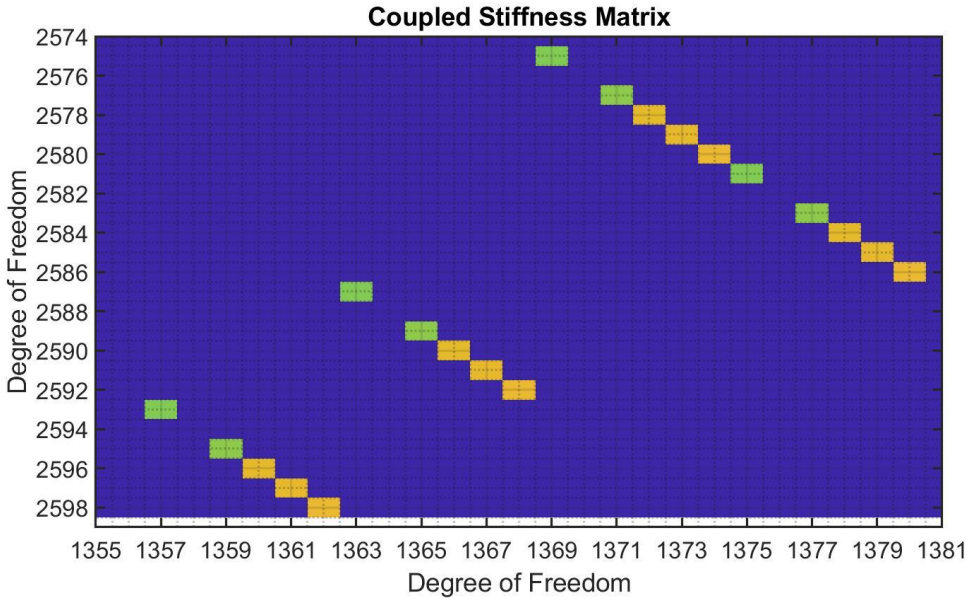

Figure 79 Closeup view of the coupling terms in the stiffness matrix.

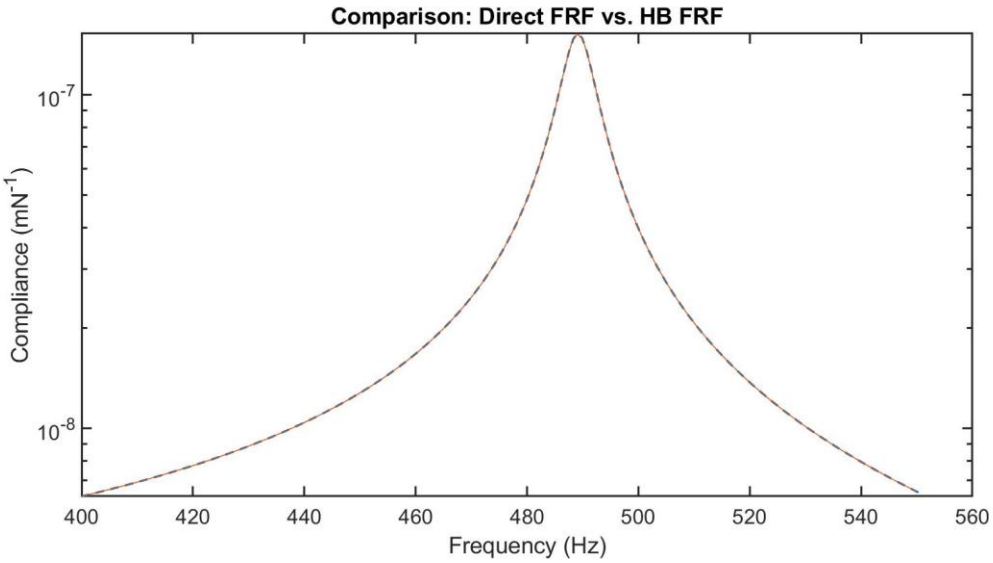

Figure 80 Comparison: Direct FRF vs. HB FRF

For the sake of this work, higher order harmonics are not required. Higher order harmonics are meant to account for energy transferred to higher frequency modes. There is no energy transfer in this case. The energy is simply spread out at the main mode of interest as a function of the nonlinear behavior of the 'spring'. The spring in this case involves the distortion of the truck body and rolling element set.

Tuning was conducted manually. The first stage of tuning was to ensure the nonlinearity *could* be activated. This was accomplished by computing the harmonic balance result at ever increasing force levels until a change in the response was determined. The engineer started at 1 kN of force applied and worked up to 10,000, kN of force. At 10 kN of force, a softening response could be observed.

Once the functionality of the model was validated, tuning began. The force levels were decreased one order of magnitude at a time while the nonlinear coefficients were increased one order of magnitude at a time. Ultimately, 200 N was utilized. This corresponded best with the experimental work discussed earlier in this work.

At 200 N, the nonlinear coefficients were evaluated to be -6e+17. This was the value required to activate and tune the nonlinearity. The value associated to the nonlinearity may seem excessive. It may be considered practical given how the nonlinearity participates in the structure. Surprisingly, all nonlinear coefficients optimize to the same value for this test article. This is attributed to the similar weakening effect experienced by all modes of interest.

Figure 81 depicts the results from the harmonic balance computations at 200 N. The low energy results are also plotted in the figure for reference. The method was capable of accurately depicting the natural frequency and damping decrease associated with the

higher forcing levels. The results do not include the mode indicated to the left of the main resonance in the red plot. That mode was not determined to be driving the response.

In addition to the capability to predict the characteristics of the FRF at resonance, the mass line is accurately depicted. Both lines shown trail off at the same rate and maintain the same shape. This was a very good result when computing responses with harmonic balance. It is worth noting, however, that the results shown in Figure 81 required approximately three days to compute.

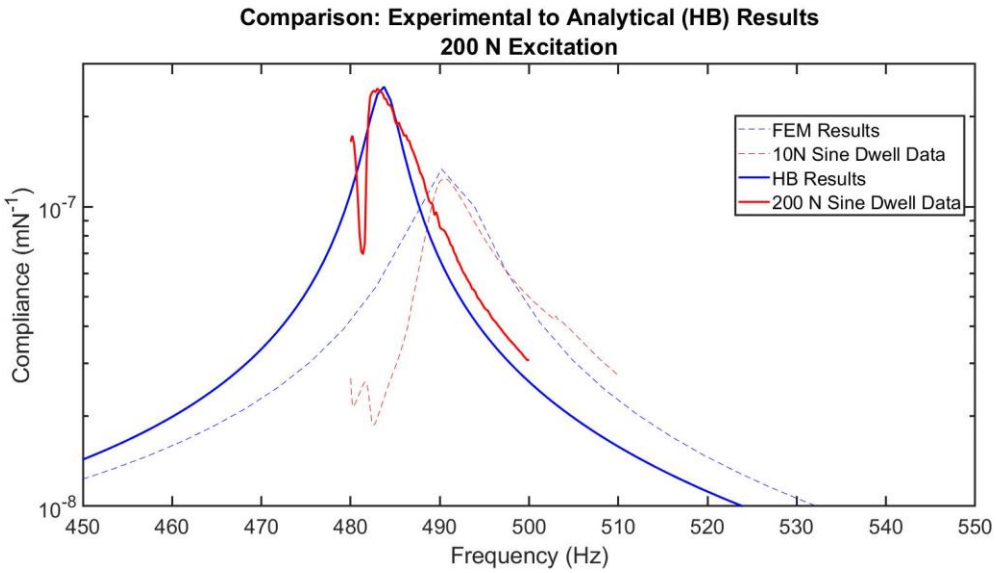

Figure 81 Comparison of experimental results to data computed with Harmonic Balance (200 N) at the first cluster of modes.

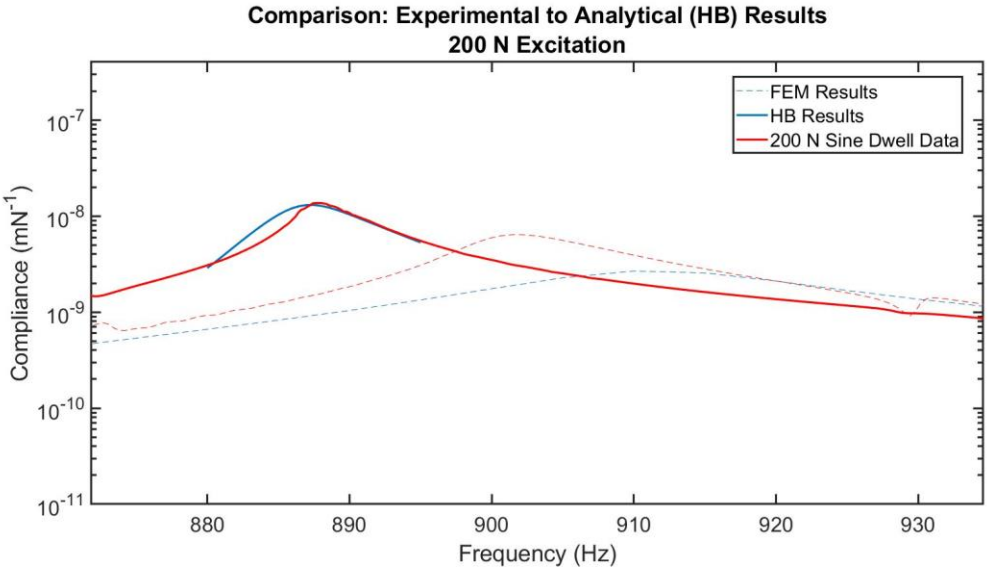

Figure 82 Comparison of experimental results to data computed with Harmonic Balance (200 N) at the second cluster of modes.

The middle band is shown above in Figure 82 and tuned similarly to the lower band of Figure 81. The upper band was not included in the analysis as it was determined to be a linear mode. Discussion on the upper band may be found in previous chapters.

The method was not able to accurately capture the fine details of the bulbous shape of the responses. The responses shown in Figure 81 and Figure 82 have a slightly leaning response which is also indicative of the softening response. The method is capable of capturing this at larger force levels. Given the overall accuracy achieved, the engineer assesses the result as good for use in stability calculations.

Future research should include automation to the tuning. The tuning procedure is very time consuming. Weeks were spent tuning the parameters. Depending on the degree to which the nonlinearity was excited, computations could take between three hours and several days. At the proper forcing levels, computations took approximately three days.

Future research should also involve a GUI. As computers become more capable, this procedure will become much more usable. This is to say that the cost will drop dramatically to conduct these analyses and they may be more commercially available. It would be very helpful for commercial FE solvers (if they are not including harmonic balance as a part of their offering) to develop a user element which may be specifically exported for solving in MATLAB. The user element may have a special property which can be flagged and parameterized for solve with MATLAB or a similar solver suite. All work conducted here involved significant knowledge of how finite element models are assembled. This is not available (or desirable) for the general practitioner. A user interface that may be deployed to specify and parameterize nonlinear elements would make this procedure much more accessible to the garden variety FE user.

The presented method has proven to be a successful methodology for capturing nonlinearity in machine tools. Chapter 5 will cover the deployment of the strategy and procedure for a full machine tool analysis. As indicated earlier – this may be taken as part of a roadmap to develop a user interface to account for nonlinearity in dynamic FE models.

4.4 Modal assembly and direct matrix update

The discerning reader may notice that this work has not made use of direct update of the system matrices to achieve agreement between experimental and analytical results. This work has also not made use of modal assembly. An opportunity is taken here to discuss utilizing modal assembly and direct model updates on the system in question.

Modal Assembly:

In highly nonlinear systems, modal assembly is not recommended because modal assembly relies on the principles of orthogonality. By definition, nonlinear systems do not exhibit orthogonality, thus linear combinations may not be utilized. The engineer

concedes that this system is slightly nonlinear and the basis assumption of this work is that the mode shapes are robust. This assumption was proven true by testing at various forcing levels and extracting mode shapes. Given the robust mode shapes, utilizing modal assembly violated the purposes of this work as outlined at the beginning.

Several adaptations have been proposed to enhance modal assembly techniques. For example, a nonlinear modal stiffness may be placed in parallel with the modal stiffness. Techniques such as harmonic balance may then be utilized to assess the response of each mode. The individual responses may then be summed. Please note that this is possible for weakly nonlinear systems. A modal assembly technique would lend itself nicely to the work presented here *if the end goals were different.* The end goal is to produce a nonlinear model which may be utilized for computations on prototype machines.

Machine assembly varies significantly with structural paradigm. A machine could be box in box – as those typically tested by the engineer. Other machines may be designed with a traveling column or a kinematic system. Each various machine type has different modal properties. To that end, a robust and simple model for the accurate prediction of responses is desired.

A modal model, though significantly less computationally expensive, associates the nonlinearity to the mode, not to the proper element causing the nonlinearity. For this reason, in this work, the engineer has not pursued modal modeling techniques.

Direct Matrix Update:

To state the purpose of this work again, a physical model of the system was desired which the engineer could use for accurately predicting response of *prototype* machine tools. While direct updating schemes would yield more accurate results for the test cases – they would not reproduce the physical significance desired. The linear and nonlinear coefficients were desired which may be utilized in different models. The analyst concedes that the new prototype model may still compute with a few percent error but it will still be significantly more accurate than other commercially available methods.

The analyst plans to look further into direct matrix update methods for future work as direct update would be beneficial for modeling loads on machines currently in use. These methods may prove the best for prediction of responses in existing machine tools when minor changes are to be made. These minor changes may be the use of different tooling.

5 Proposed Assembly Technique

Previous chapters have introduced the technique. The novel technique involves utilizing various aspects of the modern dynamic theory to evaluate nonlinearity in a structural dynamic model and solve for the critical FRFs. This methodology provides for the computation of more accurate FRFs than utilization of traditional means.

This chapter provides the proposed assembly technique on a large scale structure and introduces the overall framework. The models are not solved on a large scale structure such as the one presented. The models may not be reduced to a manageable enough degree. The methods utilized in this work are computationally very demanding. Computation of the simple test stand with either Harmonic Balance or Shooting need not be limited to including only stiffness nonlinearity. The methods may also account for damping nonlinearity. To this point, this work has focused only on capturing the stiffness nonlinearity. When the stiffness nonlinearity is accounted for, the model of the linear guides is accurate enough for good use.

A linear correlated model of the Specht 600, by MAG Automotive is shown in Figure 83. This model has tunable parameters for the joints between the linear substructures. For direct FRF computation, damping may be added between linear substructures as well. The model represents the linear case very well. The linear case would be very representative of low force applications. Be that as it may, this is a production machine and utilized for high force operations.

The modeling technique presented in this work may be utilized to make results more accurate. Several examples of joints are provided in the figures below. A joint of particular concern is the joint between the column and base. This joint is shown in Figure 83.

The joint between the column and base exhibits additional damping and nonlinear effects. This nonlinearity is introduced by local hardening from the bolt loads holding the column to the base. The column is cantilevered a significant distance above this bearing point. Loads at the top of the work zone tend to excite this joint. Several large screws are utilized to hold the components together.

Figure 85 shows the production design of the FE model presented in this work. In application, the rigid connections are utilized to help bulk the stiffnesses, damping, and nonlinear effects to a single element. This work has developed an appropriate model which may be deployed for use with the machine tool.

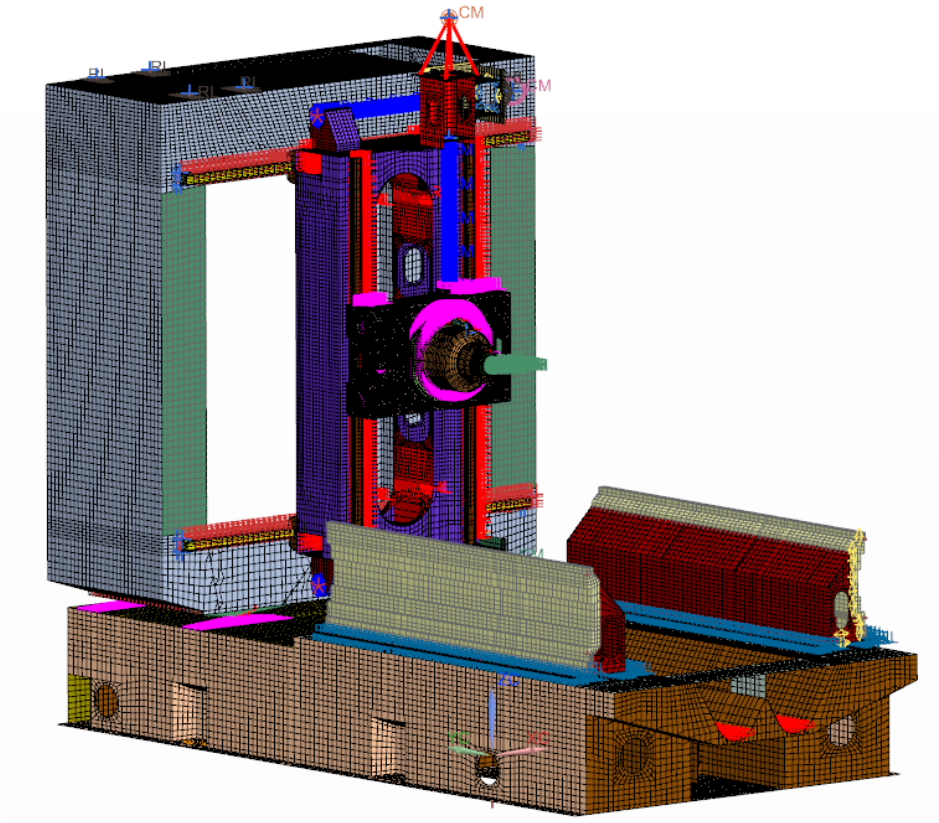

Figure 83 FEM of Specht 600 machines. A number of parameters are included in this model for update and tuning.

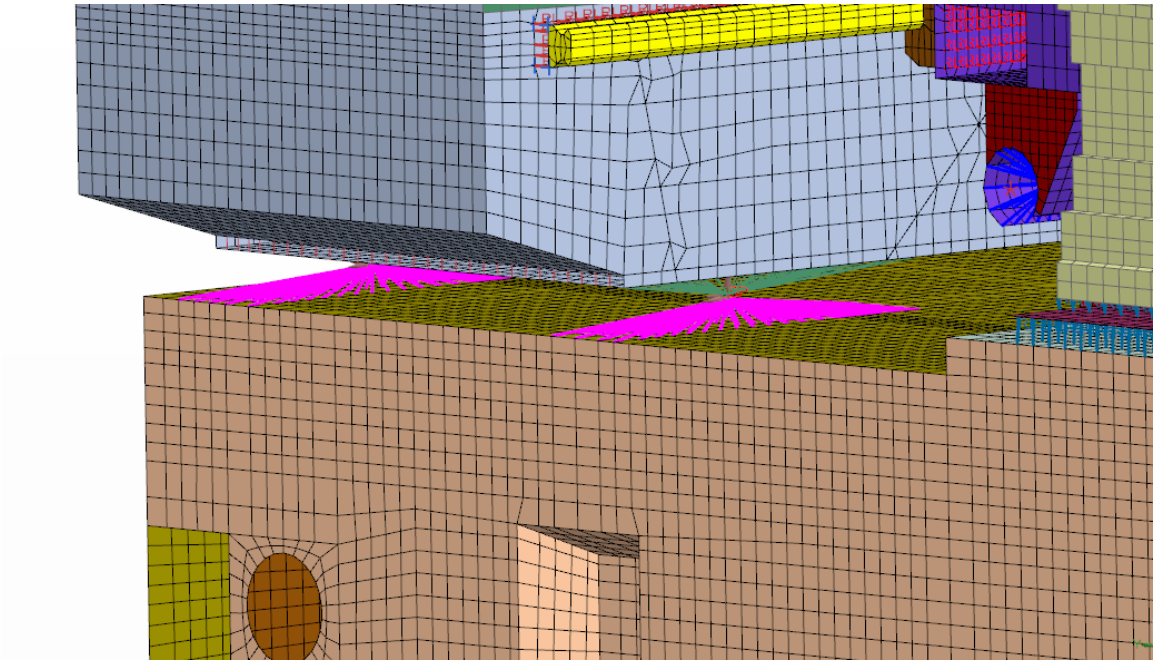

Figure 84 This is an example of the joint between the column and base.

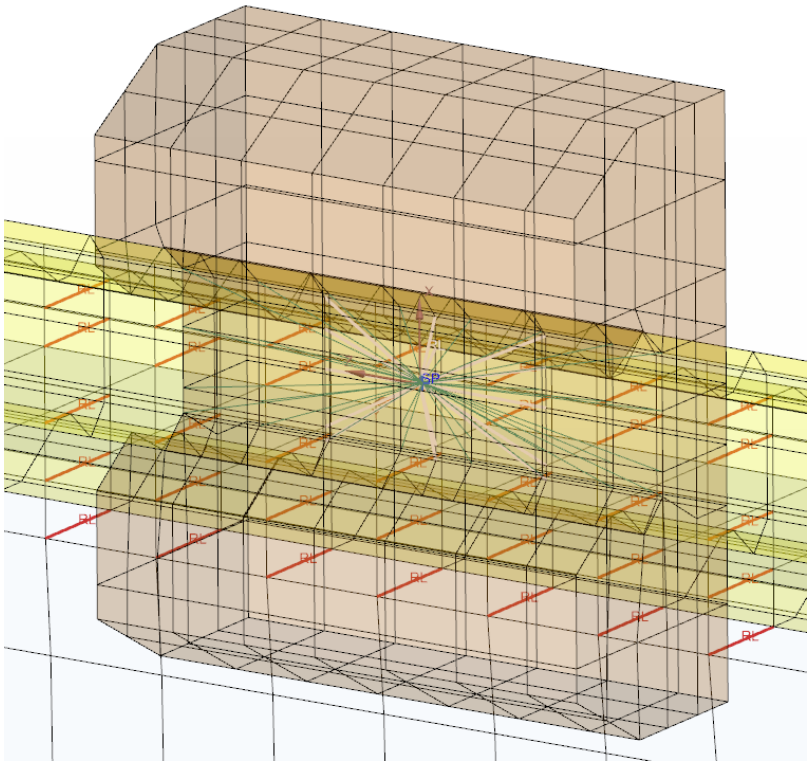

Figure 85 The linear guide model in the production FEM.

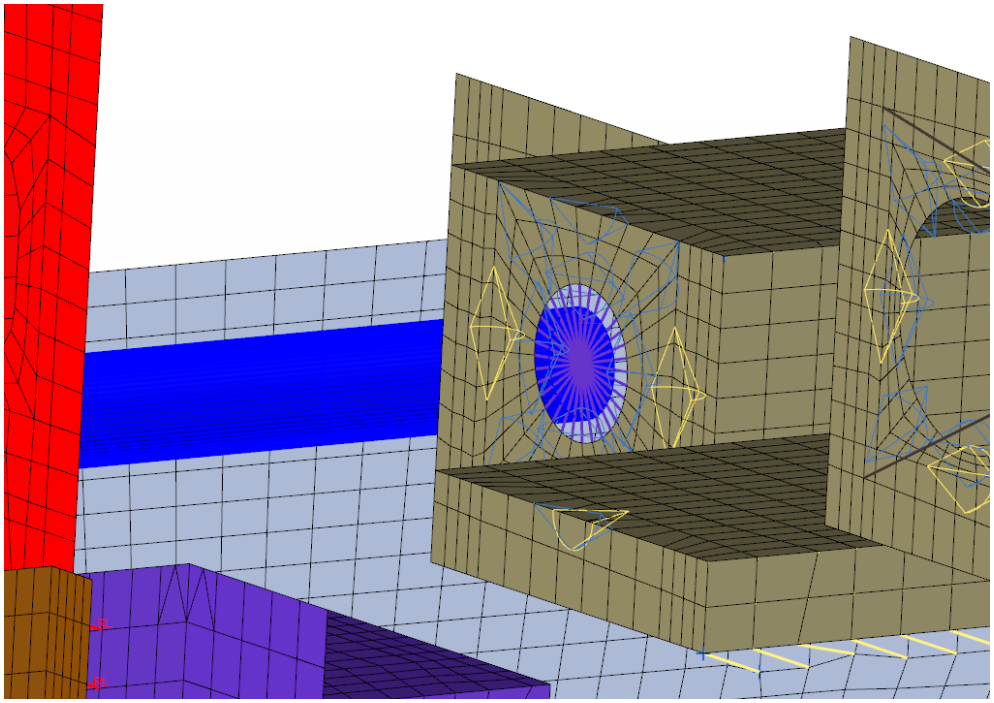

Figure 86 Model of ballscrew connection.

Another example of nonlinear connections in machine tools are the ballscrews. The ballscrew is shown in Figure 86. In this case, a beam element is utilized to model the screw shaft. The bearings on either end are represented by springs. The ballscrew is an example

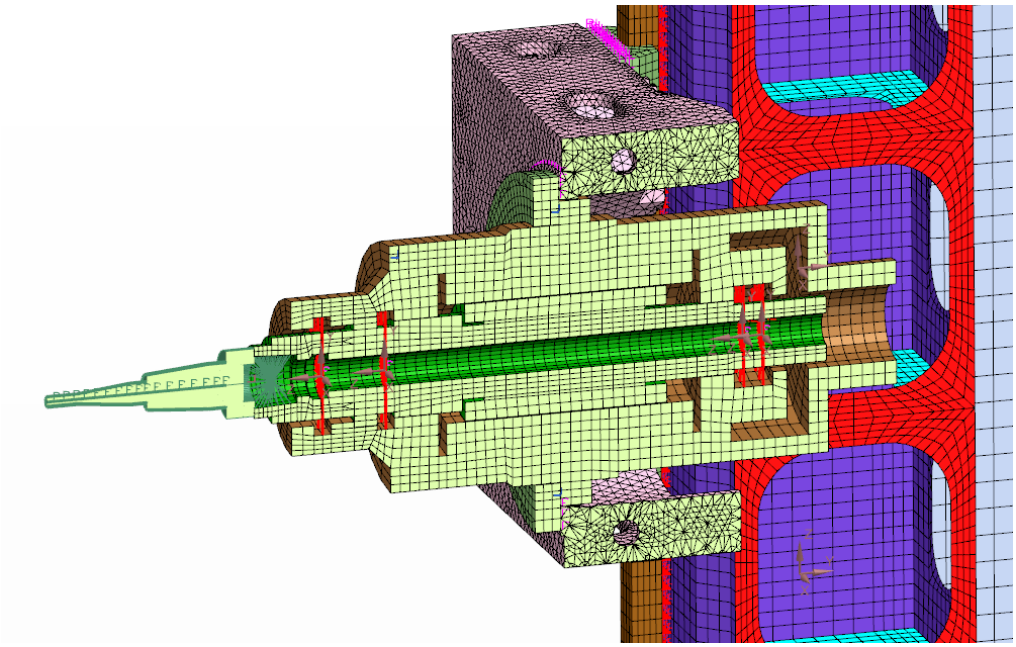

Figure 87 Section of a FE model through the spindle of the Specht 600 machine.

The spindle rounds out the discussion for the primary machine tool structural components. The spindle shown in Figure 87 has four bearings which must be studied and characterized for the model. Spindle modes are simpler to predict at lower frequencies but become more challenging at higher frequencies where they may be excited during sensitive operations. Sensitive operations which may excite spindle modes include reaming and drilling.

The topics presented in this chapter review the primary structure of the machine tool. There are other ancillary structures which are attached to the machine tool which may be considered. These include tool changers, pallet changers or pools, automation, etc.. The engineer typically represents these as masses to help reduce the size and computational expense of the models. As computational capability improves, these other models may be included for an ever more accurate model.

6 Conclusions

This work has investigated nonlinearity in machine tool structures. An extensive analysis was conducted on a physical system and test data presented. Furthermore, various modeling schemes were evaluated and presented. This work yielded a new model for linear guides and a procedure for modeling nonlinear connections in weakly nonlinear systems. The procedure involved:

1) Acquisition of modal data (this may be avoided if similar information is available for use)
2) Construction of baseline model
3) Update (tuning) of linear model with modal data
4) Application of nonlinearity to model
5) Solution of model with nonlinear technique such as shooting or harmonic balance

The model developed (the coefficients extracted) may be utilized in any application of linear guides of that size. The method is robust and may be utilized for any nonlinear element. The targeted nonlinear elements are those found in industrial machinery, particularly bearing elements.

It is beneficial for the machine tool industry to adopt such accurate models for predictive reasons. Greater and greater demands are being made of industrial machinery. The ability to have a predictive model is very valuable. Predictive modeling helps reduce time machinery spends in the technology and validation phase. Tools may be validated prior to construction. The need for trial sets of tools can be eliminated by utilizing advanced modeling techniques. The techniques presented are also very helpful with the prototype modeling of machinery. A prototype machine may be simulated accurately to eliminate necessary revisions and redesigns.

Though the modeling paradigm and procedure yielded good results, there are opportunities for further work. Responses did take a significant amount of time to compute utilizing Harmonic Balance. It is worth noting that the computer utilized was a proper simulation grade workstation with 128 GB RAM and a four core Xenon 3.5 GHz processor.

Improvement of model reduction. This work utilized various methods of model reduction to no avail. There was no technique found that could maintain the proper physical parameters of the system with improved performance. An improved model reduction algorithm which better captures the physical system properties would significantly help with computational effort. Even including only the first harmonic, computations for results presented in this chapter required several days. Once the nonlinearity is triggered, the continuation algorithms utilized must take smaller and smaller steps to track the response. Initial settings provided for a step of 20 rad / sec. Ultimately, the step reduced to approximately 0.3 rad / sec for convergence purposes.

Automation of model tuning. Manual tuning of the nonlinear coefficients took a significant amount of time. This work benefited by a single value representing several instances.

Nonlinear FBS. This method may be utilized in conjunction with FRF modeling. If the linear substructures are represented as FRFs, significant computational time may be eliminated from the procedure. The harmonic balance method may be utilized to solve the nonlinear connections between the linear substructures (represented by their respectful FRFs).

7 Bibliography

[1] R. Geissbauer, S. Schrauf, P. Berttram and F. Cheraghi, "Digital Factories 2020: Shaping the future of manufacturing," PricewaterhouseCoopers GmbH, 2017.

[2] M. Groper, "Microslip and macroslip in bolted joints," *Experimental Mechanics,* vol. 25, no. 2, pp. 171-174, 1985.

[3] A. Dadalau, M. Mottahedi and K. Groh, "Parametric modeling of ball screw spindles," *Computer Aided Engineering,* vol. 4, pp. 625-631, 2010.

[4] G.-f. Y. M.-n. S. a. X.-h. W. L. Mi, "Effects of preloads on joints on dynamic stiffness of a whole machine tool structure," *Journal of Manufacture Science and Engineering,* vol. 26, no. 2, pp. 495-508, 2012.

[5] C. Brecher, B. Eber, J. Falker and M. Fey, "Modeling of ball screw drives rolling element contact characteristics," *CIRP Annals - Manufacturing Technology,* 2018.

[6] J. S. Dhupia, A. G. Ulsoy, R. Katz and B. Powalka, "Experimental Identification of the Nonlinear Parameters of an Industrial Translational Guide for Machine Performance Evaluation," *Journal of Vibration and Control,* vol. 14, no. 5, pp. 645-668, 2008.

[7] S.-W. Kwon, V.-C. Tong and S.-W. Hong, "Five-degrees-of-freedom model for static analysis of linear roller bearing subjected to external loading," *Journal of Mechanical Engineering Science,* pp. 1-19, 2018.

[8] M. Rahmani and F. Bleicher, "Experimental and analytical investigations on normal and angular stiffness of linear guides in manufacturing systems," *CIRP,* no. 41, pp. 795-800, 2016.

[9] A. Dadalau, K. Groh, M. ReuB and A. Verl, "Modeling linear guide systems iwth CoFEM: equivalent models for rolling contact," *Computer Aided Engineering,* pp. 39-46, 2012.

[10] X. Kong, W. Sun, B. Wang and B. Wen, "Dynamic and stability analysis of the linear guide with time-varying piecewise-nonlinear stifness by multi-term incremental harmonic balance method," *Journal of Sound and Vibration,* vol. 346, pp. 265-283, 2015.

[11] F. Montevecchi, N. Grossi, A. Scippa and G. Campatelli, "Improved RCSA technique for efficient tool-tip dynamics prediction," *Precision Engineering,* vol. 44, pp. 152-162, 2016.

[12] J. Ealo, I. Garitaonandia, M. Fernandes, J. Hernandez-Vazquez and J. Munoa, "A practical study of joints in three-dimensional Inverse Receptance Coupling Substructure Analysis method in a horizontal milling machine," *International Journal of Machine Tools and Manufacture,* vol. 128, pp. 41-51, 2018.

[13] L. Guo, H. Zhang and X. Lu, "A New Orthotropic Model for the Stiffness of Machine Tool Joints," in *Proceedings of the World Congress on Engineering*, London, 2013.

[14] A. Dadalau and A. Verl, "Modeling linear guide systems with CoFEM: experimental validation," *Computer Aided Engineering,* pp. 259-265, 2012.

[15] M. Law, Position-Dependent Dynamics and Stability of Machine Tools, Vancouver: University of British Columbia, 2013.

A Bolt torques utilized in assembly of test structure

Size x Pitch	Torque (Nm)
M5 x 0.8	10.3
M6 x 1.0	17.6
M8 x 1.25	42.6
M10 x 1.5	84
M12 x 1.75	146
M16 x 2.0	365
M20 x 2.5	712

B MATLAB Codes

```
function [M,K]=importNASTRAN(aa);
%the purpose of this code is to import the NASTRAN
matrices
%K is the stiffness matrix
%aa is a structure imported to MATLAB using
aa=importdata(...)



%this location in the pch output file gives you the
dimensionality of the
%array we prealocate this space


K=zeros(aa.data(1,5));
jj=2; %jj will be the vertical location in the pch file




kk=1;
sX='MAAX';
sY=aa.textdata{kk,2};
sX_Y=strcmp(sX,sY);
while sX_Y~=1
sY=aa.textdata{kk,2};
sX_Y=strcmp(sX,sY);
kk=kk+1;
end









%% PRE-WHILE LOOP

% Locate the stars - increment until a star is found
s1='*';
```

```
s2=aa.textdata{jj,1};
s1_2=strcmp(s1,s2);
while s1_2==0
jj=jj+1;
s2=aa.textdata{jj,1};
s1_2=strcmp(s1,s2);
end

% Locate the row data and process to useful information
s1='KAAX';
s2=aa.textdata{jj-1,2};
s1_2=strcmp(s1,s2);
if s1_2==1
NodeNoRow=aa.data(jj-1,1); %This is the Node Number for
computing the row position
rowNo=aa.data(jj-1,2);%This is the DOF number for the
row
end

%determine the row index
rowIndex=((NodeNoRow-1)*6)+rowNo;

%determine the array locations for column
Node=str2double(aa.textdata{jj,2});
DOF=aa.data(jj,1);


%utilizing the row index and column value - stick the
data into the matrix
K(rowIndex,(Node-1)*6+DOF)=aa.data(jj,2);
jj=jj+1;

%% Enter Loop to Finish Matrix
while jj<kk-1
s1='*';
s2=aa.textdata{jj,1};
s1_2=strcmp(s1,s2);

while s1_2==0
jj=jj+1;
s2=aa.textdata{jj,1};
s1_2=strcmp(s1,s2);
```

```
end

s1='KAAX';
s2=aa.textdata{jj-1,2};
s1_2=strcmp(s1,s2);
if s1_2==1
NodeNoRow=aa.data(jj-1,1); %This is the Node Number for
computing the row position
rowNo=aa.data(jj-1,2);%This is the DOF number for the
row
end

%determine the row index
rowIndex=((NodeNoRow-1)*6)+rowNo;

%determine the array locations for column
Node=str2double(aa.textdata{jj,2});
DOF=aa.data(jj,1);


%utilizing the row index and column value - stick the
data into the matrix
K(rowIndex,(Node-1)*6+DOF)=aa.data(jj,2);
jj=jj+1;

end

%% MAKE THE UPPER TRIANGLE OF THE MATRIX
Klower=tril(K,-1);
K=K+transpose(Klower);


%% BUILD THE MASS MATRIX









%This section of code finds when the load matrix is
output
kk=1;
```

```
sX='VAX';
sY=aa.textdata{kk,2};
sX_Y=strcmp(sX,sY);
while sX_Y~=1
sY=aa.textdata{kk,2};
sX_Y=strcmp(sX,sY);
kk=kk+1;
end
```

```
%Create Mass Matrix
M=zeros(size(K));
```

```
% Locate the stars - increment until a star is found
s1='*';
s2=aa.textdata{jj,1};
s1_2=strcmp(s1,s2);
while s1_2==0
jj=jj+1;
s2=aa.textdata{jj,1};
s1_2=strcmp(s1,s2);
end
```

```
% Locate the row data and process to useful information
s1='MAAX';
s2=aa.textdata{jj-1,2};
s1_2=strcmp(s1,s2);
if s1_2==1
NodeNoRow=aa.data(jj-1,1); %This is the Node Number for
computing the row position
rowNo=aa.data(jj-1,2);%This is the DOF number for the
row
```

```
end

%determine the row index
rowIndex=((NodeNoRow-1)*6)+rowNo;

%determine the array locations for column
Node=str2double(aa.textdata{jj,2});
DOF=aa.data(jj,1);


%utilizing the row index and column value - stick the
data into the matrix
M(rowIndex,(Node-1)*6+DOF)=aa.data(jj,2);
jj=jj+1;




%% Enter Loop to Finish Matrix
while jj<kk-1 %kk finds the second instance. We must
stop tabulating before the first instance
s1='*';
s2=aa.textdata{jj,1};
s1_2=strcmp(s1,s2);

while s1_2==0
jj=jj+1;
s2=aa.textdata{jj,1};
s1_2=strcmp(s1,s2);
end

s1='MAAX';
s2=aa.textdata{jj-1,2};
s1_2=strcmp(s1,s2);
if s1_2==1
NodeNoRow=aa.data(jj-1,1); %This is the Node Number for
computing the row position
rowNo=aa.data(jj-1,2);%This is the DOF number for the
row
end

%determine the row index
rowIndex=((NodeNoRow-1)*6)+rowNo;
```

```
%determine the array locations for column
Node=str2double(aa.textdata{jj,2});
DOF=aa.data(jj,1);


%utilizing the row index and column value - stick the
data into the matrix
M(rowIndex,(Node-1)*6+DOF)=aa.data(jj,2);
jj=jj+1;

end
```

C FNSI and ASM Methods Explained

FNSI

FNSI or Frequency Domain Nonlinear Subspace Identification is a means of parameter estimation. As indicated earlier in the text, FNSI relies upon a specific type of excitation data to utilize the algorithm. Periodic random data is utilized to excite the test structure.

The periodic random data is played into the test structure and analyzed for periodicity. The first several periods, containing transients, are discarded. The balance of the data is utilized for the acquisition. The time data is Fourier transformed and frequency lines of interest are selected. Input and output observability matrices are then constructed and a typical procedure utilized to determine the state space matrices.

As described in the text, the dependance of this algorithm on periodic random data inhibits its use on test structures of this type. The test structure was too stiff to be adequately excited with periodic random excitation.

ASM

ASM, or the Acceleration Surface Method is a means of determining the form and magnitude of a nonlinearity. ASM is conducted with swept sine testing. A time domain signal is acquired from an accelerometer. The signal is integrated to velocity, then again to displacement. The three signals are then plotted against one another in a 3-dimensional grid. The surface obtained from the plot indicates the type and characteristic of the nonlinearity. The text gave the example of a smooth cubic softening nonlinearity.

D Copyright documentation

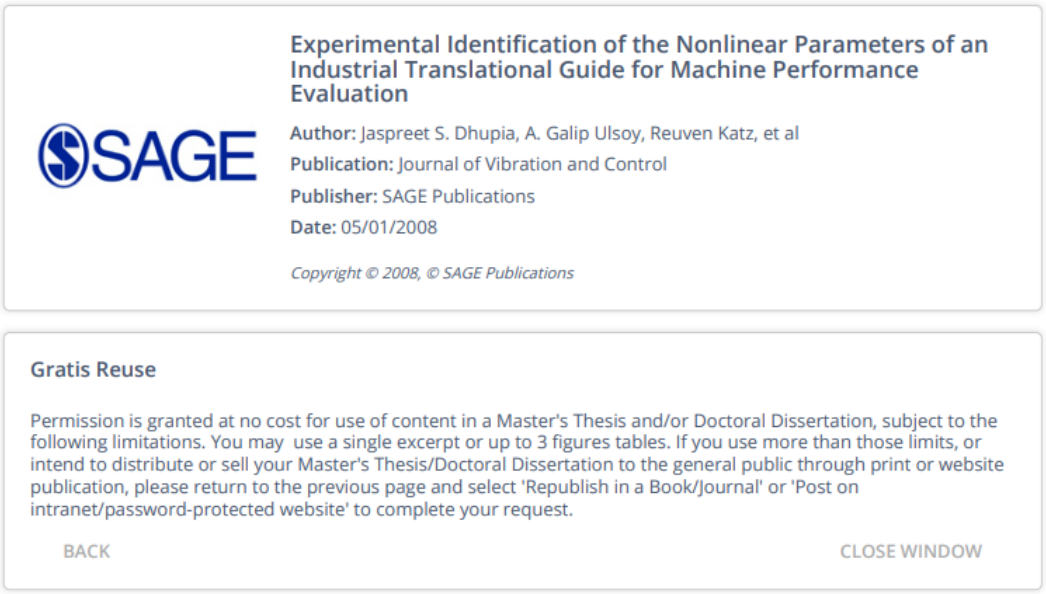

Experimental Identification of the Nonlinear Parameters of an Industrial Translational Guide for Machine Performance Evaluation

Author: Jaspreet S. Dhupia, A. Galip Ulsoy, Reuven Katz, et al

Publication: Journal of Vibration and Control

Publisher: SAGE Publications

Date: 05/01/2008

Experimental Identification of the Nonlinear Parameters of an Industrial Translational Guide for Machine Performance Evaluation

Author: Jaspreet S. Dhupia, A. Galip Ulsoy, Reuven Katz, et al

Publication: Journal of Vibration and Control

Publisher: SAGE Publications

Date: 05/01/2008

SPRINGER NATURE LICENSE
TERMS AND CONDITIONS

Feb 16, 2021

This Agreement between Michigan Technological University -- Steven Whitican ("You") and Springer Nature ("Springer Nature") consists of your license details and the terms and conditions provided by Springer Nature and Copyright Clearance Center.

License Number	5010820626776
License date	Feb 16, 2021
Licensed Content Publisher	Springer Nature
Licensed Content Publication	Production Engineering
Licensed Content Title	Modeling linear guide systems with CoFEM: equivalent models for rolling contact
Licensed Content Author	A. Dadalau et al
Licensed Content Date	Dec 6, 2011
Type of Use	Thesis/Dissertation

Requestor type	non-commercial (non-profit)
Format	print and electronic
Portion	figures/tables/illustrations
Number of figures/tables/illustrations	3
Will you be translating?	no
Circulation/distribution	1 - 29
Author of this Springer Nature content	no
Title	NOVEL NEW MODELING PROCEDURE FOR INDUSTRIAL MACHINERY WITH NONLINEAR CONNECTIONS
Institution name	Michigan Technological University
Expected presentation date	May 2021
Order reference number	Fig 1, Fig 3, Fig 10
Portions	I am using Fig 1, 3, and 10 in my literature review. I am using it to compare different methods for modeling linear guides.
	Michigan Technological University

Requestor Location

NORTH STREET, MI 48049
United States
Attn: Michigan Technological University

Total 0.00 USD

Terms and Conditions

Springer Nature Customer Service Centre GmbH
Terms and Conditions

This agreement sets out the terms and conditions of the licence (the **Licence**) between you and **Springer Nature Customer Service Centre GmbH** (the **Licensor**). By clicking 'accept' and completing the transaction for the material (**Licensed Material**), you also confirm your acceptance of these terms and conditions.

1. Grant of License

1. 1. The Licensor grants you a personal, non-exclusive, non-transferable, world-wide licence to reproduce the Licensed Material for the purpose specified in your order only. Licences are granted for the specific use requested in the order and for no other use, subject to the conditions below.

1. 2. The Licensor warrants that it has, to the best of its knowledge, the rights to license reuse of the Licensed Material. However, you should ensure that the material you are requesting is original to the Licensor and does not carry the copyright of another entity (as credited in the published version).

1. 3. If the credit line on any part of the material you have requested indicates that it was reprinted or adapted with permission from another source, then you should also seek permission from that source to reuse the material.

2. Scope of Licence

2. 1. You may only use the Licensed Content in the manner and to the extent permitted by these Ts&Cs and any applicable laws.

2. 2. A separate licence may be required for any additional use of the Licensed Material, e.g. where a licence has been purchased for print only use, separate permission must be obtained for electronic re-use. Similarly, a licence is only valid in the language selected and does not apply for editions in other languages unless additional translation rights have been granted separately in the licence. Any content owned by third parties are expressly excluded from the licence.

2. 3. Similarly, rights for additional components such as custom editions and derivatives require additional permission and may be subject to an additional fee. Please apply to Journalpermissions@springernature.com/bookpermissions@springernature.com for these rights.

2. 4. Where permission has been granted **free of charge** for material in print, permission may also be granted for any electronic version of that work, provided that the material is incidental to your work as a whole and that the electronic version is essentially equivalent to, or substitutes for, the print version.

2. 5. An alternative scope of licence may apply to signatories of the STM Permissions Guidelines, as amended from time to time.

3. Duration of Licence

3. 1. A licence for is valid from the date of purchase ('Licence Date') at the end of the relevant period in the below table:

Scope of Licence	Duration of Licence
Post on a website	12 months
Presentations	12 months
Books and journals	Lifetime of the edition in the language purchased

4. Acknowledgement

4. 1. The Licensor's permission must be acknowledged next to the Licenced Material in print. In electronic form, this acknowledgement must be visible at the same time as the figures/tables/illustrations or abstract, and must be hyperlinked to the journal/book's homepage. Our required acknowledgement format is in the Appendix below.

5. Restrictions on use

5. 1. Use of the Licensed Material may be permitted for incidental promotional use and minor editing privileges e.g. minor adaptations of single figures, changes of format, colour and/or style where the adaptation is credited as set out in Appendix 1 below. Any other changes including but not limited to, cropping, adapting, omitting material that affect the meaning, intention or moral rights of the author are strictly prohibited.

5. 2. You must not use any Licensed Material as part of any design or trademark.

5. 3. Licensed Material may be used in Open Access Publications (OAP) before publication by Springer Nature, but any Licensed Material must be removed from OAP sites prior to final publication.

6. Ownership of Rights

6. 1. Licensed Material remains the property of either Licensor or the relevant third party and any rights not explicitly granted herein are expressly reserved.

7. Warranty

IN NO EVENT SHALL LICENSOR BE LIABLE TO YOU OR ANY OTHER PARTY OR ANY OTHER PERSON OR FOR ANY SPECIAL, CONSEQUENTIAL, INCIDENTAL OR INDIRECT DAMAGES, HOWEVER CAUSED, ARISING OUT OF OR IN CONNECTION WITH THE DOWNLOADING, VIEWING OR USE OF THE MATERIALS REGARDLESS OF THE FORM OF ACTION, WHETHER FOR BREACH OF CONTRACT, BREACH OF WARRANTY, TORT, NEGLIGENCE, INFRINGEMENT OR OTHERWISE (INCLUDING, WITHOUT LIMITATION, DAMAGES BASED ON LOSS OF PROFITS, DATA, FILES, USE, BUSINESS OPPORTUNITY OR CLAIMS OF THIRD PARTIES), AND
WHETHER OR NOT THE PARTY HAS BEEN ADVISED OF THE POSSIBILITY OF SUCH DAMAGES. THIS LIMITATION SHALL APPLY NOTWITHSTANDING ANY FAILURE OF ESSENTIAL PURPOSE OF ANY LIMITED REMEDY PROVIDED HEREIN.

8. Limitations

8. 1. ***BOOKS ONLY:*** Where **'reuse in a dissertation/thesis'** has been selected the following terms apply: Print rights of the final author's accepted manuscript (for clarity, NOT the published version) for up to 100 copies, electronic rights for use only on a personal website or institutional repository as defined by the Sherpa guideline (www.sherpa.ac.uk/romeo/).

8. 2. For content reuse requests that qualify for permission under the STM Permissions Guidelines, which may be updated from time to time, the STM Permissions Guidelines supersede the terms and conditions contained in this licence.

9. Termination and Cancellation

9. 1. Licences will expire after the period shown in Clause 3 (above).

9. 2. Licensee reserves the right to terminate the Licence in the event that payment is not received in full or if there has been a breach of this agreement by you.

Appendix 1 — Acknowledgements:

For Journal Content:
Reprinted by permission from [**the Licensor**]: [**Journal Publisher** (e.g. Nature/Springer/Palgrave)] [**JOURNAL NAME**] [**REFERENCE CITATION** (Article name, Author(s) Name), [**COPYRIGHT**] (year of publication)

For **Advance Online Publication papers:**
Reprinted by permission from [**the Licensor**]: [**Journal Publisher** (e.g. Nature/Springer/Palgrave)] [**JOURNAL NAME**] [**REFERENCE CITATION** (Article name, Author(s) Name), [**COPYRIGHT**] (year of publication), advance online publication, day month year (doi: 10.1038/sj.[JOURNAL ACRONYM].)

For Adaptations/Translations:
Adapted/Translated by permission from [**the Licensor**]: [**Journal Publisher** (e.g. Nature/Springer/Palgrave)] [**JOURNAL NAME**] [**REFERENCE CITATION** (Article name, Author(s) Name), [**COPYRIGHT**] (year of publication)

Note: For any republication from the British Journal of Cancer, the following credit line style applies:

Reprinted/adapted/translated by permission from [**the Licensor**]: on behalf of Cancer Research UK: : [**Journal Publisher** (e.g. Nature/Springer/Palgrave)] [**JOURNAL NAME**] [**REFERENCE CITATION** (Article name, Author(s) Name), [**COPYRIGHT**] (year of publication)

For **Advance Online Publication** papers:
Reprinted by permission from The [**the Licensor**]: on behalf of Cancer Research UK: [**Journal Publisher** (e.g. Nature/Springer/Palgrave)] [**JOURNAL NAME**] [**REFERENCE CITATION** (Article name, Author(s) Name), [**COPYRIGHT**] (year of publication), advance online publication, day month year (doi: 10.1038/sj. [JOURNAL ACRONYM])

For Book content:
Reprinted/adapted by permission from [**the Licensor**]: [**Book Publisher** (e.g. Palgrave Macmillan, Springer etc) [**Book Title**] by [**Book author**(s)] [**COPYRIGHT**] (year of publication)

Other Conditions:

Version 1.3

Questions? customercare@copyright.com or +1-855-239-3415 (toll free in the US) or +1-978-646-2777.

ELSEVIER LICENSE
TERMS AND CONDITIONS

Feb 16, 2021

This Agreement between Michigan Technological University -- Steven Whitican ("You") and Elsevier ("Elsevier") consists of your license details and the terms and conditions provided by Elsevier and Copyright Clearance Center.

License Number	5010821385565
License date	Feb 16, 2021
Licensed Content Publisher	Elsevier
Licensed Content Publication	International Journal of Machine Tools and Manufacture
Licensed Content Title	A practical study of joints in three-dimensional Inverse Receptance Coupling Substructure Analysis method in a horizontal milling machine
Licensed Content Author	J.A. Ealo,I. Garitaonandia,M.H. Fernandes,J.M. Hernandez-Vazquez,J. Muñoa
Licensed Content Date	May 1, 2018

Licensed Content Volume	128
Licensed Content Issue	n/a
Licensed Content Pages	11
Start Page	41
End Page	51
Type of Use	reuse in a thesis/dissertation
Portion	figures/tables/illustrations
Number of figures/tables/illustrations	1
Format	both print and electronic
Are you the author of this Elsevier article?	No
Will you be translating?	No
Title	NOVEL NEW MODELING PROCEDURE FOR INDUSTRIAL MACHINERY WITH NONLINEAR CONNECTIONS

Institution name	Michigan Technological University
Expected presentation date	May 2021
Portions	I would like to use Figure 9 in my literature review.
Requestor Location	Michigan Technological University 4015 Wadhams Rd, North Street, MI, USA NORTH STREET, MI 48049 United States Attn: Michigan Technological University
Publisher Tax ID	98-0397604
Total	0.00 USD

Terms and Conditions

INTRODUCTION

1. The publisher for this copyrighted material is Elsevier. By clicking "accept" in connection with completing this licensing transaction, you agree that the following terms and conditions apply to this transaction (along with the Billing and Payment terms and conditions established by Copyright Clearance Center, Inc. ("CCC"), at the time that you opened your Rightslink account and that are available at any time at http://myaccount.copyright.com).

GENERAL TERMS

2. Elsevier hereby grants you permission to reproduce the aforementioned material subject to the terms and conditions indicated.

3. Acknowledgement: If any part of the material to be used (for example, figures) has appeared in our publication with credit or acknowledgement to another source, permission must also be sought from that source. If such permission is not obtained then that material may not be included in your publication/copies. Suitable acknowledgement to the source must be made, either as a footnote or in a reference list at the end of your publication, as follows:

"Reprinted from Publication title, Vol /edition number, Author(s), Title of article / title of chapter, Pages No., Copyright (Year), with permission from Elsevier [OR APPLICABLE SOCIETY COPYRIGHT OWNER]." Also Lancet special credit - "Reprinted from The Lancet, Vol. number, Author(s), Title of article, Pages No., Copyright (Year), with permission from Elsevier."

4. Reproduction of this material is confined to the purpose and/or media for which permission is hereby given.

5. Altering/Modifying Material: Not Permitted. However figures and illustrations may be altered/adapted minimally to serve your work. Any other abbreviations, additions, deletions and/or any other alterations shall be made only with prior written authorization of Elsevier Ltd. (Please contact Elsevier's permissions helpdesk here). No modifications can be made to any Lancet figures/tables and they must be reproduced in full.

6. If the permission fee for the requested use of our material is waived in this instance, please be advised that your future requests for Elsevier materials may attract a fee.

7. Reservation of Rights: Publisher reserves all rights not specifically granted in the combination of (i) the license details provided by you and accepted in the course of this licensing transaction, (ii) these terms and conditions and (iii) CCC's Billing and Payment terms and conditions.

8. License Contingent Upon Payment: While you may exercise the rights licensed immediately upon issuance of the license at the end of the licensing process for the transaction, provided that you have disclosed complete and accurate details of your proposed use, no license is finally effective unless and until full payment is received from you (either by publisher or by CCC) as provided in CCC's Billing and Payment terms and conditions. If

8. License Contingent Upon Payment: While you may exercise the rights licensed immediately upon issuance of the license at the end of the licensing process for the transaction, provided that you have disclosed complete and accurate details of your proposed use, no license is finally effective unless and until full payment is received from you (either by publisher or by CCC) as provided in CCC's Billing and Payment terms and conditions. If full payment is not received on a timely basis, then any license preliminarily granted shall be deemed automatically revoked and shall be void as if never granted. Further, in the event that you breach any of these terms and conditions or any of CCC's Billing and Payment terms and conditions, the license is automatically revoked and shall be void as if never granted. Use of materials as described in a revoked license, as well as any use of the materials beyond the scope of an unrevoked license, may constitute copyright infringement and publisher reserves the right to take any and all action to protect its copyright in the materials.

9. Warranties: Publisher makes no representations or warranties with respect to the licensed material.

10. Indemnity: You hereby indemnify and agree to hold harmless publisher and CCC, and their respective officers, directors, employees and agents, from and against any and all claims arising out of your use of the licensed material other than as specifically authorized pursuant to this license.

11. No Transfer of License: This license is personal to you and may not be sublicensed, assigned, or transferred by you to any other person without publisher's written permission.

12. No Amendment Except in Writing: This license may not be amended except in a writing signed by both parties (or, in the case of publisher, by CCC on publisher's behalf).

13. Objection to Contrary Terms: Publisher hereby objects to any terms contained in any purchase order, acknowledgment, check endorsement or other writing prepared by you, which terms are inconsistent with these terms and conditions or CCC's Billing and Payment terms and conditions. These terms and conditions, together with CCC's Billing and Payment terms and conditions (which are incorporated herein), comprise the entire agreement between you and publisher (and CCC) concerning this licensing transaction. In the event of any conflict between your obligations established by these terms and conditions and those established by CCC's Billing and Payment terms and conditions, these terms and conditions shall control.

14. Revocation: Elsevier or Copyright Clearance Center may deny the permissions described in this License at their sole discretion, for any reason or no reason, with a full refund payable to you. Notice of such denial will be made using the contact information provided by you. Failure to receive such notice will not alter or invalidate the denial. In no event will Elsevier or Copyright Clearance Center be responsible or liable for any costs, expenses or damage incurred by you as a result of a denial of your permission request, other than a refund of the amount(s) paid by you to Elsevier and/or Copyright Clearance Center for denied permissions.

LIMITED LICENSE

The following terms and conditions apply only to specific license types:

15. **Translation**: This permission is granted for non-exclusive world **English** rights only unless your license was granted for translation rights. If you licensed translation rights you may only translate this content into the languages you requested. A professional translator must perform all translations and reproduce the content word for word preserving the integrity of the article.

16. **Posting licensed content on any Website**: The following terms and conditions apply as follows: Licensing material from an Elsevier journal: All content posted to the web site must maintain the copyright information line on the bottom of each image; A hyper-text must be included to the Homepage of the journal from which you are licensing at http://www.sciencedirect.com/science/journal/xxxxx or the Elsevier homepage for books at http://www.elsevier.com; Central Storage: This license does not include permission for a scanned version of the material to be stored in a central repository such as that provided by Heron/XanEdu.

Licensing material from an Elsevier book: A hyper-text link must be included to the Elsevier homepage at http://www.elsevier.com . All content posted to the web site must maintain the copyright information line on the bottom of each image.

Posting licensed content on Electronic reserve: In addition to the above the following clauses are applicable: The web site must be password-protected and made available only to bona fide students registered on a relevant course. This permission is granted for 1 year only. You may obtain a new license for future website posting.

17. **For journal authors:** the following clauses are applicable in addition to the above:

Preprints:

A preprint is an author's own write-up of research results and analysis, it has not been peer-reviewed, nor has it had any other value added to it by a publisher (such as formatting, copyright, technical enhancement etc.).

Authors can share their preprints anywhere at any time. Preprints should not be added to or enhanced in any way in order to appear more like, or to substitute for, the final versions of articles however authors can update their preprints on arXiv or RePEc with their Accepted Author Manuscript (see below).

If accepted for publication, we encourage authors to link from the preprint to their formal publication via its DOI. Millions of researchers have access to the formal publications on ScienceDirect, and so links will help users to find, access, cite and use the best available version. Please note that Cell Press, The Lancet and some society-owned have different preprint policies. Information on these policies is available on the journal homepage.

Accepted Author Manuscripts: An accepted author manuscript is the manuscript of an article that has been accepted for publication and which typically includes author-incorporated changes suggested during submission, peer review and editor-author communications.

Authors can share their accepted author manuscript:

- immediately
    - via their non-commercial person homepage or blog
    - by updating a preprint in arXiv or RePEc with the accepted manuscript
    - via their research institute or institutional repository for internal institutional uses or as part of an invitation-only research collaboration work-group
    - directly by providing copies to their students or to research collaborators for their personal use
    - for private scholarly sharing as part of an invitation-only work group on commercial sites with which Elsevier has an agreement
- After the embargo period
    - via non-commercial hosting platforms such as their institutional repository
    - via commercial sites with which Elsevier has an agreement

In all cases accepted manuscripts should:

- link to the formal publication via its DOI
- bear a CC-BY-NC-ND license - this is easy to do
- if aggregated with other manuscripts, for example in a repository or other site, be shared in alignment with our hosting policy not be added to or enhanced in any way to appear more like, or to substitute for, the published journal article.

Published journal article (JPA): A published journal article (PJA) is the definitive final record of published research that appears or will appear in the journal and embodies all value-adding publishing activities including peer review co-ordination, copy-editing, formatting, (if relevant) pagination and online enrichment.

Policies for sharing publishing journal articles differ for subscription and gold open access articles:

Subscription Articles: If you are an author, please share a link to your article rather than the full-text. Millions of researchers have access to the formal publications on ScienceDirect, and so links will help your users to find, access, cite, and use the best available version.

Theses and dissertations which contain embedded PJAs as part of the formal submission can be posted publicly by the awarding institution with DOI links back to the formal publications on ScienceDirect.

If you are affiliated with a library that subscribes to ScienceDirect you have additional private sharing rights for others' research accessed under that agreement. This includes use for classroom teaching and internal training at the institution (including use in course packs and courseware programs), and inclusion of the article for grant funding purposes.

Gold Open Access Articles: May be shared according to the author-selected end-user license and should contain a CrossMark logo, the end user license, and a DOI link to the formal publication on ScienceDirect.

Please refer to Elsevier's posting policy for further information.

18. **For book authors** the following clauses are applicable in addition to the above: Authors are permitted to place a brief summary of their work online only. You are not allowed to download and post the published electronic version of your chapter, nor may you scan the printed edition to create an electronic version. **Posting to a repository:** Authors are permitted to post a summary of their chapter only in their institution's repository.

19. **Thesis/Dissertation**: If your license is for use in a thesis/dissertation your thesis may be submitted to your institution in either print or electronic form. Should your thesis be published commercially, please reapply for permission. These requirements include permission for the Library and Archives of Canada to supply single copies, on demand, of the complete thesis and include permission for Proquest/UMI to supply single copies, on demand, of the complete thesis. Should your thesis be published commercially, please reapply for permission. Theses and dissertations which contain embedded PJAs as part of the formal submission can be posted publicly by the awarding institution with DOI links back to the formal publications on ScienceDirect.

Elsevier Open Access Terms and Conditions

You can publish open access with Elsevier in hundreds of open access journals or in nearly 2000 established subscription journals that support open access publishing. Permitted third party re-use of these open access articles is defined by the author's choice of Creative Commons user license. See our open access license policy for more information.

Terms & Conditions applicable to all Open Access articles published with Elsevier:

Any reuse of the article must not represent the author as endorsing the adaptation of the article nor should the article be modified in such a way as to damage the author's honour or reputation. If any changes have been made, such changes must be clearly indicated.

The author(s) must be appropriately credited and we ask that you include the end user license and a DOI link to the formal publication on ScienceDirect.

Posting or linking by commercial companies for use by customers of those companies.

20. **Other Conditions**:

v1.10

Questions? customercare@copyright.com or +1-855-239-3415 (toll free in the US) or +1-978-646-2777.

ELSEVIER LICENSE
TERMS AND CONDITIONS

Feb 16, 2021

This Agreement between Michigan Technological University -- Steven Whitican ("You") and Elsevier ("Elsevier") consists of your license details and the terms and conditions provided by Elsevier and Copyright Clearance Center.

License Number	5010840551210
License date	Feb 16, 2021
Licensed Content Publisher	Elsevier
Licensed Content Publication	Journal of Sound and Vibration
Licensed Content Title	Dynamic and stability analysis of the linear guide with time-varying, piecewise-nonlinear stiffness by multi-term incremental harmonic balance method
Licensed Content Author	Xiangxi Kong,Wei Sun,Bo Wang,Bangchun Wen
Licensed Content Date	Jun 23, 2015

Licensed Content Issue	n/a
Licensed Content Pages	19
Start Page	265
End Page	283
Type of Use	reuse in a thesis/dissertation
Portion	figures/tables/illustrations
Number of figures/tables/illustrations	2
Format	both print and electronic
Are you the author of this Elsevier article?	No
Will you be translating?	No
Title	NOVEL NEW MODELING PROCEDURE FOR INDUSTRIAL MACHINERY WITH NONLINEAR CONNECTIONS
Institution name	Michigan Technological University

Expected presentation date	May 2021
Portions	I am using portions of Figure 21-24 (the LH graphs) in my literature review.
Requestor Location	Michigan Technological University 4015 Wadhams Rd, North Street, MI, USA NORTH STREET, MI 48049 United States Attn: Michigan Technological University
Publisher Tax ID	98-0397604
Total	0.00 USD

Terms and Conditions

INTRODUCTION

1. The publisher for this copyrighted material is Elsevier. By clicking "accept" in connection with completing this licensing transaction, you agree that the following terms and conditions apply to this transaction (along with the Billing and Payment terms and conditions established by Copyright Clearance Center, Inc. ("CCC"), at the time that you opened your Rightslink account and that are available at any time at http://myaccount.copyright.com).

GENERAL TERMS

2. Elsevier hereby grants you permission to reproduce the aforementioned material subject to the terms and conditions indicated.

3. Acknowledgement: If any part of the material to be used (for example, figures) has appeared in our publication with credit or acknowledgement to another source, permission must also be sought from that source. If such permission is not obtained then that material may not be included in your publication/copies. Suitable acknowledgement to the source must be made, either as a footnote or in a reference list at the end of your publication, as follows:

"Reprinted from Publication title, Vol /edition number, Author(s), Title of article / title of chapter, Pages No., Copyright (Year), with permission from Elsevier [OR APPLICABLE SOCIETY COPYRIGHT OWNER]." Also Lancet special credit - "Reprinted from The Lancet, Vol. number, Author(s), Title of article, Pages No., Copyright (Year), with permission from Elsevier."

4. Reproduction of this material is confined to the purpose and/or media for which permission is hereby given.

5. Altering/Modifying Material: Not Permitted. However figures and illustrations may be altered/adapted minimally to serve your work. Any other abbreviations, additions, deletions and/or any other alterations shall be made only with prior written authorization of Elsevier Ltd. (Please contact Elsevier's permissions helpdesk here). No modifications can be made to any Lancet figures/tables and they must be reproduced in full.

6. If the permission fee for the requested use of our material is waived in this instance, please be advised that your future requests for Elsevier materials may attract a fee.

7. Reservation of Rights: Publisher reserves all rights not specifically granted in the combination of (i) the license details provided by you and accepted in the course of this licensing transaction, (ii) these terms and conditions and (iii) CCC's Billing and Payment terms and conditions.

8. License Contingent Upon Payment: While you may exercise the rights licensed immediately upon issuance of the license at the end of the licensing process for the transaction, provided that you have disclosed complete and accurate details of your proposed use, no license is finally effective unless and until full payment is received from you (either by publisher or by CCC) as provided in CCC's Billing and Payment terms and conditions. If full payment is not received on a timely basis, then any license preliminarily granted shall be deemed automatically revoked and shall be void as if never granted. Further, in the event that you breach any of these terms and conditions or any of CCC's Billing and Payment terms and conditions, the license is automatically revoked and shall be void as if never granted. Use of materials as described in a revoked license, as well as any use of the

materials beyond the scope of an unrevoked license, may constitute copyright infringement and publisher reserves the right to take any and all action to protect its copyright in the materials.

9. Warranties: Publisher makes no representations or warranties with respect to the licensed material.

10. Indemnity: You hereby indemnify and agree to hold harmless publisher and CCC, and their respective officers, directors, employees and agents, from and against any and all claims arising out of your use of the licensed material other than as specifically authorized pursuant to this license.

11. No Transfer of License: This license is personal to you and may not be sublicensed, assigned, or transferred by you to any other person without publisher's written permission.

12. No Amendment Except in Writing: This license may not be amended except in a writing signed by both parties (or, in the case of publisher, by CCC on publisher's behalf).

13. Objection to Contrary Terms: Publisher hereby objects to any terms contained in any purchase order, acknowledgment, check endorsement or other writing prepared by you, which terms are inconsistent with these terms and conditions or CCC's Billing and Payment terms and conditions. These terms and conditions, together with CCC's Billing and Payment terms and conditions (which are incorporated herein), comprise the entire agreement between you and publisher (and CCC) concerning this licensing transaction. In the event of any conflict between your obligations established by these terms and conditions and those established by CCC's Billing and Payment terms and conditions, these terms and conditions shall control.

14. Revocation: Elsevier or Copyright Clearance Center may deny the permissions described in this License at their sole discretion, for any reason or no reason, with a full refund payable to you. Notice of such denial will be made using the contact information provided by you. Failure to receive such notice will not alter or invalidate the denial. In no event will Elsevier or Copyright Clearance Center be responsible or liable for any costs, expenses or damage incurred by you as a result of a denial of your permission request, other than a refund of the amount(s) paid by you to Elsevier and/or Copyright Clearance Center for denied permissions.

LIMITED LICENSE

The following terms and conditions apply only to specific license types:

15. **Translation**: This permission is granted for non-exclusive world **English** rights only unless your license was granted for translation rights. If you licensed translation rights you may only translate this content into the languages you requested. A professional translator must perform all translations and reproduce the content word for word preserving the integrity of the article.

16. **Posting licensed content on any Website**: The following terms and conditions apply as follows: Licensing material from an Elsevier journal: All content posted to the web site must maintain the copyright information line on the bottom of each image; A hyper-text must be included to the Homepage of the journal from which you are licensing at http://www.sciencedirect.com/science/journal/xxxxx or the Elsevier homepage for books at http://www.elsevier.com; Central Storage: This license does not include permission for a scanned version of the material to be stored in a central repository such as that provided by Heron/XanEdu.

Licensing material from an Elsevier book: A hyper-text link must be included to the Elsevier homepage at http://www.elsevier.com . All content posted to the web site must maintain the copyright information line on the bottom of each image.

Posting licensed content on Electronic reserve: In addition to the above the following clauses are applicable: The web site must be password-protected and made available only to bona fide students registered on a relevant course. This permission is granted for 1 year only. You may obtain a new license for future website posting.

17. **For journal authors:** the following clauses are applicable in addition to the above:

Preprints:

A preprint is an author's own write-up of research results and analysis, it has not been peer-reviewed, nor has it had any other value added to it by a publisher (such as formatting, copyright, technical enhancement etc.).

Authors can share their preprints anywhere at any time. Preprints should not be added to or enhanced in any way in order to appear more like, or to substitute for, the final versions of articles however authors can update their preprints on arXiv or RePEc with their Accepted Author Manuscript (see below).

If accepted for publication, we encourage authors to link from the preprint to their formal publication via its DOI. Millions of researchers have access to the formal publications on ScienceDirect, and so links will help users to find, access, cite and use the best available version. Please note that Cell Press, The Lancet and some society-owned have different preprint policies. Information on these policies is available on the journal homepage.

Accepted Author Manuscripts: An accepted author manuscript is the manuscript of an article that has been accepted for publication and which typically includes author-incorporated changes suggested during submission, peer review and editor-author communications.

Authors can share their accepted author manuscript:

- immediately
    - via their non-commercial person homepage or blog
    - by updating a preprint in arXiv or RePEc with the accepted manuscript
    - via their research institute or institutional repository for internal institutional uses or as part of an invitation-only research collaboration work-group
    - directly by providing copies to their students or to research collaborators for their personal use
    - for private scholarly sharing as part of an invitation-only work group on commercial sites with which Elsevier has an agreement
- After the embargo period
    - via non-commercial hosting platforms such as their institutional repository
    - via commercial sites with which Elsevier has an agreement

In all cases accepted manuscripts should:

- link to the formal publication via its DOI
- bear a CC-BY-NC-ND license - this is easy to do
- if aggregated with other manuscripts, for example in a repository or other site, be shared in alignment with our hosting policy not be added to or enhanced in any way to appear more like, or to substitute for, the published journal article.

Published journal article (JPA): A published journal article (PJA) is the definitive final

record of published research that appears or will appear in the journal and embodies all value-adding publishing activities including peer review co-ordination, copy-editing, formatting, (if relevant) pagination and online enrichment.

Policies for sharing publishing journal articles differ for subscription and gold open access articles:

Subscription Articles: If you are an author, please share a link to your article rather than the full-text. Millions of researchers have access to the formal publications on ScienceDirect, and so links will help your users to find, access, cite, and use the best available version.

Theses and dissertations which contain embedded PJAs as part of the formal submission can be posted publicly by the awarding institution with DOI links back to the formal publications on ScienceDirect.

If you are affiliated with a library that subscribes to ScienceDirect you have additional private sharing rights for others' research accessed under that agreement. This includes use for classroom teaching and internal training at the institution (including use in course packs and courseware programs), and inclusion of the article for grant funding purposes.

Gold Open Access Articles: May be shared according to the author-selected end-user license and should contain a CrossMark logo, the end user license, and a DOI link to the formal publication on ScienceDirect.

Please refer to Elsevier's posting policy for further information.

18. **For book authors** the following clauses are applicable in addition to the above: Authors are permitted to place a brief summary of their work online only. You are not allowed to download and post the published electronic version of your chapter, nor may you scan the printed edition to create an electronic version. **Posting to a repository:** Authors are permitted to post a summary of their chapter only in their institution's repository.

19. **Thesis/Dissertation**: If your license is for use in a thesis/dissertation your thesis may be submitted to your institution in either print or electronic form. Should your thesis be published commercially, please reapply for permission. These requirements include permission for the Library and Archives of Canada to supply single copies, on demand, of the complete thesis and include permission for Proquest/UMI to supply single copies, on demand, of the complete thesis. Should your thesis be published commercially, please reapply for permission. Theses and dissertations which contain embedded PJAs as part of the formal submission can be posted publicly by the awarding institution with DOI links back to the formal publications on ScienceDirect.

Elsevier Open Access Terms and Conditions

You can publish open access with Elsevier in hundreds of open access journals or in nearly 2000 established subscription journals that support open access publishing. Permitted third party re-use of these open access articles is defined by the author's choice of Creative Commons user license. See our open access license policy for more information.

Terms & Conditions applicable to all Open Access articles published with Elsevier:

Any reuse of the article must not represent the author as endorsing the adaptation of the article nor should the article be modified in such a way as to damage the author's honour or reputation. If any changes have been made, such changes must be clearly indicated.

The author(s) must be appropriately credited and we ask that you include the end user license and a DOI link to the formal publication on ScienceDirect.

If any part of the material to be used (for example, figures) has appeared in our publication with credit or acknowledgement to another source it is the responsibility of the user to ensure their reuse complies with the terms and conditions determined by the rights holder.

Additional Terms & Conditions applicable to each Creative Commons user license:

CC BY: The CC-BY license allows users to copy, to create extracts, abstracts and new works from the Article, to alter and revise the Article and to make commercial use of the Article (including reuse and/or resale of the Article by commercial entities), provided the user gives appropriate credit (with a link to the formal publication through the relevant DOI), provides a link to the license, indicates if changes were made and the licensor is not represented as endorsing the use made of the work. The full details of the license are available at http://creativecommons.org/licenses/by/4.0.

CC BY NC SA: The CC BY-NC-SA license allows users to copy, to create extracts, abstracts and new works from the Article, to alter and revise the Article, provided this is not done for commercial purposes, and that the user gives appropriate credit (with a link to the formal publication through the relevant DOI), provides a link to the license, indicates if changes were made and the licensor is not represented as endorsing the use made of the work. Further, any new works must be made available on the same conditions. The full details of the license are available at http://creativecommons.org/licenses/by-nc-sa/4.0.

CC BY NC ND: The CC BY-NC-ND license allows users to copy and distribute the Article, provided this is not done for commercial purposes and further does not permit distribution of the Article if it is changed or edited in any way, and provided the user gives appropriate credit (with a link to the formal publication through the relevant DOI), provides a link to the license, and that the licensor is not represented as endorsing the use made of the work. The full details of the license are available at http://creativecommons.org/licenses/by-nc-nd/4.0. Any commercial reuse of Open Access articles published with a CC BY NC SA or CC BY NC ND license requires permission from Elsevier and will be subject to a fee.

Commercial reuse includes:

- Associating advertising with the full text of the Article
- Charging fees for document delivery or access
- Article aggregation
- Systematic distribution via e-mail lists or share buttons

Posting or linking by commercial companies for use by customers of those companies.

20. **Other Conditions**:

v1.10

Questions? customercare@copyright.com or +1-855-239-3415 (toll free in the US) or +1-978-646-2777.